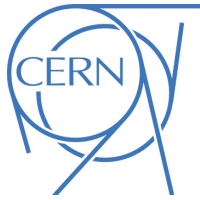


EUROPEAN ORGANISATION FOR NUCLEAR RESEARCH (CERN)



Eur. Phys. J. C 79 (2019) 666
DOI: [10.1140/epjc/s10052-019-7162-0](https://doi.org/10.1140/epjc/s10052-019-7162-0)



CERN-EP-2019-064
2nd December 2019

Measurement of distributions sensitive to the underlying event in inclusive Z-boson production in pp collisions at $\sqrt{s} = 13$ TeV with the ATLAS detector

The ATLAS Collaboration

This paper presents measurements of charged-particle distributions sensitive to the properties of the underlying event in events containing a Z boson decaying into a muon pair. The data were obtained using the ATLAS detector at the LHC in proton–proton collisions at a centre-of-mass energy of 13 TeV with an integrated luminosity of 3.2 fb^{-1} . Distributions of the charged-particle multiplicity and of the charged-particle transverse momentum are measured in regions of the azimuth defined relative to the Z boson direction. The measured distributions are compared with the predictions of various Monte Carlo generators which implement different underlying-event models. The Monte Carlo model predictions qualitatively describe the data well, but with some significant discrepancies.

Contents

1	Introduction	2
2	Underlying-event observables and measurement strategy	3
3	The ATLAS detector	5
4	Data and simulated event samples	5
5	Event and track selection	6
6	Corrections and systematic uncertainties	8
6.1	Unfolding	8
6.2	Background subtraction	8
6.3	Systematic uncertainties	8
7	Unfolded observables and comparison with model predictions	13
7.1	Overview of the results	13
7.2	Differential distributions	13
7.3	Underlying-event activity as a function of p_T^Z	15
7.4	Comparison with other centre-of-mass energies	17
8	Discussion and conclusion	23

1 Introduction

A typical proton–proton (pp) collision studied at the LHC consists of a short-distance hard-scattering process and accompanying activity collectively termed the underlying event (UE). The hard scattering processes have a momentum transfer sufficiently large that the strong coupling constant is small and the cross-section may be calculated perturbatively in quantum chromodynamics (QCD). The driving mechanisms for the production of the UE are at a much lower momentum scale. These mechanisms include partons not participating in the hard-scattering process (beam remnants), radiation processes and additional hard and semi-hard scatters in the same pp collision, termed multiple parton interactions (MPI). Phenomenological models are required to describe these processes using several free parameters determined from experiment. In addition to furthering the understanding of the proton’s internal structure and the related soft-QCD processes, accurate modelling of the UE is crucial for many data analyses at a hadron collider, either to precisely determine Standard Model quantities or to search for new particles and interactions.

The UE is not distinguishable from the hard scatter on an event-by-event basis. However, there are observables which are sensitive to the UE properties, as first introduced by the CDF Collaboration in proton–antiproton ($p\bar{p}$) collisions at a centre-of-mass energy of 1.8 TeV [1]. An example of such an

observable can be defined by topological considerations, based on the activity measurement in the direction transverse¹ to a reference object.

The object in the event with the leading transverse momentum relates the UE activity to the scale of the momentum transfer in the hard interaction. In general, processes with leptonic final states like Drell–Yan events are experimentally clean and theoretically well understood, allowing reliable identification of the particles from the UE. The absence of QCD final-state radiation (FSR) permits a study of different kinematic regions with varying transverse momenta of the Z boson due to harder or softer initial-state radiation (ISR).

Previous measurements of distributions sensitive to the properties of the UE in Drell–Yan events were performed in pp collisions at a centre-of-mass energy of 7 TeV by the ATLAS [2] and CMS [3] Collaborations and at a centre-of-mass energy of 13 TeV by the CMS Collaboration [4]. Both measurements at $\sqrt{s} = 7$ TeV verified that the dependence of the UE activity on the dimuon invariant mass is qualitatively well described by the PowHEG+PYTHIA8 and Herwig++ sets of tuned parameters but with some significant discrepancies. Reference [2] provides distributions which are sensitive to the choice of parameters used in the various UE models.

This paper presents distributions of four observables sensitive to the UE in events containing a Z boson produced in pp collisions at a centre-of-mass energy of 13 TeV in the ATLAS detector at the LHC, where the singly produced Z boson decays into $\mu^+\mu^-$. Observables measured as a function of the transverse momentum of the Z boson, p_T^Z , in various regions of phase space are compared with predictions from several Monte Carlo (MC) event generators.

2 Underlying-event observables and measurement strategy

Events containing two muons originating from the decay of a singly produced Z boson form a particularly interesting sample for studying the UE. The final-state Z boson is well-identified and colour neutral, so that interaction between the final-state leading particle and the UE is minimal. Gluon radiation from the quarks or gluons initiating the hard scatter are, however, an important consideration as these give the remainder of the event a non-zero transverse momentum and change the kinematics of the final-state. Observables are therefore measured in different regions of the transverse plane, which are defined relative to the direction of the Z boson as illustrated in Figure 1.

A charged particle lies in the *away* region if its azimuthal angle relative to the Z boson direction $|\Delta\phi|$ is greater than 120° . This region is heavily dominated by the hadronic recoil against the Z boson from initial state quark/gluon radiation and is therefore not particularly sensitive to the UE. The *toward* ($|\Delta\phi| \leq 60^\circ$) and *transverse* ($60^\circ < |\Delta\phi| \leq 120^\circ$) regions contain less contamination from the hard process after subtraction of the two muons from the Z boson. The transverse region is sensitive to the UE because, by construction, it is perpendicular to the direction of the Z boson and hence is expected to have a lower level of activity from the hard-scattering process than the away region. The two *transverse* regions are differentiated on an event-by-event basis by their scalar sum of charged-particle p_T . The one with the larger

¹ ATLAS uses a right-handed coordinate system with its origin at the nominal interaction point (IP) in the centre of the detector and the z -axis along the beam pipe. The x -axis points from the IP to the centre of the LHC ring, and the y -axis points upwards. Cylindrical coordinates (r, ϕ) are used in the transverse plane, ϕ being the azimuthal angle around the z -axis. The pseudorapidity is defined in terms of the polar angle θ as $\eta = -\ln \tan(\theta/2)$. Angular distance is measured in units of $\Delta R \equiv \sqrt{(\Delta\eta)^2 + (\Delta\phi)^2}$.

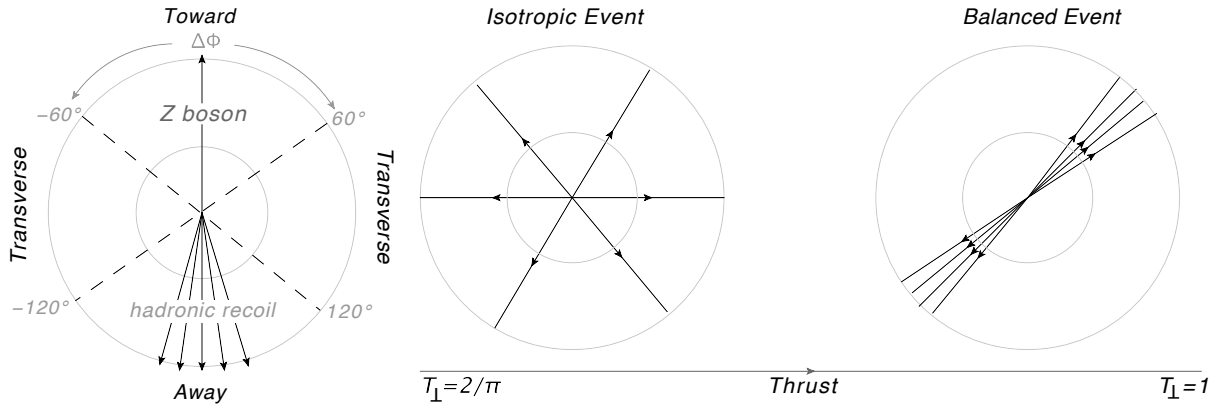


Figure 1: (a) Illustration of away, transverse, and towards regions in the transverse plane defined relative to the direction of the Z boson. (b) Illustration of an isotropic and a balanced event topology in the transverse plane with their corresponding values of thrust T_{\perp} . In these figures, the beams are travelling perpendicular to the plane of the page.

sum is labelled *trans-max* and the other *trans-min* [5, 6]. The trans-min region is highly sensitive to the UE activity because it is less likely that activity from recoiling jets leaks into this region.

Four distributions are studied to understand the UE activity. The first is the charged-particle transverse momentum $dN_{\text{ch}}/dp_{\text{T}}^{\text{ch}}$ distribution inclusive over all selected particles. The final spectrum for this variable is accumulated over all events and then normalized. The next three are evaluated on an event-by-event basis: the charged-particle multiplicity $dN_{\text{ev}}/d(\sum N_{\text{ch}}/\delta\eta\delta\phi)$, the scalar sum of the transverse momentum of those particles $dN_{\text{ev}}/d(\sum p_{\text{T}}/\delta\eta\delta\phi)$, and the mean transverse momentum $dN_{\text{ev}}/d(\text{mean } p_{\text{T}})$, where mean p_{T} is the quotient of $\sum p_{\text{T}}$ and N_{ch} (provided $N_{\text{ch}} > 0$ in the corresponding region). The distributions of these variables are produced separately for charged particles lying in each of the regions described above. The charged-particle multiplicity and the scalar sum of transverse momenta are normalized relative to the area of the corresponding region in the η - ϕ space. This simplifies the comparison of the activity in different regions. The distributions are distinguished in different ranges of the Z boson transverse momentum p_{T}^Z and for two regions of transverse thrust T_{\perp} [7]. Transverse thrust characterizes the topology of the tracks in the event and is

$$T_{\perp} = \frac{\sum_i |\vec{p}_{\text{T},i} \cdot \hat{n}|}{\sum_i |\vec{p}_{\text{T},i}|}. \quad (1)$$

The thrust axis \hat{n} is the unit vector which maximizes T_{\perp} . Here the summation is done on an event-by-event basis over the transverse momenta p_{T} of all charged particles except the two muons. Transverse thrust has a maximum value of 1 for a pencil-like dijet topology and a minimum value of $2/\pi$ for a circularly symmetric distribution of particles in the transverse plane, as illustrated in Figure 1. As proposed in Ref. [8], events with lower values of T_{\perp} are more sensitive to the MPI component of the UE. The two regions of thrust examined in this paper are $T_{\perp} \leq 0.75$ and $T_{\perp} > 0.75$, which are optimized to distinguish extra jet activity from the actual UE activity. A measurement of transverse thrust in combination with the UE activity was done at $\sqrt{s} = 7$ TeV [9], but it did not distinguish the transverse regions.

In this paper, all measurements are also performed inclusively in T_{\perp} . In total, the spectra of the four observables are measured in 96 regions of phase space, i.e. in eight bins of p_{T}^Z ; in the away, toward, trans-max, and trans-min regions; and for low, high, and inclusive T_{\perp} . The bin boundaries in p_{T}^Z are (0, 10, 20, 40, 60, 80, 120, 200, 500) GeV. In addition to distributions of the four observables, the arithmetic

means $\langle N_{\text{ch}} \rangle$, $\langle \Sigma p_{\text{T}} \rangle$, and $\langle \text{mean } p_{\text{T}} \rangle$ are evaluated as functions of p_{T}^Z in each of the various regions of phase space.

3 The ATLAS detector

The ATLAS detector [10–12] at the LHC covers nearly the entire solid angle around the collision point. It consists of an inner tracking detector (ID) surrounded by a thin superconducting solenoid, electromagnetic and hadronic calorimeters, and a muon spectrometer (MS) incorporating three large superconducting toroid magnets.

The ID is immersed in a 2 T axial magnetic field and provides charged-particle tracking in the range $|\eta| < 2.5$. A high-granularity silicon pixel detector typically provides four measurements per track and is surrounded by a silicon microstrip tracker (SCT), which usually provides four three-dimensional measurement points per track. These silicon detectors are complemented by a transition radiation tracker, which enables radially extended track reconstruction up to $|\eta| = 2.0$.

The MS comprises separate trigger and precision tracking chambers which measure the deflection of muons in a magnetic field generated by superconducting air-core toroids. The precision chamber system covers the region $|\eta| < 2.7$ with three layers of monitored drift tubes, complemented by cathode-strip chambers in the forward region, where the background is highest. The muon trigger system covers the range $|\eta| < 2.4$ with resistive-plate chambers in the barrel and thin-gap chambers in the endcap regions.

A two-level trigger system is used to select interesting events [13]. The level-1 trigger is implemented in hardware and uses a subset of the muon spectrometer and calorimeter information to reduce the event rate to around 100 kHz. This is followed by a software-based trigger which runs offline reconstruction algorithms and reduces the event rate to approximately 1 kHz.

4 Data and simulated event samples

Data recorded in 2015 with the ATLAS detector at the LHC in proton–proton collisions at a centre-of-mass energy of 13 TeV are used in this analysis. The data set corresponds to an integrated luminosity of 3.2 fb^{-1} . Only events recorded when the detector was fully operational are considered.

Simulated MC events are used both to estimate the contamination from background processes in data and to correct the measured data for detector inefficiency and resolution effects (Section 6.1).

The $Z \rightarrow \mu\mu$ signal process was simulated using the next-to-leading-order PowHEG [14, 15] event generator with the CT10 set of parton distribution functions (PDFs) [16] and interfaced to the PYTHIA 8.170 event generator [17, 18] to simulate the parton shower, hadronization and UE with the CTEQ6L1 PDF set and the AZNLO set of tuned parameters [19]. The latter option tunes the event generator to the p_{T}^Z measurement at $\sqrt{s} = 7 \text{ TeV}$ [19]. Hence, it retunes the overall UE activity by adjusting the PYTHIA MPI cut-off parameter to the UE activity of the previous measurement [2] in the lowest p_{T}^Z bin (0 to 5 GeV). PHOTOS [20] was used to simulate final-state electromagnetic radiation. The PYTHIA generator uses p_{T} -ordered parton showers and a hadronization model based on the fragmentation of colour strings. Its MPI model interleaves the ISR and FSR emissions with MPI scatters.

An alternative signal sample used for cross-checks and systematic uncertainty evaluations was simulated

using **SHERPA** 2.2.0 [21], which has an independent implementation of the parton shower, hadronization, UE and FSR. The **SHERPA** samples utilize the NNPDF30NNLO PDF set [22] and were generated with the nominal tune set of version 2.2.0. The **SHERPA** generator uses leading-order matrix elements with a model for MPI similar to that of **PYTHIA** 8 but without interleaving the FSR. It implements a cluster hadronization model similar to that of **Herwig++**. **SHERPA** and **PYTHIA** impose the infrared cut-off for MPI as a smooth function. In contrast, **Herwig++** implements it as a step function. A signal sample produced with the MC generator **Herwig++** [23] using the UE-EE-5 tune [24] provided by the generator’s authors and the corresponding CTEQ6L1 PDF set is compared with unfolded data in Section 7. This tuning uses energy extrapolation and was developed to describe the UE and double parton interaction effective cross-section. **Herwig++** uses, similarly to **PYTHIA**, a leading-logarithm parton shower model matched to leading-order matrix element calculations, but it implements a cluster hadronization scheme with parton showering ordered by emission angle.

Three sources of background are estimated using MC samples: $Z \rightarrow \tau\tau$, $WW \rightarrow \mu\nu\mu\nu$, and the $t\bar{t}$ process, each of which was simulated using PowHEG [25, 26] interfaced to **PYTHIA**8 or **PYTHIA**6 for $t\bar{t}$. The **PYTHIA** tune set for $Z \rightarrow \tau\tau$ and $WW \rightarrow \mu\nu\mu\nu$ is the same as was used for the signal process (AZNLO). The Perugia 2012 [27] tune set was used for simulation of the $t\bar{t}$ process.

Overlaid MC-generated minimum-bias events [28] simulate the effect of multiple interactions in the same bunch crossing (pile-up). These samples were produced with **PYTHIA** 8 using the A2 tune set [29] in combination with the MSTW2008LO PDF set. The A2 tune set was matched to the ATLAS minimum-bias measurement at $\sqrt{s} = 7$ TeV [30]. The mean number of interactions per bunch crossing $\langle\mu\rangle$ during the 2015 data-taking with 25 ns bunch spacing was 13.5. The simulated samples are reweighted to reproduce the distribution of the number of interactions per bunch crossing observed in the data.

The **GEANT4** [31] program simulated the passage of particles through the ATLAS detector. Differences in muon reconstruction, trigger, and isolation efficiencies between MC simulation and data are evaluated using a tag-and-probe method [32], and the simulation is corrected accordingly. Additional factors applied to the MC events correct for the description of the muon energy and momentum scales and resolution, which are determined from fits to the observed Z boson line shapes in data and MC simulations [32]. Finally, correction factors adjust the distribution of the longitudinal position of the primary pp collision vertex [33] to the one observed in the data.

5 Event and track selection

Candidate $Z \rightarrow \mu\mu$ events are selected by requiring that at least one out of two single-muon triggers be satisfied. A high-threshold trigger requires a muon to have $p_T > 40$ GeV, whilst a low-threshold trigger requires $p_T > 20$ GeV and the muon to be isolated from additional nearby tracks. All events are required to have a primary vertex (PV). The PV is defined as the reconstructed vertex in the event with the highest Σp_T of the associated tracks, consistent with the beam-spot position (spatial region inside the detector where collisions take place) and with at least two associated tracks with $p_T > 400$ MeV.

The main selections to define the regions of phase space are summarized in Table 1. The reconstruction procedure for muon candidates combines tracks reconstructed in the inner detector with tracks reconstructed in the MS [32]. The reconstructed muons are required to have $p_T > 25$ GeV and $|\eta| < 2.4$. Track quality requirements are imposed to suppress backgrounds, and the muon candidate is required to be isolated using

a p_T - and η -dependent ‘gradient’ isolation criterion [32] based on track and calorimeter information. Muon candidates consistent with having originated from the decay of a heavy quark are rejected by requiring the significance of the transverse impact parameter ($|d_0/\sigma(d_0)|$, with d_0 representing the transverse impact parameter and $\sigma(d_0)$ the related uncertainty) to be below 3. Furthermore, the muon candidates must be associated to the PV, i.e. the longitudinal ($|z_0 \sin \theta|$) impact parameter is less than 0.5 mm. The variables d_0 and z_0 are measured relative to the PV.

Events are required to have exactly two opposite-charged muons satisfying the selection criteria above. The invariant mass of the dimuon system must be between 66 GeV and 116 GeV.

Tracks reconstructed in the ID from the passage of charged particles are used to form the UE observables. Each reconstructed track is required to have $p_T > 0.5$ GeV, $|\eta| < 2.5$, one hit in the innermost layer is required (if expected) and in total at least one hit in the pixel detector and at least six hits in the SCT. The tracks must have been assigned to the PV, i.e. the transverse and longitudinal impact parameters of the tracks relative to the PV must be smaller than 2 mm and 1.5 mm respectively. An additional requirement on the quality of the fit of the track to the hits in the detector applies to tracks with $p_T > 10$ GeV in order to suppress mismeasured tracks at high p_T . This criterion affects mainly the tracks associated with the muon candidates and has little impact on the predominantly low- p_T tracks of the UE activity.

The kinematics of the Z boson and of the charged particles in the event define the phase space of the fiducial region (particle level). This closely reflects the selection made on measured detector quantities outlined before. Simulated events are required to have two prompt muons that satisfy $p_T > 25$ GeV and $|\eta| < 2.4$ with each muon defined at the ‘bare’ level (after final-state QED radiation). The measurements are all reported in bins of p_T^Z , the results presented in this paper are not sensitive to the predicted shape of the p_T^Z spectrum, even though they are sensitive to jet activity in the event. As a cross-check the observables are constructed as defined before but the muons are unfolded to the ‘dressed’ level (i.e. collinear QED FSR is added to the ‘bare’ level muons) similar to the previous UE measurement in Z events [2]. The difference between the results after unfolding to different generator levels is below the percent level and is less than the uncertainty related to the unfolding procedure. Charged particles must be stable, i.e. have a proper lifetime with $c\tau > 10$ mm, with $p_T > 0.5$ GeV. and $|\eta| < 2.5$.

The statistical uncertainties of the data and the MC simulations are propagated using the bootstrap method [34]. While the statistical error of the data is the limiting factor for all distributions at high p_T^Z , it does not limit the measurements in phase-space regions of lower p_T^Z , which are particularly important for tuning MC simulations.

Table 1: A summary of the fiducial volume definition of the measurement, the particle-level definition, and the main observables. The first row lists selection criteria for the signal muons (indicated with an μ as superscript) limited by the detector geometry, while the cut on the dimuon invariant mass $m^{\ell\ell}$ yields a low background contamination.

Fiducial volume (for muon selection)	$p_T^\mu > 25$ GeV, $ \eta < 2.4$, $66 \text{ GeV} < m^{\mu\mu} < 116$ GeV
Particle-level definition	$p_T > 0.5$ GeV, $ \eta < 2.5$, charge $\neq 0$, stable (i.e. a proper lifetime of $c\tau > 10$ mm)

6 Corrections and systematic uncertainties

6.1 Unfolding

An iterative Bayesian unfolding technique is used to correct the data for detector inefficiencies and resolution [35–37]. Response matrices connect each observable at the detector and particle levels; these are constructed using the PowHEG+PYTHIA8 signal MC sample which is overlayed with pile-up events at detector level. Each response matrix corresponds to a bin of p_T^Z or thrust, with the migration of events between p_T^Z or thrust bins corrected using a per-bin purity correction factor. In the context of MC simulations, the purity of one bin is defined as the fraction of events that are reconstructed in the same bin as the original particle level quantity. The bin intervals in p_T^Z and thrust are chosen to yield high purities (> 0.9 for the bins in p_T^Z and > 0.85 for the two bins in T_\perp) enabling the per-bin corrections. For the observable $dN_{\text{ch}}/dp_T^{\text{ch}}$, two unfolding iterations are sufficient for convergence of the unfolding results, while for all other observables eight iterations are performed. The evaluation of the mean value of each observable in a bin of p_T^Z and thrust occurs after unfolding. The bin boundaries are the same at both the detector and particle levels.

6.2 Background subtraction

The background contributions to the selected data from the $Z \rightarrow \tau\tau$, $t\bar{t}$, and $WW \rightarrow \mu\nu\mu\nu$ processes are estimated using MC simulations. In total, these are about 0.7% of selected data events. This fraction varies from 0.9% for the lowest bin in p_T^Z to the per mille level for the highest p_T^Z bin. The background contribution from multijet processes is estimated using a data-driven technique based on the isolation and charge of the two reconstructed muons, similar to previous analyses [2]. The size of the multijet contribution in the data is less than 0.1%. The unfolding of the data is done after the subtraction of all MC and data-driven background estimates.

6.3 Systematic uncertainties

Systematic uncertainties can arise due to possible mismodelling of the muon momentum scale or resolution, as well as the reconstruction, identification, and isolation efficiencies. Furthermore, limited knowledge of the ID material distribution [38] dominates the uncertainties in the track reconstruction inefficiencies. Also the effect of falsely reconstructed tracks (when there is no corresponding charged particle) contributes to all observables.

All uncertainties related to imperfect modelling of the detector are assessed using MC simulations. The data are first unfolded using the nominal MC simulation samples. Then the data are unfolded with MC samples where the parameter of the simulation which is affected by the mismodelling is varied by $\pm 1\sigma$ of its estimated uncertainty. The average of the up and down shifts is assigned as the corresponding systematic uncertainty.

Since the observables are primarily track-based, the track-related systematic uncertainties dominate the total detector-related uncertainty. These are of the order of 2% regardless of the observable and region. Systematic uncertainties related to the muon reconstruction are a negligible fraction of the overall uncertainty.

Uncertainties due to mismodelling of the background processes are also considered. For the background processes modelled with MC simulations, the electroweak background normalization is varied by $\pm 5\%$ and the $t\bar{t}$ background normalization by $\pm 15\%$ (approximately within their theoretical uncertainties [39, 40]) and the effect on the final measurements is estimated. The full effect of including the multijet background or not is taken as an uncertainty. The combined background-related uncertainties form a negligible fraction of the total systematic uncertainty. The dependence of the background uncertainty on p_T^Z is negligible for this measurement.

An important consideration for these measurements is the modelling of the pile-up, since the MC simulations must correct for contamination from pile-up tracks through the unfolding procedure. When averaging over all simulated events about 13% of the selected tracks which are compatible with the primary vertex originate from pile-up.

A variation in the pile-up reweighting of the MC simulations is included to cover the uncertainty on the ratio between the predicted and measured inelastic cross-section in the fiducial volume defined by $M_X > 13 \text{ GeV}$ where M_X is the mass of the hadronic system [41]. The value of $\langle \mu \rangle$ assumed in the MC simulations for the unfolding process is varied by $\pm 9\%$ from the nominal value. This uncertainty in the pile-up modelling is one of the largest sources of systematic uncertainty in the tails of the distributions of p_T , N_{ch} , Σp_T , and mean p_T , and for the mean distributions. The uncertainties related to the inaccuracies of the detector and pile-up modelling are combined and referred to as the ‘Detector’ uncertainty in the following figures.

Two additional cross-checks validate the pile-up modelling and the consistency of removing the pile-up effects via the unfolding technique. First, the unfolding procedure for all observables in all measurement bins is repeated for three intervals of $\langle \mu \rangle$, namely [8–10], [11–13] and [14–16]. A mismodelling of pile-up in MC simulations would manifest itself less in the interval of $8 \leq \langle \mu \rangle \leq 10$ and more in the interval of $14 \leq \langle \mu \rangle \leq 16$. The unfolded results for the three intervals are found to be fully compatible within their associated statistical uncertainties, confirming the consistency of the handling of pile-up in the unfolding process.

Secondly, a complementary data-driven technique based on the *Hit Backspace Once More* (HBOM) method [42] is used. The intention is to reproduce pile-up contaminations as realistically as possible. Hence, the track information associated with non-primary vertices in the data is bundled to form a pile-up library. A random sample is drawn from this library and used as an example of pile-up effects in data. If this random sample is added to an individual event, the pile-up effect increases. A sampling of the library is subsequently used to pollute events with additional pile-up. Six iterations of pollution are applied, i.e. up to six random samples from the pile-up library are added to each event. Then the observables are constructed from these additionally contaminated events. Assuming the values of the observables evolve smoothly with each iteration of additional pile-up, an extrapolation in each bin to the value with zero pile-up vertices yields the HBOM estimate of pile-up subtracted data. The data are subsequently unfolded using a version of the POWHEG+PYTHIA signal MC samples without pile-up vertices. The results obtained using this method are consistent with the nominal procedure, and no additional uncertainty is assigned.

The uncertainty associated with the unfolding technique is evaluated using a data-driven method. It accounts for the dependence of the unfolding on the usage of prior knowledge from the MC simulation, i.e. the particle level quantities. The ratio of data to simulation at detector-level is evaluated and smoothed for each observable. The smoothed ratio is then used to reweight the simulations by applying the event-weight according to the particle level quantity. The reweighted detector-level distribution is then unfolded using the regular response matrix. The relative difference between the reweighted particle-level distribution and the reweighted and unfolded detector-level distribution is treated as a systematic uncertainty. This dependence

on prior knowledge from the MC simulation is the dominant systematic uncertainty in most distributions at lower values of p_T^Z . An additional method of estimating the uncertainty related to the unfolding is to unfold the detector-level MC distributions generated with SHERPA using the unfolding matrices based on the POWHEG+PYTHIA MC sample. The results are compared with the particle level quantities predicted by SHERPA. After taking the uncertainty due to the MC prior into account, a slight discrepancy between the unfolded SHERPA sample and the particle-level distributions remains. Therefore, an additional contribution to the MC prior uncertainty is introduced to cover this remaining non-closure of the unfolded result and the SHERPA generator level. In general, it does not exceed the 2–4% level and is smoothed over the full range of the observable. In a few cases, this non-closure component dominates the MC prior uncertainty. These two separate unfolding uncertainties are added in quadrature in all figures.

All sources of systematic uncertainty are considered uncorrelated and are combined in quadrature. The MC prior uncertainty is one of the largest contributors to the total systematic uncertainty at all values of p_T and in each p_T^Z region. The statistical uncertainty of the data rises with increasing p_T^Z , contributing a significant fraction of the overall uncertainty. The breakdown of the individual sources of uncertainties for the four observables, p_T , N_{ch} , Σp_T , and mean p_T is illustrated in Figure 2 for the example of events with $10 < p_T^Z < 20$ GeV in the trans-min region (the region most sensitive to the UE), inclusively in T_\perp .

Figure 3 shows the systematic uncertainties in the arithmetic mean of the N_{ch} and Σp_T spectra in the trans-min region as a function of p_T^Z inclusively in T_\perp . The largest contributions to the total systematic uncertainties of the mean distributions at all p_T^Z values come from either the MC prior uncertainty or the track-related uncertainties. The statistical uncertainties of the data become large for p_T^Z greater than around 200 GeV.

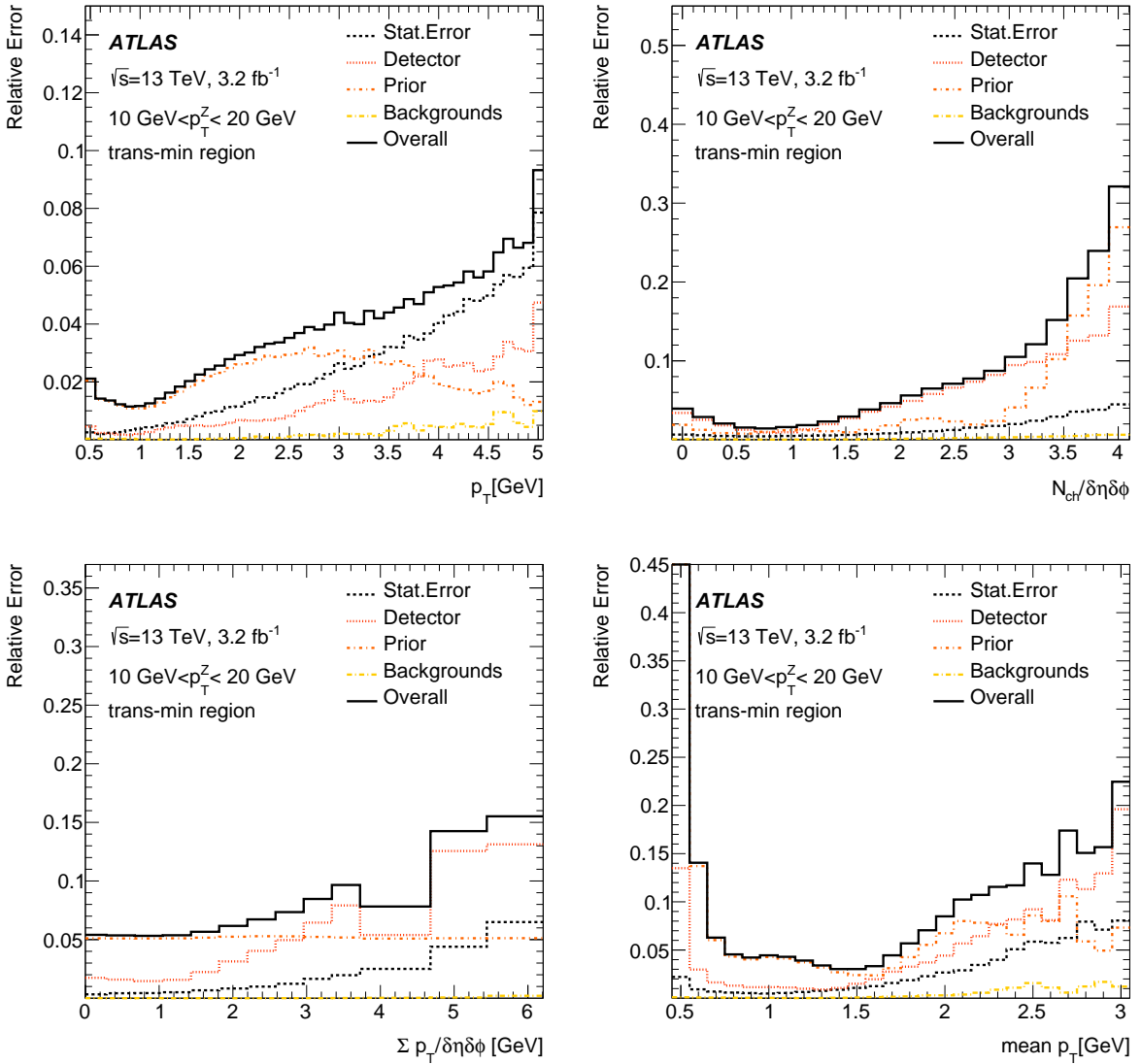


Figure 2: Breakdown of systematic uncertainties in the p_T spectrum (upper left), the charged-particle multiplicity (N_{ch} , upper right), the scalar sum of the transverse momenta (Σp_T , lower left) and the mean transverse momentum (mean p_T , lower right) for events with $10 < p_T^Z < 20$ GeV in the trans-min region inclusively in T_\perp . Here ‘Prior’ combines the two approaches to estimate the unfolding-related uncertainties. ‘Detector’ includes the modelling of the detector and the pile-up conditions.

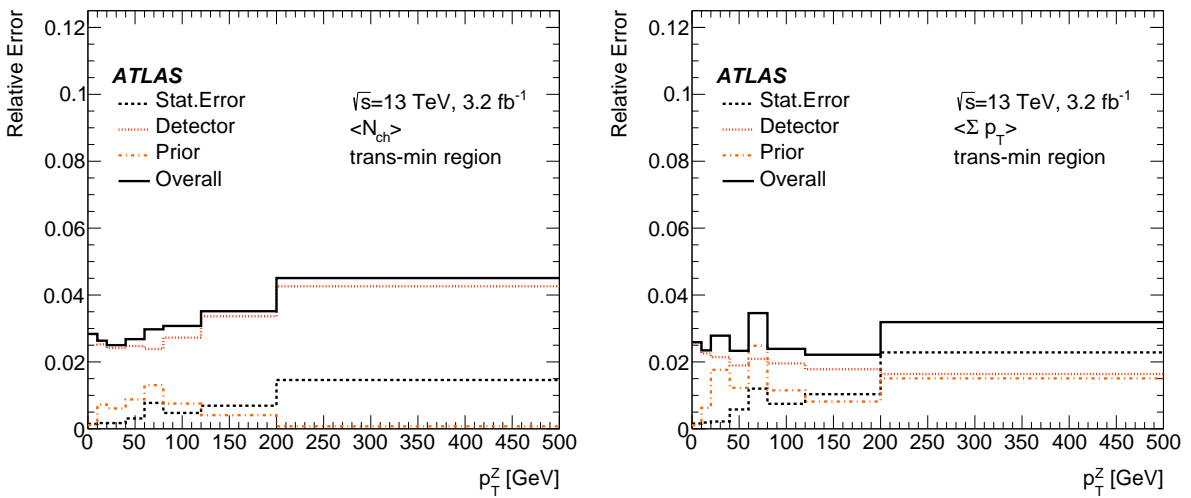


Figure 3: A summary of the systematic uncertainties in the arithmetic mean of the N_{ch} and Σp_T spectra in the trans-min region as a function of p_T^Z . Here ‘Prior’ combines the two approaches to estimate the unfolding-related uncertainties. ‘Detector’ includes the modelling of the detector and the pile-up conditions.

7 Unfolded observables and comparison with model predictions

7.1 Overview of the results

Distributions of p_T , N_{ch} , Σp_T , and mean p_T are obtained in slices of p_T^Z for the different regions defined in the transverse plane and different regions of T_\perp . The results for N_{ch} and Σp_T are normalized relative to the area of the region in η and ϕ . In addition to the measurements in slices of p_T^Z , the arithmetic means of N_{ch} , Σp_T , and mean p_T ($\langle N_{\text{ch}} \rangle$, $\langle \Sigma p_T \rangle$, and $\langle \text{mean } p_T \rangle$) are measured as a function of p_T^Z . Only a selection of the most relevant results is discussed in this section: the comparison of the unfolded data to the predictions of different MC generators focuses on the trans-min region. While the toward region provides insights of similar importance for tuning MC generators after having removed the two muons, the discussion focuses on the trans-min region to better facilitate comparison with previous measurements. The UE activity in the toward region is higher compared with that in trans-min. This is expected since the trans-min region is defined as the subregion of the transverse region with the lower activity and for $Z \rightarrow \mu\mu$ events the UE activity is expected to be of similar magnitude in the toward and transverse regions. The trans-min region is statistically less affected by radiation and it is essentially the region where the contribution from ISR is subtracted. Apart from this difference in the amount of activity, the predictive performance of the different MC generators is comparable in the toward and trans-min regions. No significant difference in the predictive power between these regions is observed. Both $\langle N_{\text{ch}} \rangle$ and $\langle \Sigma p_T \rangle$ measured in the trans-min are compared with previous measurements of the UE in Z boson events at lower centre-of-mass energies.

7.2 Differential distributions

Figures 4 and 5 show the unfolded p_T spectrum, N_{ch} , Σp_T , and mean p_T for the trans-min region inclusively in T_\perp for events with p_T^Z between 10 and 20 GeV and between 120 and 200 GeV. The predictions from Powheg+Pythia, Sherpa, and Herwig++ are compared with the data. The ratio of prediction to data is shown beneath each plot. None of the tested MC generators describes all aspects of the data well and in some regions the differences exceed the 70% level. Generally, the MC generators predict a higher number of particles with small p_T than is observed in data (see top left of Figures 4 and 5). This is consistent with the MC predictions tending to lower values of mean p_T , as is shown on the lower right plots of Figures 4 and 5. The largest differences between data and simulation are at low N_{ch} and low Σp_T , and arise due to the steeper transverse momentum spectrum of charged particles in MC simulations. Powheg+Pythia and Sherpa predict a higher fraction of events with fewer charged particles and a consistently smaller sum of p_T . However, Herwig++ slightly overestimates the fraction of particles with $p_T > 2.5$ GeV and is qualitatively closer to the shape of the distributions of N_{ch} and Σp_T . With rising p_T^Z , the data p_T spectrum becomes harder, and N_{ch} , Σp_T , and mean p_T increase. The relative discrepancy remains the same in comparisons with the generator predictions.

The dependence on T_\perp is illustrated in Figure 6 for the unfolded p_T spectrum in the trans-min region for events with $10 < p_T^Z < 20$ GeV and $120 < p_T^Z < 200$ GeV. Similar to the results for the measurement inclusive in T_\perp , the MC generators predict a higher fraction of particles with low p_T than present in data. The predictions of Powheg+Pythia are closer to the measured distributions in the lower p_T^Z region, but Sherpa describes better the full p_T range in the higher p_T^Z bin. The Herwig++ simulations have significant statistical fluctuations at higher p_T . The most striking difference between the different regions in T_\perp is observed for the Powheg+Pythia generator when focusing on the low p_T^Z bins for N_{ch} as presented in Figure 7. In MPI-sensitive regions (left plot in Figure 7) the distribution of N_{ch} by Powheg+Pythia is

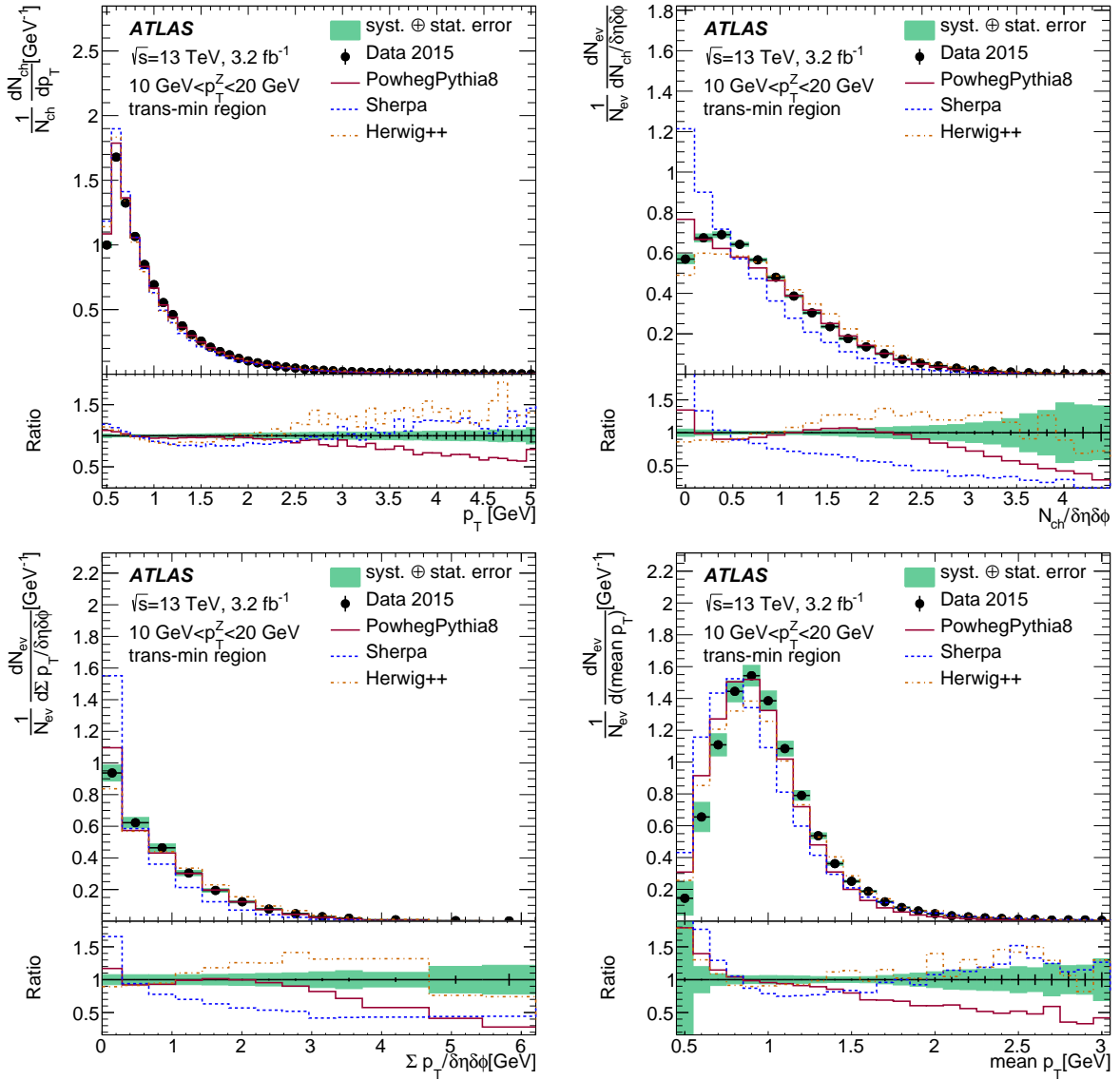


Figure 4: Measured spectra of p_T (upper left), the charged-particle multiplicity, N_{ch} (upper right), the scalar sum of the transverse momentum of those particles, Σp_T , (lower left) and the mean transverse momentum, $\text{mean } p_T$ (lower right) in the trans-min region inclusively in T_\perp for events with $10 < p_T^Z < 20 \text{ GeV}$. Predictions of POWHEG+PYTHIA, SHERPA, and Herwig++ are compared with the data. The ratios shown are predictions over data.

shifted towards higher numbers of charged-particles relative to the data, i.e. overshooting the data in the range $1 \leq N_{\text{ch}}/\delta\eta\delta\phi \leq 2.5$. But in the high thrust region (right plot) the MC generator underestimates the data almost over the full range except for the first two bins. In contrast, the performances of SHERPA and Herwig++ are consistent when comparing the low and high thrust regions for N_{ch} ; Herwig++ overestimates N_{ch} , and SHERPA underestimates it. The same effect is observed for the distributions of Σp_T but is less significant and therefore not presented. As pointed out in Ref. [8], the regions of high values of T_\perp are dominated by extra jet activity which is not adequately modelled in POWHEG+PYTHIA, as shown in the right plots in Figures 6 and 7.

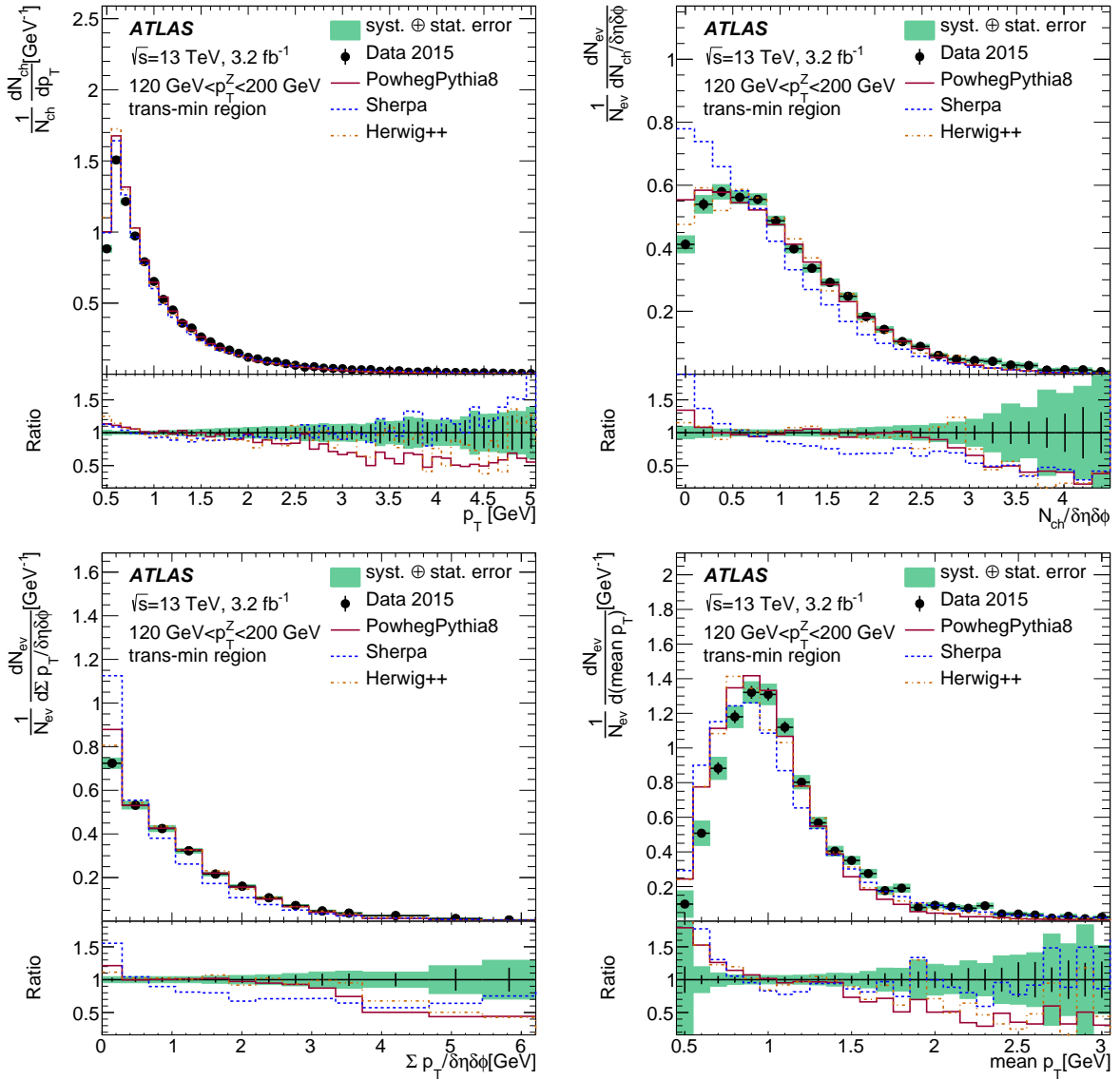


Figure 5: Measured p_T spectra (upper left), the charged-particle multiplicity N_{ch} (upper right), the scalar sum of the transverse momentum of those particles Σp_T (lower left), and the mean transverse momentum, $\text{mean } p_T$ (lower right) in the trans-min region inclusively in T_\perp for events with $120 < p_T^Z < 200 \text{ GeV}$. Predictions of POWHEG+PYTHIA, SHERPA, and Herwig++ are compared with the data. The ratios shown are predictions over data.

7.3 Underlying-event activity as a function of p_T^Z

Figure 8 shows the mean number of charged particles and the mean of the scalar sum of the transverse momenta of those particles per unit $\eta-\phi$ space as a function of p_T^Z in the transverse, trans-min, and trans-max regions inclusively in T_\perp . The trans-min region is further separated by T_\perp in the right plots of Figure 8. In the trans-min region, the UE-sensitive variables N_{ch} and Σp_T rise slowly with increasing Z boson transverse momentum. In contrast, the observables in the trans-max region have a strong dependence on p_T^Z . This is because it is heavily contaminated with the Z boson hadronic recoil leaking into the transverse region. The slope of the UE activity in the trans-min region as a function of p_T^Z for events of high T_\perp is similar to the

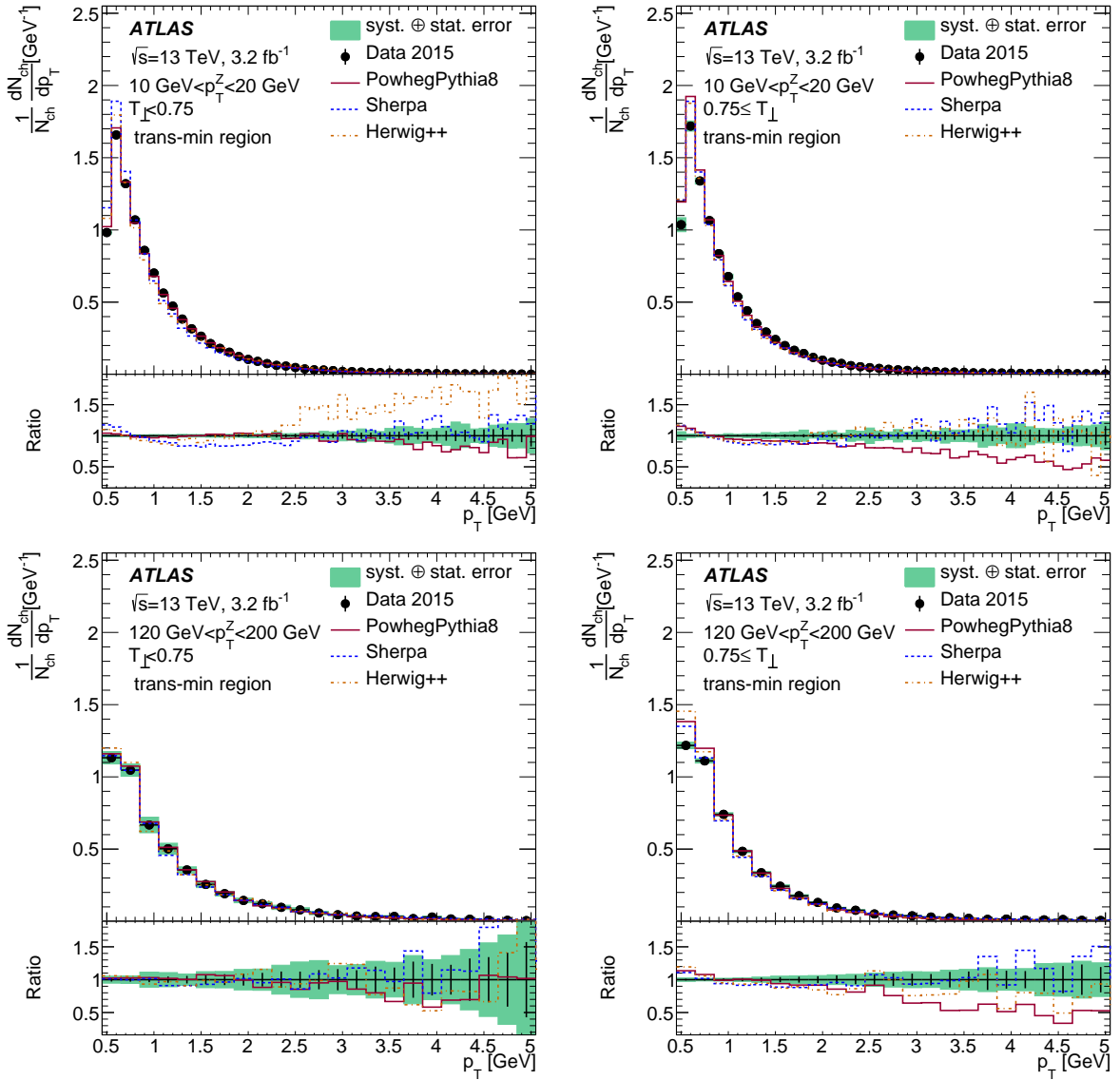


Figure 6: Measured p_T spectra in the trans-min region for $T_\perp < 0.75$ (left) and $0.75 \leq T_\perp$ (right) for events with $10 < p_T^Z < 20 \text{ GeV}$ (upper row) and $120 < p_T^Z < 200 \text{ GeV}$ (lower row). Predictions of Powheg+Pythia, Sherpa, and Herwig++ are compared with the data. The ratios shown are predictions over data.

inclusive measurement. The total amount of activity measured in the trans-min region for events with high T_\perp is lower than the inclusive measurement due to the correlation of activity in the transverse region and T_\perp . Furthermore, the right-hand plots of Figure 8 demonstrate that the UE activity is higher for events with lower T_\perp , as expected [8]. Lower values of T_\perp also increase the dependence on p_T^Z in the trans-min region.

The MC modelling of individual measurements in all 96 phase-space regions is further investigated by comparing the measured arithmetic means of the N_{ch} , Σp_T , and mean p_T as functions of p_T^Z . Figures 9 and 10 show comparisons with the predictions of Powheg+Pythia, Sherpa, and Herwig++ for the trans-min and towards regions inclusively in T_\perp . The predictions fail to describe the data in either of the regimes.

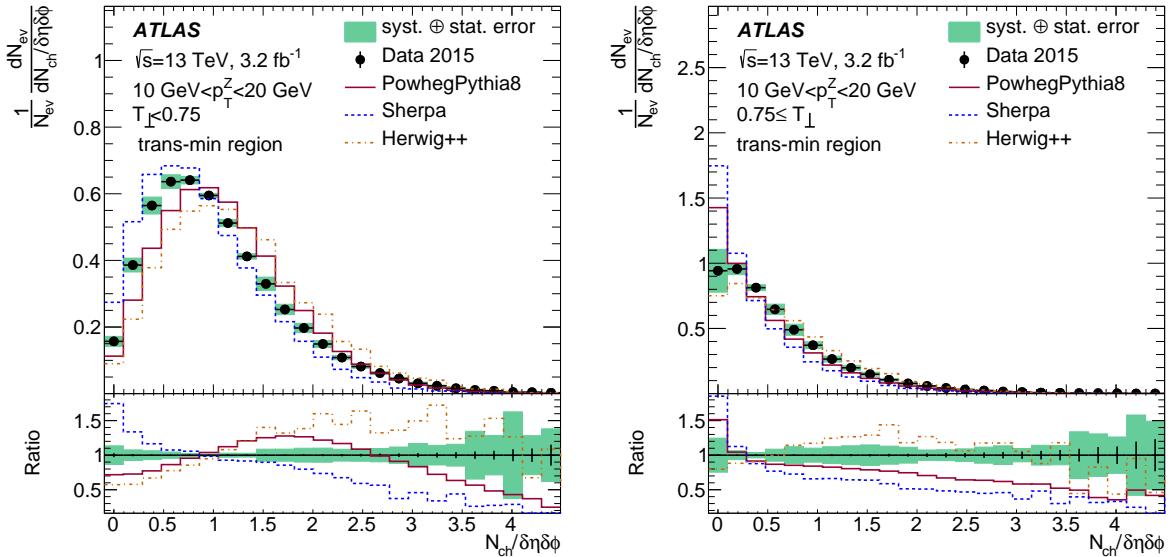


Figure 7: Measured number of charged particles in the trans-min region for $T_{\perp} < 0.75$ (left) and $0.75 \leq T_{\perp}$ (right) for events with $10 < p_T^Z < 20$ GeV. Predictions of POWHEG+PYTHIA, SHERPA, and HERWIG++ are compared with the data. The ratios shown are predictions over data.

For $p_T^Z > 20$ GeV, HERWIG++ predicts a slower rise in UE activity with rising p_T^Z than in the measured distributions. On the other hand, POWHEG+PYTHIA and SHERPA qualitatively describe the ‘turn-on’ effect of the UE activity, i.e. a steeper slope at low p_T^Z which vanishes at higher values of p_T^Z . For POWHEG+PYTHIA, the rise of the UE activity is underestimated, and hence the discrepancy with data grows with p_T^Z and stabilizes around $p_T^Z = 100$ GeV. Only in the toward region of the mean of the mean p_T is SHERPA in good agreement with the data.

The p_T^Z dependence for the two regions of T_{\perp} in the trans-min region is summarized in Figures 11 and 12. In the low T_{\perp} region, the prediction by SHERPA improves, e.g. for N_{ch} the discrepancy shrinks from about 30% to roughly 10%. Referring to the same observable, POWHEG+PYTHIA is in agreement with data for $p_T^Z > 80$ GeV in the low T_{\perp} regime within the uncertainties. For the selection on high T_{\perp} all generators underestimate the UE activity. SHERPA provides the best description of the data in $\langle \text{mean } p_T \rangle$. Apart from the toward region, it tends to a constant underestimation but agrees with the overall shape. The agreement of POWHEG+PYTHIA with data is better for $T_{\perp} < 0.75$ than for the inclusive measurement. The predictions of HERWIG++ in the trans-min region improve with higher values of p_T^Z and also in events of lower T_{\perp} . However, the discrepancy between HERWIG++ and the data in the lowest bins remains regardless of the selected region.

7.4 Comparison with other centre-of-mass energies

Figure 13 presents a comparison of the measured $\langle N_{\text{ch}} \rangle$ and $\langle \Sigma p_T \rangle$ for different centre-of-mass energies. The results for $\sqrt{s} = 7$ TeV are taken from the previous ATLAS measurement of the UE activity in Z boson events [2]. The event selection criteria are similar to the analysis presented in this paper, but the previous measurement also includes the $Z \rightarrow e^+ e^-$ channel. The CDF measurements at $\sqrt{s} = 1.96$ TeV [43] are also included in the comparison. The CDF analyses used Drell–Yan lepton pairs in a smaller invariant mass window ($70 < m_{\mu\mu} < 110$ GeV) in $p\bar{p}$ collisions. The relative uncertainties of the two ATLAS

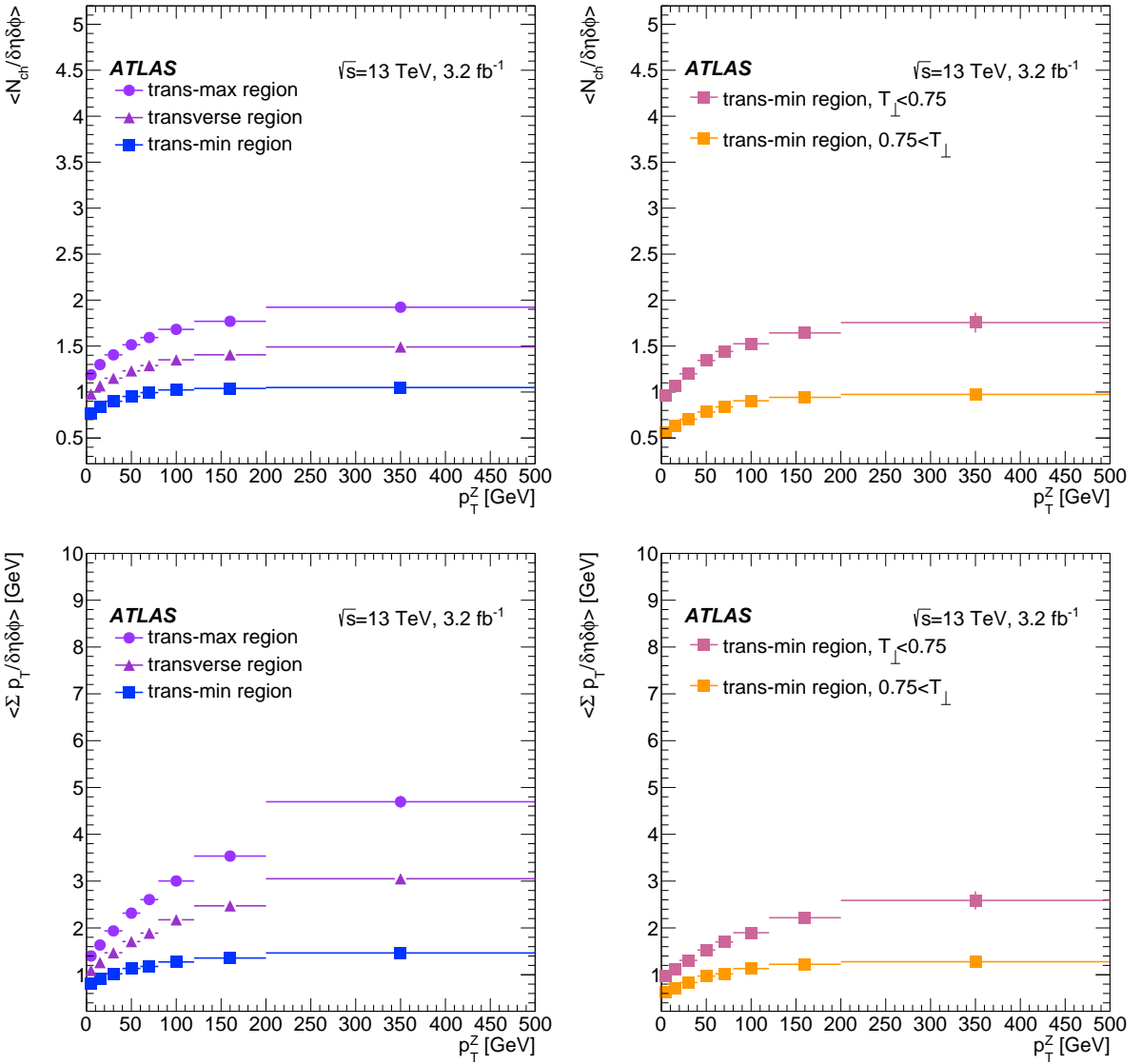


Figure 8: The mean number of charged particles (upper row) and the mean of the scalar sum of the transverse momentum of those particles (lower row) per unit $\eta-\phi$ space as a function of p_T^Z in the full transverse region and for the trans-min and trans-max regions inclusively in T_\perp (left) and in the trans-min region separated in T_\perp (right).

measurements are of similar sizes, while the CDF measurements have large statistical fluctuations for $p_T^{Z/\mu\mu} > 30 \text{ GeV}$. All three measurements show qualitatively the same behaviour, i.e. a growing UE activity with higher values of p_T^Z . With higher centre-of-mass energies, more energy is available for the processes forming the UE e.g. MPI. Hence, the rise of the UE activity as a function of \sqrt{s} is expected.

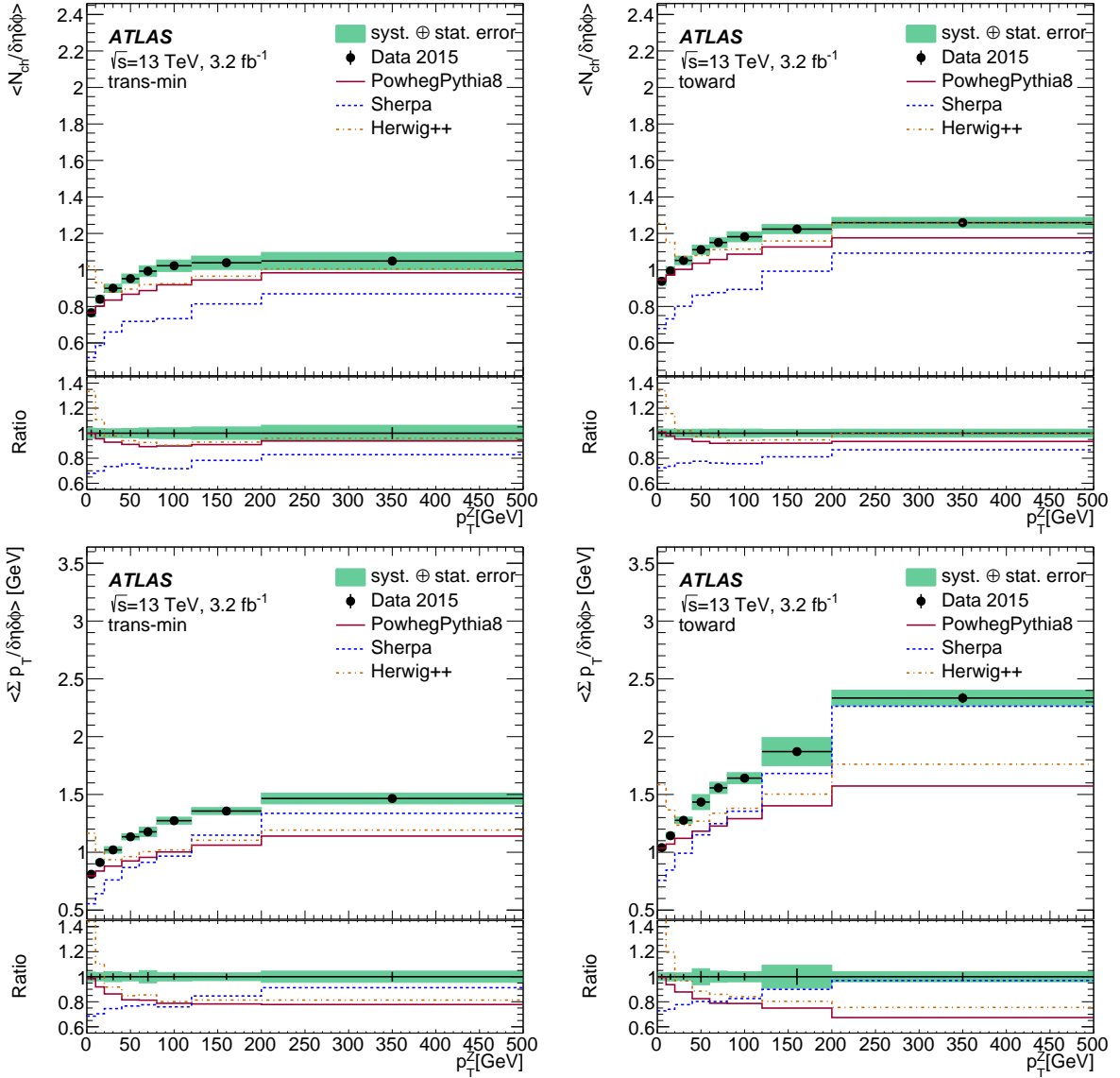


Figure 9: Comparison of measured arithmetic means of the N_{ch} (upper row) and Σp_T (lower row) as functions of p_T^Z for the trans-min (left) and towards (right) region inclusively in T_\perp . Predictions of Powheg+PYTHIA, SHERPA and Herwig++ are compared with the data. The ratios shown are predictions over data.

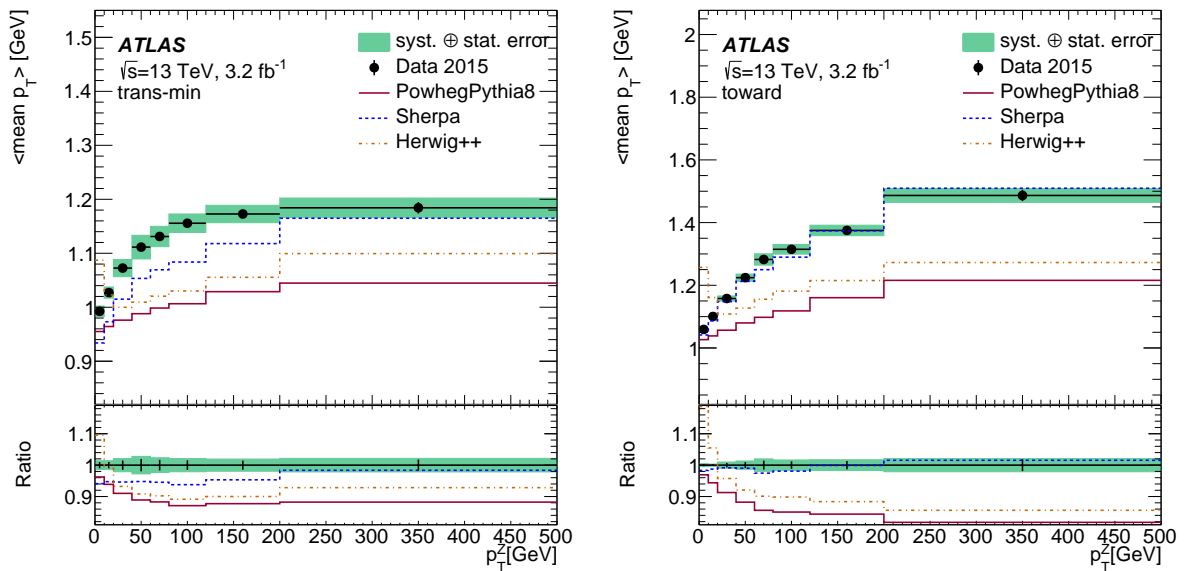


Figure 10: Comparison of measured arithmetic means of mean p_T as functions of p_T^Z for the trans-min (left) and towards (right) regions inclusively, and in regions of T_\perp . Predictions of POWHEG+PYTHIA, SHERPA, and Herwig++ are compared with the data. The ratios shown are predictions over data.

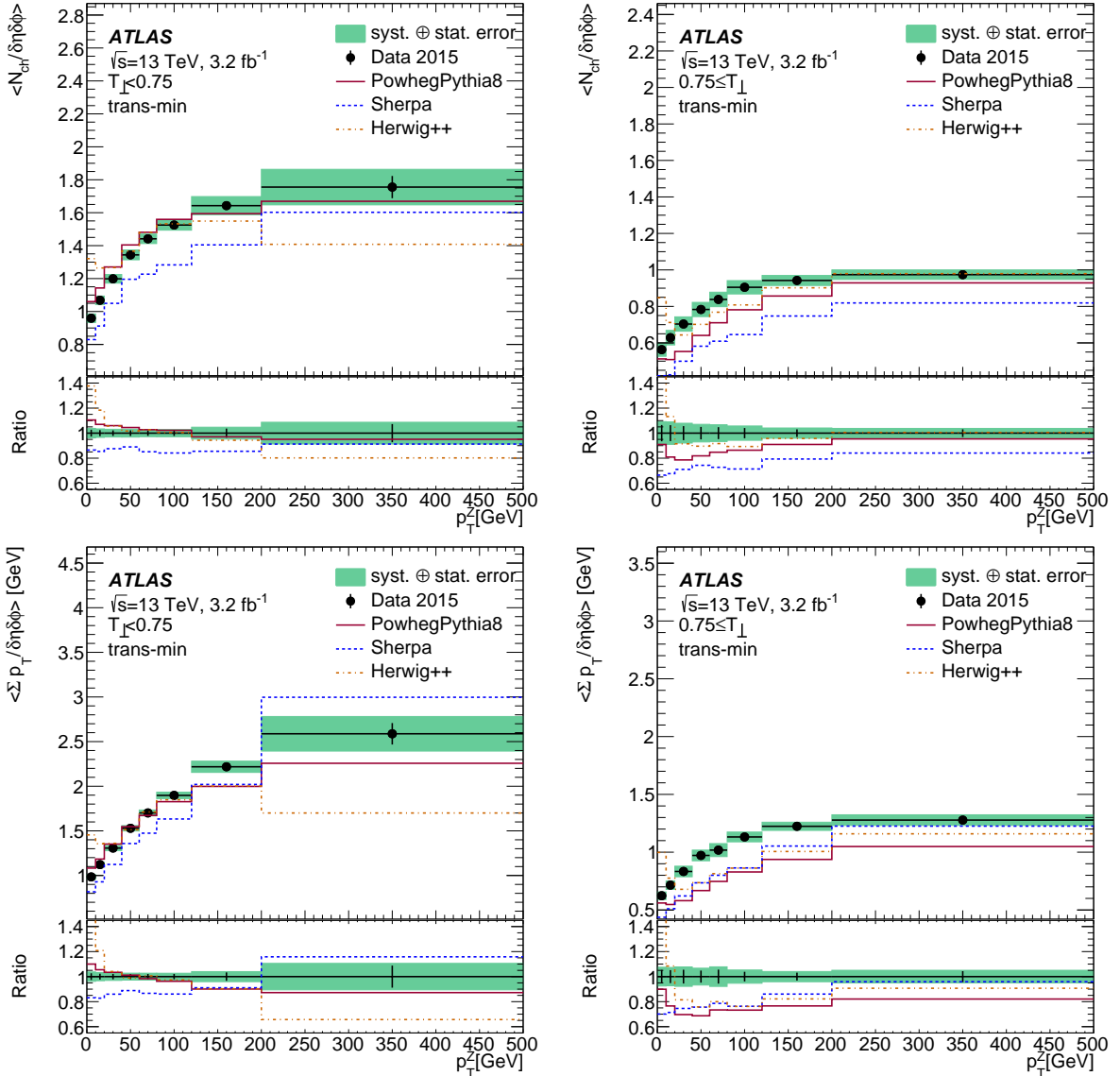


Figure 11: Comparison of measured arithmetic means of the N_{ch} (upper row) and Σp_T (lower row) as functions of p_T^Z for $T_\perp < 0.75$ (left) and $0.75 \leq T_\perp$ (right) for the trans-min region. Predictions of Powheg+PYTHIA, SHERPA, and Herwig++ are compared with the data. The ratios shown are predictions over data.

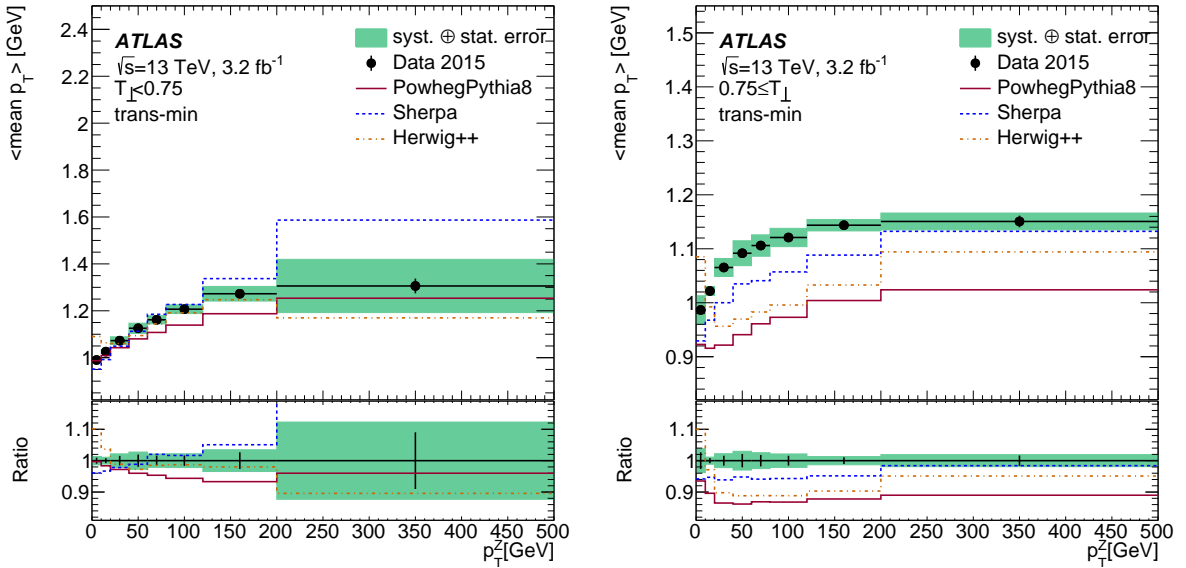


Figure 12: Comparison of the measured arithmetic mean of mean p_T as a function of p_T^Z for ranges of T_\perp in the trans-min region. Predictions of Powheg+Pythia, Sherpa, and Herwig++ are compared with the data. The ratios shown are predictions over data.

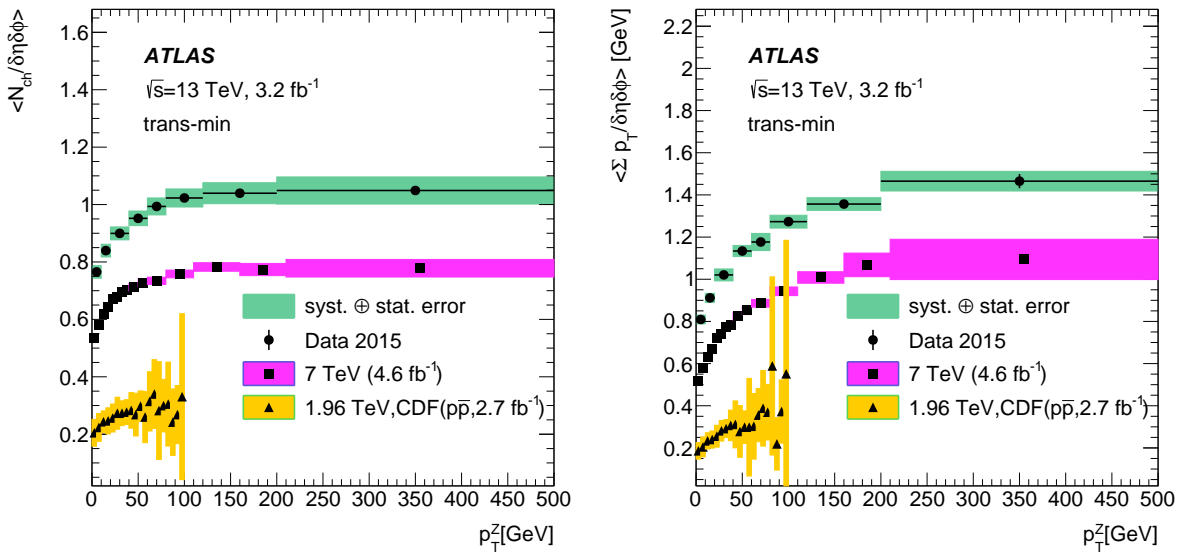


Figure 13: The distributions of $\langle N_{ch} \rangle$ and $\langle \Sigma p_T \rangle$ measured at $\sqrt{s} = 13$ TeV compared with the results of the previous ATLAS measurements at $\sqrt{s} = 7$ TeV [2] and the CDF measurements at $\sqrt{s}=1.96$ TeV [43]. The error bars correspond to the full uncertainties of the corresponding measurement.

8 Discussion and conclusion

Measurements of four observables sensitive to the activity of the UE in $Z \rightarrow \mu\mu$ events are presented using 3.2 fb⁻¹ of $\sqrt{s} = 13$ TeV pp collision data collected with the ATLAS detector at the LHC in 2015. Those observables are the p_T of charged particles, the number of charged particles per event (N_{ch}), the sum of charged-particle p_T per event (Σp_T), and the mean of charged-particle p_T per event (mean p_T). They are measured in intervals of the Z boson p_T and in different azimuthal regions of the detector relative to the Z boson direction. The arithmetic means of the distributions are plotted as functions of the Z boson p_T , inclusively of and in regions of transverse thrust.

The predictions from three Monte Carlo generators (POWHEG+PYTHIA8, SHERPA and Herwig++) are compared with the data. In general, all tested generators and tunes show significant deviations from the data distributions regardless of the observable. The arithmetic means of the observables deduced from the predictions of POWHEG+PYTHIA8 and SHERPA match the main features of the UE activity in the fiducial region. The turn-on effect, i.e. the rising activity as a function of the hard-scatter scale (here p_T^Z), is visible as is a saturation of this effect for higher values of p_T^Z . In contrast to the other generators, Herwig++ fails to reproduce the turn-on effect at low p_T^Z as it predicts that the UE activity decreases as a function of p_T^Z when considered only in the $p_T^Z < 20$ GeV region. Otherwise, all generators underestimate the activity of the UE when quantified as the arithmetic mean of the observables for inclusive T_\perp . The generators predict the mean values better in comparison with the data when focusing on the MPI-sensitive regions. POWHEG+PYTHIA8 is in agreement with data within the uncertainties for $\langle N_{ch} \rangle$ and $\langle \Sigma p_T \rangle$, indicating an adequate handling of the MPI activity. However, since the predictive power shrinks for the region with $T_\perp > 0.75$ in comparison with the inclusive measurement, the simulation of contributions other than MPI to the UE activity needs to be improved. Reference [8] points out that the region with $T_\perp > 0.75$ is dominated by extra jet activity, giving a first indication for a possible improvement of the MC generator prediction. This conclusion is valid when focusing on POWHEG+PYTHIA8 for different regions of T_\perp for individual bins of p_T^Z .

In comparison with the measurements at $\sqrt{s} = 7$ TeV [2], the performance of Herwig++ is consistent for $p_T^Z > 20$ GeV. Both measurements use the energy-extrapolation tunes [24] provided by the Herwig++ authors, i.e. UE-EE-3 for $\sqrt{s} = 7$ TeV and in the analysis presented here UE-EE-5. The latter tune was additionally validated against Tevatron and LHC measurements at $\sqrt{s} = 900$ GeV and $\sqrt{s} = 7$ TeV [44]. The prediction of Herwig++ is slightly better for the distributions of $\langle N_{ch} \rangle$ and $\langle \Sigma p_T \rangle$ at higher values of p_T^Z . In the previous measurements, the divergence increased with p_T^Z , which might be related to improper modelling of the impact parameter. Apart from overestimating the mean activity, Herwig++ improved relative to the $\sqrt{s} = 7$ TeV measurements in the description of the shape of $dN_{ev}/d(\Sigma p_T/\delta\eta\delta\phi)$, $dN_{ev}/d(\text{mean } p_T)$, and $dN_{ev}/d(N_{ch}/\delta\eta\delta\phi)$ in the presented p_T^Z -bins. Qualitatively it performs better than the other generators.

POWHEG+PYTHIA8 performs as well at $\sqrt{s} = 13$ TeV as it does at $\sqrt{s} = 7$ TeV, but is tuned with AU2 (only the MPI part was tuned by ATLAS using $\sqrt{s} = 7$ TeV UE data) in the previous measurements. Nevertheless, this indicates that the MPI energy extrapolation of PYTHIA8 works well, which is in agreement with the better description for distributions at low T_\perp .

In contrast, while at $\sqrt{s} = 7$ TeV SHERPA version 1.4.0 with the CT10 PDF set consistently overestimates the UE activity metrics $\langle N_{ch} \rangle$ and $\langle \Sigma p_T \rangle$ by 5% to 15%, the present analysis and SHERPA version reveal a continuous underestimation. At $\sqrt{s} = 13$ TeV, the discrepancy relative to the data decreases with higher values of p_T^Z .

Acknowledgements

We thank CERN for the very successful operation of the LHC, as well as the support staff from our institutions without whom ATLAS could not be operated efficiently.

We acknowledge the support of ANPCyT, Argentina; YerPhI, Armenia; ARC, Australia; BMWFW and FWF, Austria; ANAS, Azerbaijan; SSTC, Belarus; CNPq and FAPESP, Brazil; NSERC, NRC and CFI, Canada; CERN; CONICYT, Chile; CAS, MOST and NSFC, China; COLCIENCIAS, Colombia; MSMT CR, MPO CR and VSC CR, Czech Republic; DNRF and DNSRC, Denmark; IN2P3-CNRS, CEA-DRF/IRFU, France; SRNSFG, Georgia; BMBF, HGF, and MPG, Germany; GSRT, Greece; RGC, Hong Kong SAR, China; ISF and Benoziyo Center, Israel; INFN, Italy; MEXT and JSPS, Japan; CNRST, Morocco; NWO, Netherlands; RCN, Norway; MNiSW and NCN, Poland; FCT, Portugal; MNE/IFA, Romania; MES of Russia and NRC KI, Russian Federation; JINR; MESTD, Serbia; MSSR, Slovakia; ARRS and MIZŠ, Slovenia; DST/NRF, South Africa; MINECO, Spain; SRC and Wallenberg Foundation, Sweden; SERI, SNSF and Cantons of Bern and Geneva, Switzerland; MOST, Taiwan; TAEK, Turkey; STFC, United Kingdom; DOE and NSF, United States of America. In addition, individual groups and members have received support from BCKDF, CANARIE, CRC and Compute Canada, Canada; COST, ERC, ERDF, Horizon 2020, and Marie Skłodowska-Curie Actions, European Union; Investissements d’Avenir Labex and Idex, ANR, France; DFG and AvH Foundation, Germany; Herakleitos, Thales and Aristeia programmes co-financed by EU-ESF and the Greek NSRF, Greece; BSF-NSF and GIF, Israel; CERCA Programme Generalitat de Catalunya, Spain; The Royal Society and Leverhulme Trust, United Kingdom.

The crucial computing support from all WLCG partners is acknowledged gratefully, in particular from CERN, the ATLAS Tier-1 facilities at TRIUMF (Canada), NDGF (Denmark, Norway, Sweden), CC-IN2P3 (France), KIT/GridKA (Germany), INFN-CNAF (Italy), NL-T1 (Netherlands), PIC (Spain), ASGC (Taiwan), RAL (UK) and BNL (USA), the Tier-2 facilities worldwide and large non-WLCG resource providers. Major contributors of computing resources are listed in Ref. [45].

References

- [1] CDF Collaboration, *Charged jet evolution and the underlying event in $p\bar{p}$ collisions at 1.8 TeV*, *Phys. Rev. D* **65** (2002) 092002.
- [2] ATLAS Collaboration, *Measurement of distributions sensitive to the underlying event in inclusive Z-boson production in pp collisions at $\sqrt{s} = 7$ TeV with the ATLAS detector*, *Eur. Phys. J. C* **74** (2014) 3195, arXiv: [1409.3433 \[hep-ex\]](#).
- [3] CMS Collaboration, *Measurement of the underlying event in the Drell-Yan process in proton–proton collisions at $\sqrt{s} = 7$ TeV*, *Eur. Phys. J. C* **72** (2012) 2080, arXiv: [1204.1411 \[hep-ex\]](#).
- [4] CMS Collaboration, *Measurement of the underlying event activity in inclusive Z boson production in proton–proton collisions at $\sqrt{s} = 13$ TeV*, *JHEP* **07** (2018) 032, arXiv: [1711.04299 \[hep-ex\]](#).
- [5] G. Marchesini and B. R. Webber, *Associated transverse energy in hadronic jet production*, *Phys. Rev. D* **38** (1988) 3419.
- [6] J. Pumplin, *Hard underlying event correction to inclusive jet cross-sections*, *Phys. Rev. D* **57** (1998) 5787, arXiv: [hep-ph/9708464 \[hep-ph\]](#).

- [7] A. Banfi, G. P. Salam and G. Zanderighi, *Phenomenology of event shapes at hadron colliders*, *JHEP* **06** (2010) 038, arXiv: [1001.4082 \[hep-ph\]](#).
- [8] D. Kar and D. S. Rafanoharana, *Probing underlying event in Z-boson events using event shape observables*, *Int. J. Mod. Phys. A* **34** (2018) 1950022, arXiv: [1801.05218 \[hep-ph\]](#).
- [9] ATLAS Collaboration, *Measurement of event-shape observables in $Z \rightarrow \ell^+ \ell^-$ events in pp collisions at $\sqrt{s} = 7$ TeV with the ATLAS detector at the LHC*, *Eur. Phys. J. C* **76** (2016) 375, arXiv: [1602.08980 \[hep-ex\]](#).
- [10] ATLAS Collaboration, *The ATLAS Experiment at the CERN Large Hadron Collider*, *JINST* **3** (2008) S08003.
- [11] ATLAS Collaboration, *ATLAS Insertable B-Layer Technical Design Report*, ATLAS-TDR-19, 2010, URL: <https://cds.cern.ch/record/1291633>, Addendum: ATLAS-TDR-19-ADD-1, 2012, URL: <https://cds.cern.ch/record/1451888>.
- [12] B. Abbott et al., *Production and integration of the ATLAS Insertable B-Layer*, *JINST* **13** (2018) T05008, arXiv: [1803.00844 \[physics.ins-det\]](#).
- [13] ATLAS Collaboration, *Performance of the ATLAS trigger system in 2015*, *Eur. Phys. J. C* **77** (2017) 317, arXiv: [1611.09661 \[hep-ex\]](#).
- [14] S. Alioli, P. Nason, C. Oleari and E. Re, *NLO vector-boson production matched with shower in POWHEG*, *JHEP* **07** (2008) 060, arXiv: [0805.4802 \[hep-ph\]](#).
- [15] S. Alioli, P. Nason, C. Oleari and E. Re, *A general framework for implementing NLO calculations in shower Monte Carlo programs: the POWHEG BOX*, *JHEP* **06** (2010) 043, arXiv: [1002.2581 \[hep-ph\]](#).
- [16] J. Pumplin et al., *New Generation of Parton Distributions with Uncertainties from Global QCD Analysis*, *JHEP* **07** (2002) 012, arXiv: [hep-ph/0201195](#).
- [17] T. Sjöstrand, S. Mrenna and P. Z. Skands, *PYTHIA 6.4 physics and manual*, *JHEP* **05** (2006) 026, arXiv: [hep-ph/0603175](#).
- [18] T. Sjöstrand, S. Mrenna and P. Z. Skands, *A brief introduction to PYTHIA 8.1*, *Comput. Phys. Commun.* **178** (2008) 852, arXiv: [0710.3820 \[hep-ph\]](#).
- [19] ATLAS Collaboration, *Measurement of the Z/γ^* boson transverse momentum distribution in pp collisions at $\sqrt{s} = 7$ TeV with the ATLAS detector*, *JHEP* **09** (2014) 145, arXiv: [1406.3660 \[hep-ex\]](#).
- [20] P. Gononka and Z. Was, *PHOTOS Monte Carlo: A precision tool for QED corrections in Z and W decays*, *Eur. Phys. J. C* **45** (2006) 97, arXiv: [hep-ph/0506026](#).
- [21] T. Gleisberg et al., *Event generation with SHERPA 1.1*, *JHEP* **02** (2009) 007, arXiv: [0811.4622 \[hep-ph\]](#).
- [22] R. D. Ball et al., *Parton distributions for the LHC Run II*, *JHEP* **04** (2015) 040, arXiv: [1410.8849 \[hep-ph\]](#).
- [23] M. Bähr et al., *Herwig++ physics and manual*, *Eur. Phys. J. C* **58** (2008) 639, arXiv: [0803.0883 \[hep-ph\]](#).
- [24] S. Gieseke, C. Rohr and A. Siódmiak, *Colour reconnections in Herwig++*, *Eur. Phys. J. C* **72** (2012) 2225, arXiv: [1206.0041 \[hep-ph\]](#).

- [25] T. Melia, P. Nason, R. Röntsch and G. Zanderighi, *W+W-, WZ and ZZ production in the POWHEG BOX*, *JHEP* **2011** (2011) 78, arXiv: [1107.5051 \[hep-ph\]](#).
- [26] S. Frixione, P. Nason and G. Ridolfi, *A Positive-weight next-to-leading-order Monte Carlo for heavy flavour hadroproduction*, *JHEP* **09** (2007) 126, arXiv: [0707.3088 \[hep-ph\]](#).
- [27] P. Z. Skands, *Tuning Monte Carlo generators: The Perugia tunes*, *Phys. Rev. D* **82** (2010) 074018, arXiv: [1005.3457 \[hep-ph\]](#).
- [28] ATLAS Collaboration, *The ATLAS Simulation Infrastructure*, *Eur. Phys. J. C* **70** (2010) 823, arXiv: [1005.4568 \[physics.ins-det\]](#).
- [29] ATLAS Collaboration, *Further ATLAS tunes of PYTHIA 6 and Pythia 8*, ATL-PHYS-PUB-2011-014, 2011, URL: <https://cds.cern.ch/record/1400677>.
- [30] ATLAS Collaboration, *Measurement of the jet fragmentation function and transverse profile in proton–proton collisions at a center-of-mass energy of 7 TeV with the ATLAS detector*, *Eur. Phys. J. C* **71** (2011) 1795, arXiv: [1109.5816 \[hep-ex\]](#).
- [31] S. Agostinelli et al., *GEANT4—A simulation toolkit*, *Nucl. Instrum. Meth. A* **506** (2003) 250.
- [32] ATLAS Collaboration, *Muon reconstruction performance of the ATLAS detector in proton–proton collision data at $\sqrt{s} = 13$ TeV*, *Eur. Phys. J. C* **76** (2016) 292, arXiv: [1603.05598 \[hep-ex\]](#).
- [33] ATLAS Collaboration, *Performance of primary vertex reconstruction in proton–proton collisions at $\sqrt{s} = 7$ TeV in the ATLAS experiment*, ATLAS-CONF-2010-069, 2010, URL: <https://cds.cern.ch/record/1281344>.
- [34] B. Efron, *Bootstrap Methods: Another Look at the Jackknife*, *Ann. Statist.* **7** (1979) 1.
- [35] G. D’Agostini, *A Multidimensional unfolding method based on Bayes’ theorem*, *Nucl. Instrum. Meth. A* **362** (1995) 487.
- [36] G. D’Agostini, *Improved iterative Bayesian unfolding*, (2010), arXiv: [1010.0632 \[physics.data-an\]](#).
- [37] T. Adye, *Unfolding algorithms and tests using RooUnfold*, (2011), arXiv: [1105.1160 \[physics.data-an\]](#).
- [38] ATLAS Collaboration, *Study of the material of the ATLAS inner detector for Run 2 of the LHC*, *JINST* **12** (2017) P12009, arXiv: [1707.02826 \[hep-ex\]](#).
- [39] ATLAS Collaboration, *Measurement of the WW cross section in $\sqrt{s} = 7$ TeV pp collisions with the ATLAS detector and limits on anomalous gauge couplings*, *Phys. Lett. B* **712** (2012) 289, arXiv: [1203.6232 \[hep-ex\]](#).
- [40] ATLAS Collaboration, *Measurement of the top quark pair production cross section in pp collisions at $\sqrt{s} = 7$ TeV in dilepton final states with ATLAS*, *Phys. Lett. B* **707** (2012) 459, arXiv: [1108.3699 \[hep-ex\]](#).
- [41] ATLAS Collaboration, *Measurement of the Inelastic Proton–Proton Cross Section at $\sqrt{s} = 13$ TeV with the ATLAS Detector at the LHC*, *Phys. Rev. Lett.* **117** (2016) 182002, arXiv: [1606.02625 \[hep-ex\]](#).
- [42] J. W. Monk and C. Oropesa-Barrera, *The HBOM method for unfolding detector effects*, *Nucl. Instrum. Meth. A* **701** (2013) 17, arXiv: [1111.4896 \[hep-ex\]](#).
- [43] CDF Collaboration, *Studying the underlying event in Drell-Yan and high transverse momentum jet production at the Tevatron*, *Phys. Rev. D* **82** (2010) 034001, arXiv: [1003.3146 \[hep-ex\]](#).
- [44] M. H. Seymour and A. Siomok, *Constraining MPI models using σ_{eff} and recent Tevatron and LHC Underlying Event data*, *JHEP* **10** (2013) 113, arXiv: [1307.5015 \[hep-ph\]](#).

- [45] ATLAS Collaboration, *ATLAS Computing Acknowledgements*, ATL-GEN-PUB-2016-002, URL: <https://cds.cern.ch/record/2202407>.

The ATLAS Collaboration

G. Aad¹⁰¹, B. Abbott¹²⁸, D.C. Abbott¹⁰², O. Abdinov^{13,*}, A. Abed Abud^{70a,70b}, K. Abeling⁵³, D.K. Abhayasinghe⁹³, S.H. Abidi¹⁶⁷, O.S. AbouZeid⁴⁰, N.L. Abraham¹⁵⁶, H. Abramowicz¹⁶¹, H. Abreu¹⁶⁰, Y. Abulaiti⁶, B.S. Acharya^{66a,66b,p}, B. Achkar⁵³, S. Adachi¹⁶³, L. Adam⁹⁹, C. Adam Bourdarios¹³², L. Adamczyk^{83a}, L. Adamek¹⁶⁷, J. Adelman¹²⁰, M. Adersberger¹¹³, A. Adiguzel^{12c,ak}, S. Adorni⁵⁴, T. Adye¹⁴⁴, A.A. Affolder¹⁴⁶, Y. Afik¹⁶⁰, C. Agapopoulou¹³², M.N. Agaras³⁸, A. Aggarwal¹¹⁸, C. Agheorghiesei^{27c}, J.A. Aguilar-Saavedra^{140f,140a,aj}, F. Ahmadov⁷⁹, W.S. Ahmed¹⁰³, X. Ai^{15a}, G. Aielli^{73a,73b}, S. Akatsuka⁸⁵, T.P.A. Åkesson⁹⁶, E. Akilli⁵⁴, A.V. Akimov¹¹⁰, K. Al Khoury¹³², G.L. Alberghi^{23b,23a}, J. Albert¹⁷⁶, M.J. Alconada Verzini¹⁶¹, S. Alderweireldt³⁶, M. Aleksa³⁶, I.N. Aleksandrov⁷⁹, C. Alexa^{27b}, D. Alexandre¹⁹, T. Alexopoulos¹⁰, A. Alfonsi¹¹⁹, M. Alhroob¹²⁸, B. Ali¹⁴², G. Alimonti^{68a}, J. Alison³⁷, S.P. Alkire¹⁴⁸, C. Allaire¹³², B.M.M. Allbrooke¹⁵⁶, B.W. Allen¹³¹, P.P. Allport²¹, A. Aloisio^{69a,69b}, A. Alonso⁴⁰, F. Alonso⁸⁸, C. Alpigiani¹⁴⁸, A.A. Alshehri⁵⁷, M. Alvarez Estevez⁹⁸, D. Álvarez Piqueras¹⁷⁴, M.G. Alviggi^{69a,69b}, Y. Amaral Coutinho^{80b}, A. Ambler¹⁰³, L. Ambroz¹³⁵, C. Amelung²⁶, D. Amidei¹⁰⁵, S.P. Amor Dos Santos^{140a}, S. Amoroso⁴⁶, C.S. Amrouche⁵⁴, F. An⁷⁸, C. Anastopoulos¹⁴⁹, N. Andari¹⁴⁵, T. Andeen¹¹, C.F. Anders^{61b}, J.K. Anders²⁰, A. Andreazza^{68a,68b}, V. Andrei^{61a}, C.R. Anelli¹⁷⁶, S. Angelidakis³⁸, A. Angerami³⁹, A.V. Anisenkov^{121b,121a}, A. Annovi^{71a}, C. Antel^{61a}, M.T. Anthony¹⁴⁹, M. Antonelli⁵¹, D.J.A. Antrim¹⁷¹, F. Anulli^{72a}, M. Aoki⁸¹, J.A. Aparisi Pozo¹⁷⁴, L. Aperio Bella³⁶, G. Arabidze¹⁰⁶, J.P. Araque^{140a}, V. Araujo Ferraz^{80b}, R. Araujo Pereira^{80b}, C. Arcangeletti⁵¹, A.T.H. Arce⁴⁹, F.A. Arduh⁸⁸, J-F. Arguin¹⁰⁹, S. Argyropoulos⁷⁷, J.-H. Arling⁴⁶, A.J. Armbruster³⁶, L.J. Armitage⁹², A. Armstrong¹⁷¹, O. Arnaez¹⁶⁷, H. Arnold¹¹⁹, A. Artamonov^{123,*}, G. Artoni¹³⁵, S. Artz⁹⁹, S. Asai¹⁶³, N. Asbah⁵⁹, E.M. Asimakopoulou¹⁷², L. Asquith¹⁵⁶, K. Assamagan²⁹, R. Astalos^{28a}, R.J. Atkin^{33a}, M. Atkinson¹⁷³, N.B. Atlay¹⁵¹, H. Atmani¹³², K. Augsten¹⁴², G. Avolio³⁶, R. Avramidou^{60a}, M.K. Ayoub^{15a}, A.M. Azoulay^{168b}, G. Azuelos^{109,az}, M.J. Baca²¹, H. Bachacou¹⁴⁵, K. Bachas^{67a,67b}, M. Backes¹³⁵, F. Backman^{45a,45b}, P. Bagnaia^{72a,72b}, M. Bahmani⁸⁴, H. Bahrasemani¹⁵², A.J. Bailey¹⁷⁴, V.R. Bailey¹⁷³, J.T. Baines¹⁴⁴, M. Bajic⁴⁰, C. Bakalis¹⁰, O.K. Baker¹⁸³, P.J. Bakker¹¹⁹, D. Bakshi Gupta⁸, S. Balaji¹⁵⁷, E.M. Baldin^{121b,121a}, P. Balek¹⁸⁰, F. Balli¹⁴⁵, W.K. Balunas¹³⁵, J. Balz⁹⁹, E. Banas⁸⁴, A. Bandyopadhyay²⁴, Sw. Banerjee^{181,j}, A.A.E. Bannoura¹⁸², L. Barak¹⁶¹, W.M. Barbe³⁸, E.L. Barberio¹⁰⁴, D. Barberis^{55b,55a}, M. Barbero¹⁰¹, T. Barillari¹¹⁴, M-S. Barisits³⁶, J. Barkeloo¹³¹, T. Barklow¹⁵³, R. Barnea¹⁶⁰, S.L. Barnes^{60c}, B.M. Barnett¹⁴⁴, R.M. Barnett¹⁸, Z. Barnovska-Blenessy^{60a}, A. Baroncelli^{60a}, G. Barone²⁹, A.J. Barr¹³⁵, L. Barranco Navarro¹⁷⁴, F. Barreiro⁹⁸, J. Barreiro Guimarães da Costa^{15a}, S. Barsov¹³⁸, R. Bartoldus¹⁵³, G. Bartolini¹⁰¹, A.E. Barton⁸⁹, P. Bartos^{28a}, A. Basalaev⁴⁶, A. Bassalat^{132,as}, R.L. Bates⁵⁷, S.J. Batista¹⁶⁷, S. Batlamous^{35e}, J.R. Batley³², B. Batool¹⁵¹, M. Battaglia¹⁴⁶, M. Bauce^{72a,72b}, F. Bauer¹⁴⁵, K.T. Bauer¹⁷¹, H.S. Bawa^{31,n}, J.B. Beacham⁴⁹, T. Beau¹³⁶, P.H. Beauchemin¹⁷⁰, F. Becherer⁵², P. Bechtle²⁴, H.C. Beck⁵³, H.P. Beck^{20,t}, K. Becker⁵², M. Becker⁹⁹, C. Becot⁴⁶, A. Beddall^{12d}, A.J. Beddall^{12a}, V.A. Bednyakov⁷⁹, M. Bedognetti¹¹⁹, C.P. Bee¹⁵⁵, T.A. Beermann⁷⁶, M. Begalli^{80b}, M. Begel²⁹, A. Behera¹⁵⁵, J.K. Behr⁴⁶, F. Beisiegel²⁴, A.S. Bell⁹⁴, G. Bella¹⁶¹, L. Bellagamba^{23b}, A. Bellerive³⁴, P. Bellos⁹, K. Beloborodov^{121b,121a}, K. Belotskiy¹¹¹, N.L. Belyaev¹¹¹, D. Benchekroun^{35a}, N. Benekos¹⁰, Y. Benhammou¹⁶¹, D.P. Benjamin⁶, M. Benoit⁵⁴, J.R. Bensinger²⁶, S. Bentvelsen¹¹⁹, L. Beresford¹³⁵, M. Beretta⁵¹, D. Berge⁴⁶, E. Bergeaas Kuutmann¹⁷², N. Berger⁵, B. Bergmann¹⁴², L.J. Bergsten²⁶, J. Beringer¹⁸, S. Berlendis⁷, N.R. Bernard¹⁰², G. Bernardi¹³⁶, C. Bernius¹⁵³, F.U. Bernlochner²⁴, T. Berry⁹³, P. Berta⁹⁹, C. Bertella^{15a}, I.A. Bertram⁸⁹, G.J. Besjes⁴⁰, O. Bessidskaia Bylund¹⁸², N. Besson¹⁴⁵, A. Bethani¹⁰⁰, S. Bethke¹¹⁴, A. Betti²⁴, A.J. Bevan⁹², J. Beyer¹¹⁴, R. Bi¹³⁹, R.M. Bianchi¹³⁹, O. Biebel¹¹³, D. Biedermann¹⁹, R. Bielski³⁶, K. Bierwagen⁹⁹, N.V. Biesuz^{71a,71b}, M. Biglietti^{74a}, T.R.V. Billoud¹⁰⁹, M. Bindi⁵³, A. Bingul^{12d}, C. Bini^{72a,72b}, S. Biondi^{23b,23a}, M. Birman¹⁸⁰, T. Bisanz⁵³,

J.P. Biswal¹⁶¹, A. Bitadze¹⁰⁰, C. Bittrich⁴⁸, K. Bjørke¹³⁴, K.M. Black²⁵, T. Blazek^{28a}, I. Bloch⁴⁶,
 C. Blocker²⁶, A. Blue⁵⁷, U. Blumenschein⁹², G.J. Bobbink¹¹⁹, V.S. Bobrovnikov^{121b,121a}, S.S. Bocchetta⁹⁶,
 A. Bocci⁴⁹, D. Boerner⁴⁶, D. Bogavac¹⁴, A.G. Bogdanchikov^{121b,121a}, C. Bohm^{45a}, V. Boisvert⁹³,
 P. Bokan^{53,172}, T. Bold^{83a}, A.S. Boldyrev¹¹², A.E. Bolz^{61b}, M. Bomben¹³⁶, M. Bona⁹², J.S. Bonilla¹³¹,
 M. Boonekamp¹⁴⁵, H.M. Borecka-Bielska⁹⁰, A. Borisov¹²², G. Borissov⁸⁹, J. Bortfeldt³⁶, D. Bortolotto¹³⁵,
 V. Bortolotto^{73a,73b}, D. Boscherini^{23b}, M. Bosman¹⁴, J.D. Bossio Sola¹⁰³, K. Bouaouda^{35a}, J. Boudreau¹³⁹,
 E.V. Bouhova-Thacker⁸⁹, D. Boumediene³⁸, S.K. Boutle⁵⁷, A. Boveia¹²⁶, J. Boyd³⁶, D. Boye^{33b,at},
 I.R. Boyko⁷⁹, A.J. Bozson⁹³, J. Bracinik²¹, N. Brahimi¹⁰¹, G. Brandt¹⁸², O. Brandt^{61a}, F. Braren⁴⁶,
 B. Brau¹⁰², J.E. Brau¹³¹, W.D. Breaden Madden⁵⁷, K. Brendlinger⁴⁶, L. Brenner⁴⁶, R. Brenner¹⁷²,
 S. Bressler¹⁸⁰, B. Brickwedde⁹⁹, D.L. Briglin²¹, D. Britton⁵⁷, D. Britzger¹¹⁴, I. Brock²⁴, R. Brock¹⁰⁶,
 G. Brooijmans³⁹, W.K. Brooks^{147c}, E. Brost¹²⁰, J.H. Broughton²¹, P.A. Bruckman de Renstrom⁸⁴,
 D. Bruncko^{28b}, A. Bruni^{23b}, G. Bruni^{23b}, L.S. Bruni¹¹⁹, S. Bruno^{73a,73b}, B.H. Brunt³², M. Bruschi^{23b},
 N. Bruscino¹³⁹, P. Bryant³⁷, L. Bryngemark⁹⁶, T. Buanes¹⁷, Q. Buat³⁶, P. Buchholz¹⁵¹, A.G. Buckley⁵⁷,
 I.A. Budagov⁷⁹, M.K. Bugge¹³⁴, F. Bührer⁵², O. Bulekov¹¹¹, T.J. Burch¹²⁰, S. Burdin⁹⁰, C.D. Burgard¹¹⁹,
 A.M. Burger¹²⁹, B. Burghgrave⁸, J.T.P. Bur⁴⁶, J.C. Burzynski¹⁰², V. Büscher⁹⁹, E. Buschmann⁵³,
 P.J. Bussey⁵⁷, J.M. Butler²⁵, C.M. Buttar⁵⁷, J.M. Butterworth⁹⁴, P. Butti³⁶, W. Buttinger³⁶, A. Buzatu¹⁵⁸,
 A.R. Buzykaev^{121b,121a}, G. Cabras^{23b,23a}, S. Cabrera Urbán¹⁷⁴, D. Caforio⁵⁶, H. Cai¹⁷³, V.M.M. Cairo¹⁵³,
 O. Cakir^{4a}, N. Calace³⁶, P. Calafiura¹⁸, A. Calandri¹⁰¹, G. Calderini¹³⁶, P. Calfayan⁶⁵, G. Callea⁵⁷,
 L.P. Caloba^{80b}, S. Calvente Lopez⁹⁸, D. Calvet³⁸, S. Calvet³⁸, T.P. Calvet¹⁵⁵, M. Calvetti^{71a,71b},
 R. Camacho Toro¹³⁶, S. Camarda³⁶, D. Camarero Munoz⁹⁸, P. Camarri^{73a,73b}, D. Cameron¹³⁴,
 R. Caminal Armadans¹⁰², C. Camincher³⁶, S. Campana³⁶, M. Campanelli⁹⁴, A. Camplani⁴⁰,
 A. Campoverde¹⁵¹, V. Canale^{69a,69b}, A. Canesse¹⁰³, M. Cano Bret^{60c}, J. Cantero¹²⁹, T. Cao¹⁶¹, Y. Cao¹⁷³,
 M.D.M. Capeans Garrido³⁶, M. Capua^{41b,41a}, R. Cardarelli^{73a}, F. Cardillo¹⁴⁹, I. Carli¹⁴³, T. Carli³⁶,
 G. Carlino^{69a}, B.T. Carlson¹³⁹, L. Carminati^{68a,68b}, R.M.D. Carney^{45a,45b}, S. Caron¹¹⁸, E. Carquin^{147c},
 S. Carrá⁴⁶, J.W.S. Carter¹⁶⁷, M.P. Casado^{14,f}, A.F. Casha¹⁶⁷, D.W. Casper¹⁷¹, R. Castelijn¹¹⁹,
 F.L. Castillo¹⁷⁴, V. Castillo Gimenez¹⁷⁴, N.F. Castro^{140a,140e}, A. Catinaccio³⁶, J.R. Catmore¹³⁴, A. Cattai³⁶,
 J. Caudron²⁴, V. Cavalieri²⁹, E. Cavallaro¹⁴, D. Cavalli^{68a}, M. Cavalli-Sforza¹⁴, V. Cavasinni^{71a,71b},
 E. Celebi^{12b}, F. Ceradini^{74a,74b}, L. Cerdà Alberich¹⁷⁴, K. Cerny¹³⁰, A.S. Cerqueira^{80a}, A. Cerri¹⁵⁶,
 L. Cerrito^{73a,73b}, F. Cerutti¹⁸, A. Cervelli^{23b,23a}, S.A. Cetin^{12b}, D. Chakraborty¹²⁰, S.K. Chan⁵⁹,
 W.S. Chan¹¹⁹, W.Y. Chan⁹⁰, J.D. Chapman³², B. Chargeishvili^{159b}, D.G. Charlton²¹, T.P. Charman⁹²,
 C.C. Chau³⁴, S. Che¹²⁶, A. Chegwidden¹⁰⁶, S. Chekanov⁶, S.V. Chekulaev^{168a}, G.A. Chelkov^{79,ay},
 M.A. Chelstowska³⁶, B. Chen⁷⁸, C. Chen^{60a}, C.H. Chen⁷⁸, H. Chen²⁹, J. Chen^{60a}, J. Chen³⁹, S. Chen¹³⁷,
 S.J. Chen^{15c}, X. Chen^{15b,ax}, Y. Chen⁸², Y-H. Chen⁴⁶, H.C. Cheng^{63a}, H.J. Cheng^{15a,15d}, A. Cheplakov⁷⁹,
 E. Cheremushkina¹²², R. Cherkaoui El Moursli^{35e}, E. Cheu⁷, K. Cheung⁶⁴, T.J.A. Chevaléries¹⁴⁵,
 L. Chevalier¹⁴⁵, V. Chiarella⁵¹, G. Chiarelli^{71a}, G. Chiodini^{67a}, A.S. Chisholm^{36,21}, A. Chitan^{27b},
 I. Chiu¹⁶³, Y.H. Chiu¹⁷⁶, M.V. Chizhov⁷⁹, K. Choi⁶⁵, A.R. Chomont^{72a,72b}, S. Chouridou¹⁶²,
 Y.S. Chow¹¹⁹, M.C. Chu^{63a}, J. Chudoba¹⁴¹, A.J. Chuinard¹⁰³, J.J. Chwastowski⁸⁴, L. Chytka¹³⁰,
 K.M. Ciesla⁸⁴, D. Cinca⁴⁷, V. Cindro⁹¹, I.A. Cioara^{27b}, A. Ciocio¹⁸, F. Cirotto^{69a,69b}, Z.H. Citron^{180,l},
 M. Citterio^{68a}, D.A. Ciubotaru^{27b}, B.M. Ciungu¹⁶⁷, A. Clark⁵⁴, M.R. Clark³⁹, P.J. Clark⁵⁰,
 C. Clement^{45a,45b}, Y. Coadou¹⁰¹, M. Cobal^{66a,66c}, A. Coccaro^{55b}, J. Cochran⁷⁸, H. Cohen¹⁶¹,
 A.E.C. Coimbra³⁶, L. Colasurdo¹¹⁸, B. Cole³⁹, A.P. Colijn¹¹⁹, J. Collot⁵⁸, P. Conde Muñoz^{140a,g},
 E. Coniavitis⁵², S.H. Connell^{33b}, I.A. Connelly⁵⁷, S. Constantinescu^{27b}, F. Conventi^{69a,ba},
 A.M. Cooper-Sarkar¹³⁵, F. Cormier¹⁷⁵, K.J.R. Cormier¹⁶⁷, L.D. Corpe⁹⁴, M. Corradi^{72a,72b},
 E.E. Corrigan⁹⁶, F. Corriveau^{103,af}, A. Cortes-Gonzalez³⁶, M.J. Costa¹⁷⁴, F. Costanza⁵, D. Costanzo¹⁴⁹,
 G. Cowan⁹³, J.W. Cowley³², J. Crane¹⁰⁰, K. Cranmer¹²⁴, S.J. Crawley⁵⁷, R.A. Creager¹³⁷,
 S. Crépé-Renaudin⁵⁸, F. Crescioli¹³⁶, M. Cristinziani²⁴, V. Croft¹¹⁹, G. Crosetti^{41b,41a}, A. Cueto⁵,
 T. Cuhadar Donszelmann¹⁴⁹, A.R. Cukierman¹⁵³, S. Czekierda⁸⁴, P. Czodrowski³⁶,

M.J. Da Cunha Sargedas De Sousa^{60b}, J.V. Da Fonseca Pinto^{80b}, C. Da Via¹⁰⁰, W. Dabrowski^{83a},
 T. Dado^{28a}, S. Dahbi^{35e}, T. Dai¹⁰⁵, C. Dallapiccola¹⁰², M. Dam⁴⁰, G. D'amen^{23b,23a}, V. D'Amico^{74a,74b},
 J. Damp⁹⁹, J.R. Dandoy¹³⁷, M.F. Daneri³⁰, N.P. Dang^{181,j}, N.S. Dann¹⁰⁰, M. Danninger¹⁷⁵, V. Dao³⁶,
 G. Darbo^{55b}, O. Dartsi⁵, A. Dattagupta¹³¹, T. Daubney⁴⁶, S. D'Auria^{68a,68b}, W. Davey²⁴, C. David⁴⁶,
 T. Davidek¹⁴³, D.R. Davis⁴⁹, I. Dawson¹⁴⁹, K. De⁸, R. De Asmundis^{69a}, M. De Beurs¹¹⁹,
 S. De Castro^{23b,23a}, S. De Cecco^{72a,72b}, N. De Groot¹¹⁸, P. de Jong¹¹⁹, H. De la Torre¹⁰⁶, A. De Maria^{15c},
 D. De Pedis^{72a}, A. De Salvo^{72a}, U. De Sanctis^{73a,73b}, M. De Santis^{73a,73b}, A. De Santo¹⁵⁶,
 K. De Vasconcelos Corga¹⁰¹, J.B. De Vivie De Regie¹³², C. Debenedetti¹⁴⁶, D.V. Dedovich⁷⁹,
 A.M. Deiana⁴², M. Del Gaudio^{41b,41a}, J. Del Peso⁹⁸, Y. Delabat Diaz⁴⁶, D. Delgove¹³², F. Deliot^{145,s},
 C.M. Delitzsch⁷, M. Della Pietra^{69a,69b}, D. Della Volpe⁵⁴, A. Dell'Acqua³⁶, L. Dell'Asta^{73a,73b},
 M. Delmastro⁵, C. Delporte¹³², P.A. Delsart⁵⁸, D.A. DeMarco¹⁶⁷, S. Demers¹⁸³, M. Demichev⁷⁹,
 G. Demontigny¹⁰⁹, S.P. Denisov¹²², D. Denysiuk¹¹⁹, L. D'Eramo¹³⁶, D. Derendarz⁸⁴, J.E. Derkaoui^{35d},
 F. Derue¹³⁶, P. Dervan⁹⁰, K. Desch²⁴, C. Deterre⁴⁶, K. Dette¹⁶⁷, C. Deutsch²⁴, M.R. Devesa³⁰,
 P.O. Deviveiros³⁶, A. Dewhurst¹⁴⁴, S. Dhaliwal²⁶, F.A. Di Bello⁵⁴, A. Di Ciaccio^{73a,73b}, L. Di Ciaccio⁵,
 W.K. Di Clemente¹³⁷, C. Di Donato^{69a,69b}, A. Di Girolamo³⁶, G. Di Gregorio^{71a,71b}, B. Di Micco^{74a,74b},
 R. Di Nardo¹⁰², K.F. Di Petrillo⁵⁹, R. Di Sipio¹⁶⁷, D. Di Valentino³⁴, C. Diaconu¹⁰¹, F.A. Dias⁴⁰,
 T. Dias Do Vale^{140a}, M.A. Diaz^{147a}, J. Dickinson¹⁸, E.B. Diehl¹⁰⁵, J. Dietrich¹⁹, S. Díez Cornell⁴⁶,
 A. Dimitrievska¹⁸, W. Ding^{15b}, J. Dingfelder²⁴, F. Dittus³⁶, F. Djama¹⁰¹, T. Djobava^{159b}, J.I. Djuvsland¹⁷,
 M.A.B. Do Vale^{80c}, M. Dobre^{27b}, D. Dodsworth²⁶, C. Doglioni⁹⁶, J. Dolejsi¹⁴³, Z. Dolezal¹⁴³,
 M. Donadelli^{80d}, J. Donini³⁸, A. D'onofrio⁹², M. D'Onofrio⁹⁰, J. Dopke¹⁴⁴, A. Doria^{69a}, M.T. Dova⁸⁸,
 A.T. Doyle⁵⁷, E. Drechsler¹⁵², E. Dreyer¹⁵², T. Dreyer⁵³, A.S. Drobac¹⁷⁰, Y. Duan^{60b}, F. Dubinin¹¹⁰,
 M. Dubovsky^{28a}, A. Dubreuil⁵⁴, E. Duchovni¹⁸⁰, G. Duckeck¹¹³, A. Ducourthial¹³⁶, O.A. Ducu¹⁰⁹,
 D. Duda¹¹⁴, A. Dudarev³⁶, A.C. Dudder⁹⁹, E.M. Duffield¹⁸, L. Duflot¹³², M. Dührssen³⁶, C. Dülsen¹⁸²,
 M. Dumancic¹⁸⁰, A.E. Dumitriu^{27b}, A.K. Duncan⁵⁷, M. Dunford^{61a}, A. Duperrin¹⁰¹, H. Duran Yildiz^{4a},
 M. Düren⁵⁶, A. Durglishvili^{159b}, D. Duschinger⁴⁸, B. Dutta⁴⁶, D. Duvnjak¹, G.I. Dyckes¹³⁷, M. Dyndal³⁶,
 S. Dysch¹⁰⁰, B.S. Dziedzic⁸⁴, K.M. Ecker¹¹⁴, R.C. Edgar¹⁰⁵, T. Eifert³⁶, G. Eigen¹⁷, K. Einsweiler¹⁸,
 T. Ekelof¹⁷², M. El Kacimi^{35c}, R. El Kosseifi¹⁰¹, V. Ellajosyula¹⁷², M. Ellert¹⁷², F. Ellinghaus¹⁸²,
 A.A. Elliot⁹², N. Ellis³⁶, J. Elmsheuser²⁹, M. Elsing³⁶, D. Emeliyanov¹⁴⁴, A. Emerman³⁹, Y. Enari¹⁶³,
 J.S. Ennis¹⁷⁸, M.B. Epland⁴⁹, J. Erdmann⁴⁷, A. Ereditato²⁰, M. Errenst³⁶, M. Escalier¹³², C. Escobar¹⁷⁴,
 O. Estrada Pastor¹⁷⁴, E. Etzion¹⁶¹, H. Evans⁶⁵, A. Ezhilov¹³⁸, F. Fabbri⁵⁷, L. Fabbri^{23b,23a}, V. Fabiani¹¹⁸,
 G. Facini⁹⁴, R.M. Faisca Rodrigues Pereira^{140a}, R.M. Fakhrutdinov¹²², S. Falciano^{72a}, P.J. Falke⁵,
 S. Falke⁵, J. Faltova¹⁴³, Y. Fang^{15a}, Y. Fang^{15a}, G. Fanourakis⁴⁴, M. Fanti^{68a,68b}, A. Farbin⁸, A. Farilla^{74a},
 E.M. Farina^{70a,70b}, T. Farooque¹⁰⁶, S. Farrell¹⁸, S.M. Farrington¹⁷⁸, P. Farthouat³⁶, F. Fassi^{35e},
 P. Fassnacht³⁶, D. Fassouliotis⁹, M. Facci Giannelli⁵⁰, W.J. Fawcett³², L. Fayard¹³², O.L. Fedin^{138,q},
 W. Fedorko¹⁷⁵, M. Feickert⁴², S. Feigl¹³⁴, L. Feligioni¹⁰¹, A. Fell¹⁴⁹, C. Feng^{60b}, E.J. Feng³⁶, M. Feng⁴⁹,
 M.J. Fenton⁵⁷, A.B. Fenyuk¹²², J. Ferrando⁴⁶, A. Ferrante¹⁷³, A. Ferrari¹⁷², P. Ferrari¹¹⁹, R. Ferrari^{70a},
 D.E. Ferreira de Lima^{61b}, A. Ferrer¹⁷⁴, D. Ferrere⁵⁴, C. Ferretti¹⁰⁵, F. Fiedler⁹⁹, A. Filipčič⁹¹,
 F. Filthaut¹¹⁸, K.D. Finelli²⁵, M.C.N. Fiolhais^{140a,140c,a}, L. Fiorini¹⁷⁴, F. Fischer¹¹³, W.C. Fisher¹⁰⁶,
 I. Fleck¹⁵¹, P. Fleischmann¹⁰⁵, R.R.M. Fletcher¹³⁷, T. Flick¹⁸², B.M. Flierl¹¹³, L. Flores¹³⁷,
 L.R. Flores Castillo^{63a}, F.M. Follega^{75a,75b}, N. Fomin¹⁷, J.H. Foo¹⁶⁷, G.T. Forcolin^{75a,75b}, A. Formica¹⁴⁵,
 F.A. Förster¹⁴, A.C. Forti¹⁰⁰, A.G. Foster²¹, M.G. Foti¹³⁵, D. Fournier¹³², H. Fox⁸⁹, P. Francavilla^{71a,71b},
 S. Francescato^{72a,72b}, M. Franchini^{23b,23a}, S. Franchino^{61a}, D. Francis³⁶, L. Franconi²⁰, M. Franklin⁵⁹,
 A.N. Fray⁹², B. Freund¹⁰⁹, W.S. Freund^{80b}, E.M. Freundlich⁴⁷, D.C. Frizzell¹²⁸, D. Froidevaux³⁶,
 J.A. Frost¹³⁵, C. Fukunaga¹⁶⁴, E. Fullana Torregrosa¹⁷⁴, E. Fumagalli^{55b,55a}, T. Fusayasu¹¹⁵, J. Fuster¹⁷⁴,
 A. Gabrielli^{23b,23a}, A. Gabrielli¹⁸, G.P. Gach^{83a}, S. Gadatsch⁵⁴, P. Gadow¹¹⁴, G. Gagliardi^{55b,55a},
 L.G. Gagnon¹⁰⁹, C. Galea^{27b}, B. Galhardo^{140a}, G.E. Gallardo¹³⁵, E.J. Gallas¹³⁵, B.J. Gallop¹⁴⁴,
 P. Gallus¹⁴², G. Galster⁴⁰, R. Gamboa Goni⁹², K.K. Gan¹²⁶, S. Ganguly¹⁸⁰, J. Gao^{60a}, Y. Gao⁹⁰,

Y.S. Gao^{31,n}, C. García¹⁷⁴, J.E. García Navarro¹⁷⁴, J.A. García Pascual^{15a}, C. Garcia-Argos⁵², M. Garcia-Sciveres¹⁸, R.W. Gardner³⁷, N. Garelli¹⁵³, S. Gargiulo⁵², V. Garonne¹³⁴, A. Gaudiello^{55b,55a}, G. Gaudio^{70a}, I.L. Gavrilenco¹¹⁰, A. Gavrilyuk¹²³, C. Gay¹⁷⁵, G. Gaycken²⁴, E.N. Gazis¹⁰, A.A. Geanta^{27b}, C.N.P. Gee¹⁴⁴, J. Geisen⁵³, M. Geisen⁹⁹, M.P. Geisler^{61a}, C. Gemme^{55b}, M.H. Genest⁵⁸, C. Geng¹⁰⁵, S. Gentile^{72a,72b}, S. George⁹³, T. Geralis⁴⁴, L.O. Gerlach⁵³, P. Gessinger-Befurt⁹⁹, G. Gessner⁴⁷, S. Ghasemi¹⁵¹, M. Ghasemi Bostanabad¹⁷⁶, A. Ghosh⁷⁷, B. Giacobbe^{23b}, S. Giagu^{72a,72b}, N. Giangiacomi^{23b,23a}, P. Giannetti^{71a}, A. Giannini^{69a,69b}, S.M. Gibson⁹³, M. Gignac¹⁴⁶, D. Gillberg³⁴, G. Gilles¹⁸², D.M. Gingrich^{3,az}, M.P. Giordani^{66a,66c}, F.M. Giorgi^{23b}, P.F. Giraud¹⁴⁵, G. Giugliarelli^{66a,66c}, D. Giugni^{68a}, F. Giuli^{73a,73b}, S. Gkaitatzis¹⁶², I. Gkialas^{9,i}, E.L. Gkougkousis¹⁴, P. Gkountoumis¹⁰, L.K. Gladilin¹¹², C. Glasman⁹⁸, J. Glatzer¹⁴, P.C.F. Glaysher⁴⁶, A. Glazov⁴⁶, M. Goblirsch-Kolb²⁶, S. Goldfarb¹⁰⁴, T. Golling⁵⁴, D. Golubkov¹²², A. Gomes^{140a,140b}, R. Goncalves Gama⁵³, R. Gonçalo^{140a,140b}, G. Gonella⁵², L. Gonella²¹, A. Gongadze⁷⁹, F. Gonnella²¹, J.L. Gonski⁵⁹, S. González de la Hoz¹⁷⁴, S. Gonzalez-Sevilla⁵⁴, G.R. Gonzalvo Rodriguez¹⁷⁴, L. Goossens³⁶, P.A. Gorbounov¹²³, H.A. Gordon²⁹, B. Gorini³⁶, E. Gorini^{67a,67b}, A. Gorišek⁹¹, A.T. Goshaw⁴⁹, M.I. Gostkin⁷⁹, C.A. Gottardo²⁴, M. Gouighri^{35b}, D. Goujdami^{35c}, A.G. Goussiou¹⁴⁸, N. Govender^{33b,b}, C. Goy⁵, E. Gozani¹⁶⁰, I. Grabowska-Bold^{83a}, E.C. Graham⁹⁰, J. Gramling¹⁷¹, E. Gramstad¹³⁴, S. Grancagnolo¹⁹, M. Grandi¹⁵⁶, V. Gratchev¹³⁸, P.M. Gravila^{27f}, F.G. Gravili^{67a,67b}, C. Gray⁵⁷, H.M. Gray¹⁸, C. Grefe²⁴, K. Gregersen⁹⁶, I.M. Gregor⁴⁶, P. Grenier¹⁵³, K. Grevtsov⁴⁶, N.A. Grieser¹²⁸, J. Griffiths⁸, A.A. Grillo¹⁴⁶, K. Grimm^{31,m}, S. Grinstein^{14,z}, J.-F. Grivaz¹³², S. Groh⁹⁹, E. Gross¹⁸⁰, J. Grosse-Knetter⁵³, Z.J. Grout⁹⁴, C. Grud¹⁰⁵, A. Grummer¹¹⁷, L. Guan¹⁰⁵, W. Guan¹⁸¹, J. Guenther³⁶, A. Guerguichon¹³², F. Guescini¹¹⁴, D. Guest¹⁷¹, R. Gugel⁵², B. Gui¹²⁶, T. Guillemin⁵, S. Guindon³⁶, U. Gul⁵⁷, J. Guo^{60c}, W. Guo¹⁰⁵, Y. Guo^{60a,u}, Z. Guo¹⁰¹, R. Gupta⁴⁶, S. Gurbuz^{12c}, G. Gustavino¹²⁸, P. Gutierrez¹²⁸, C. Gutschow⁹⁴, C. Guyot¹⁴⁵, M.P. Guzik^{83a}, C. Gwenlan¹³⁵, C.B. Gwilliam⁹⁰, A. Haas¹²⁴, C. Haber¹⁸, H.K. Hadavand⁸, N. Haddad^{35e}, A. Hadef^{60a}, S. Hageböck³⁶, M. Hagihara¹⁶⁹, M. Haleem¹⁷⁷, J. Haley¹²⁹, G. Halladjian¹⁰⁶, G.D. Hallewell¹⁰¹, K. Hamacher¹⁸², P. Hamal¹³⁰, K. Hamano¹⁷⁶, H. Hamdaoui^{35e}, G.N. Hamity¹⁴⁹, K. Han^{60a,am}, L. Han^{60a}, S. Han^{15a,15d}, K. Hanagaki^{81,x}, M. Hance¹⁴⁶, D.M. Handl¹¹³, B. Haney¹³⁷, R. Hankache¹³⁶, E. Hansen⁹⁶, J.B. Hansen⁴⁰, J.D. Hansen⁴⁰, M.C. Hansen²⁴, P.H. Hansen⁴⁰, E.C. Hanson¹⁰⁰, K. Hara¹⁶⁹, A.S. Hard¹⁸¹, T. Harenberg¹⁸², S. Harkusha¹⁰⁷, P.F. Harrison¹⁷⁸, N.M. Hartmann¹¹³, Y. Hasegawa¹⁵⁰, A. Hasib⁵⁰, S. Hassani¹⁴⁵, S. Haug²⁰, R. Hauser¹⁰⁶, L.B. Havener³⁹, M. Havranek¹⁴², C.M. Hawkes²¹, R.J. Hawkings³⁶, D. Hayden¹⁰⁶, C. Hayes¹⁵⁵, R.L. Hayes¹⁷⁵, C.P. Hays¹³⁵, J.M. Hays⁹², H.S. Hayward⁹⁰, S.J. Haywood¹⁴⁴, F. He^{60a}, M.P. Heath⁵⁰, V. Hedberg⁹⁶, L. Heelan⁸, S. Heer²⁴, K.K. Heidegger⁵², W.D. Heidorn⁷⁸, J. Heilman³⁴, S. Heim⁴⁶, T. Heim¹⁸, B. Heinemann^{46,au}, J.J. Heinrich¹³¹, L. Heinrich³⁶, C. Heinz⁵⁶, J. Hejbal¹⁴¹, L. Helary^{61b}, A. Held¹⁷⁵, S. Hellesund¹³⁴, C.M. Helling¹⁴⁶, S. Hellman^{45a,45b}, C. Helsens³⁶, R.C.W. Henderson⁸⁹, Y. Heng¹⁸¹, S. Henkelmann¹⁷⁵, A.M. Henriques Correia³⁶, G.H. Herbert¹⁹, H. Herde²⁶, V. Herget¹⁷⁷, Y. Hernández Jiménez^{33c}, H. Herr⁹⁹, M.G. Herrmann¹¹³, T. Herrmann⁴⁸, G. Herten⁵², R. Hertenberger¹¹³, L. Hervas³⁶, T.C. Herwig¹³⁷, G.G. Hesketh⁹⁴, N.P. Hessey^{168a}, A. Higashida¹⁶³, S. Higashino⁸¹, E. Higón-Rodríguez¹⁷⁴, K. Hildebrand³⁷, E. Hill¹⁷⁶, J.C. Hill³², K.K. Hill²⁹, K.H. Hiller⁴⁶, S.J. Hillier²¹, M. Hils⁴⁸, I. Hinchliffe¹⁸, F. Hinterkeuser²⁴, M. Hirose¹³³, S. Hirose⁵², D. Hirschbuehl¹⁸², B. Hiti⁹¹, O. Hladík¹⁴¹, D.R. Hlálučka^{33c}, X. Hoad⁵⁰, J. Hobbs¹⁵⁵, N. Hod¹⁸⁰, M.C. Hodgkinson¹⁴⁹, A. Hoecker³⁶, F. Hoenig¹¹³, D. Hohn⁵², D. Hohov¹³², T.R. Holmes³⁷, M. Holzbock¹¹³, L.B.A.H Hommels³², S. Honda¹⁶⁹, T. Honda⁸¹, T.M. Hong¹³⁹, A. Hönlé¹¹⁴, B.H. Hooberman¹⁷³, W.H. Hopkins⁶, Y. Horii¹¹⁶, P. Horn⁴⁸, L.A. Horyn³⁷, J.-Y. Hostachy⁵⁸, A. Hostiuc¹⁴⁸, S. Hou¹⁵⁸, A. Hoummada^{35a}, J. Howarth¹⁰⁰, J. Hoya⁸⁸, M. Hrabovsky¹³⁰, J. Hrdinka⁷⁶, I. Hristova¹⁹, J. Hrivnac¹³², A. Hrynevich¹⁰⁸, T. Hrynevich⁵, P.J. Hsu⁶⁴, S.-C. Hsu¹⁴⁸, Q. Hu²⁹, S. Hu^{60c}, Y. Huang^{15a}, Z. Hubacek¹⁴², F. Hubaut¹⁰¹, M. Huebner²⁴, F. Huegging²⁴, T.B. Huffman¹³⁵, M. Huhtinen³⁶, R.F.H. Hunter³⁴, P. Huo¹⁵⁵, A.M. Hupe³⁴, N. Huseynov^{79,ah}, J. Huston¹⁰⁶, J. Huth⁵⁹, R. Hyneman¹⁰⁵, S. Hyrych^{28a}, G. Iacobucci⁵⁴, G. Iakovidis²⁹,

I. Ibragimov¹⁵¹, L. Iconomidou-Fayard¹³², Z. Idrissi^{35e}, P. Iengo³⁶, R. Ignazzi⁴⁰, O. Igonkina^{119,ab,*},
 R. Iguchi¹⁶³, T. Iizawa⁵⁴, Y. Ikegami⁸¹, M. Ikeno⁸¹, D. Iliadis¹⁶², N. Illic¹¹⁸, F. Iltzsche⁴⁸, G. Introzzi^{70a,70b},
 M. Iodice^{74a}, K. Iordanidou^{168a}, V. Ippolito^{72a,72b}, M.F. Isacson¹⁷², M. Ishino¹⁶³, M. Ishitsuka¹⁶⁵,
 W. Islam¹²⁹, C. Issever¹³⁵, S. Istin¹⁶⁰, F. Ito¹⁶⁹, J.M. Iturbe Ponce^{63a}, R. Iuppa^{75a,75b}, A. Ivina¹⁸⁰,
 H. Iwasaki⁸¹, J.M. Izen⁴³, V. Izzo^{69a}, P. Jacka¹⁴¹, P. Jackson¹, R.M. Jacobs²⁴, B.P. Jaeger¹⁵², V. Jain²,
 G. Jäkel¹⁸², K.B. Jakobi⁹⁹, K. Jakobs⁵², S. Jakobsen⁷⁶, T. Jakoubek¹⁴¹, J. Jamieson⁵⁷, K.W. Janas^{83a},
 R. Jansky⁵⁴, J. Janssen²⁴, M. Janus⁵³, P.A. Janus^{83a}, G. Jarlskog⁹⁶, N. Javadov^{79,ah}, T. Javůrek³⁶,
 M. Javurkova⁵², F. Jeanneau¹⁴⁵, L. Jeanty¹³¹, J. Jejelava^{159a,ai}, A. Jelinskas¹⁷⁸, P. Jenni^{52,c}, J. Jeong⁴⁶,
 N. Jeong⁴⁶, S. Jézéquel⁵, H. Ji¹⁸¹, J. Jia¹⁵⁵, H. Jiang⁷⁸, Y. Jiang^{60a}, Z. Jiang^{153,r}, S. Jiggins⁵²,
 F.A. Jimenez Morales³⁸, J. Jimenez Pena¹⁷⁴, S. Jin^{15c}, A. Jinaru^{27b}, O. Jinnouchi¹⁶⁵, H. Jivan^{33c},
 P. Johansson¹⁴⁹, K.A. Johns⁷, C.A. Johnson⁶⁵, K. Jon-And^{45a,45b}, R.W.L. Jones⁸⁹, S.D. Jones¹⁵⁶, S. Jones⁷,
 T.J. Jones⁹⁰, J. Jongmanns^{61a}, P.M. Jorge^{140a}, J. Jovicevic³⁶, X. Ju¹⁸, J.J. Junggeburth¹¹⁴,
 A. Juste Rozas^{14,z}, A. Kaczmarska⁸⁴, M. Kado^{72a,72b}, H. Kagan¹²⁶, M. Kagan¹⁵³, C. Kahra⁹⁹, T. Kaji¹⁷⁹,
 E. Kajomovitz¹⁶⁰, C.W. Kalderon⁹⁶, A. Kaluza⁹⁹, A. Kamenshchikov¹²², L. Kanjir⁹¹, Y. Kano¹⁶³,
 V.A. Kantserov¹¹¹, J. Kanzaki⁸¹, L.S. Kaplan¹⁸¹, D. Kar^{33c}, M.J. Kareem^{168b}, E. Karentzos¹⁰,
 S.N. Karpov⁷⁹, Z.M. Karpova⁷⁹, V. Kartvelishvili⁸⁹, A.N. Karyukhin¹²², L. Kashif¹⁸¹, R.D. Kass¹²⁶,
 A. Kastanas^{45a,45b}, Y. Kataoka¹⁶³, C. Kato^{60d,60c}, J. Katzy⁴⁶, K. Kawade⁸², K. Kawagoe⁸⁷,
 T. Kawaguchi¹¹⁶, T. Kawamoto¹⁶³, G. Kawamura⁵³, E.F. Kay¹⁷⁶, V.F. Kazanin^{121b,121a}, R. Keeler¹⁷⁶,
 R. Kehoe⁴², J.S. Keller³⁴, E. Kellermann⁹⁶, D. Kelsey¹⁵⁶, J.J. Kempster²¹, J. Kendrick²¹, O. Kepka¹⁴¹,
 S. Kersten¹⁸², B.P. Kerševan⁹¹, S. Ketabchi Haghighat¹⁶⁷, M. Khader¹⁷³, F. Khalil-Zada¹³,
 M. Khandoga¹⁴⁵, A. Khanov¹²⁹, A.G. Kharlamov^{121b,121a}, T. Kharlamova^{121b,121a}, E.E. Khoda¹⁷⁵,
 A. Khodinov¹⁶⁶, T.J. Khoo⁵⁴, E. Khramov⁷⁹, J. Khubua^{159b}, S. Kido⁸², M. Kiehn⁵⁴, C.R. Kilby⁹³,
 Y.K. Kim³⁷, N. Kimura^{66a,66c}, O.M. Kind¹⁹, B.T. King^{90,*}, D. Kirchmeier⁴⁸, J. Kirk¹⁴⁴, A.E. Kiryunin¹¹⁴,
 T. Kishimoto¹⁶³, D.P. Kisliuk¹⁶⁷, V. Kitali⁴⁶, O. Kivernyk⁵, E. Kladiva^{28b,*}, T. Klapdor-Kleingrothaus⁵²,
 M. Klassen^{61a}, M.H. Klein¹⁰⁵, M. Klein⁹⁰, U. Klein⁹⁰, K. Kleinknecht⁹⁹, P. Klimek¹²⁰, A. Klimentov²⁹,
 T. Klingl²⁴, T. Klioutchnikova³⁶, F.F. Klitzner¹¹³, P. Kluit¹¹⁹, S. Kluth¹¹⁴, E. Kneringer⁷⁶,
 E.B.F.G. Knoops¹⁰¹, A. Knue⁵², D. Kobayashi¹⁶³, M. Kobel⁴⁸, M. Kocian¹⁵³, P. Kodys¹⁴³,
 P.T. Koenig²⁴, T. Koffas³⁴, N.M. Köhler¹¹⁴, T. Koi¹⁵³, M. Kolb^{61b}, I. Koletsou⁵, T. Komarek¹³⁰,
 T. Kondo⁸¹, N. Kondrashova^{60c}, K. Köneke⁵², A.C. König¹¹⁸, T. Kono¹²⁵, R. Konoplich^{124,ap},
 V. Konstantinides⁹⁴, N. Konstantinidis⁹⁴, B. Konya⁹⁶, R. Kopeliansky⁶⁵, S. Koperny^{83a}, K. Korcyl⁸⁴,
 K. Kordas¹⁶², G. Koren¹⁶¹, A. Korn⁹⁴, I. Korolkov¹⁴, E.V. Korolkova¹⁴⁹, N. Korotkova¹¹², O. Kortner¹¹⁴,
 S. Kortner¹¹⁴, T. Kosek¹⁴³, V.V. Kostyukhin²⁴, A. Kotwal⁴⁹, A. Koumouris¹⁰,
 A. Kourkoumeli-Charalampidi^{70a,70b}, C. Kourkoumelis⁹, E. Kourlitis¹⁴⁹, V. Kouskoura²⁹,
 A.B. Kowalewska⁸⁴, R. Kowalewski¹⁷⁶, C. Kozakai¹⁶³, W. Kozanecki¹⁴⁵, A.S. Kozhin¹²²,
 V.A. Kramarenko¹¹², G. Kramberger⁹¹, D. Krasnopenvtsev^{60a}, M.W. Krasny¹³⁶, A. Krasznahorkay³⁶,
 D. Krauss¹¹⁴, J.A. Kremer^{83a}, J. Kretzschmar⁹⁰, P. Krieger¹⁶⁷, F. Krieter¹¹³, A. Krishnan^{61b}, K. Krizka¹⁸,
 K. Kroeninger⁴⁷, H. Kroha¹¹⁴, J. Kroll¹⁴¹, J. Kroll¹³⁷, J. Krstic¹⁶, U. Kruchonak⁷⁹, H. Krüger²⁴,
 N. Krumnack⁷⁸, M.C. Kruse⁴⁹, J.A. Krzysiak⁸⁴, T. Kubota¹⁰⁴, S. Kuday^{4b}, J.T. Kuechler⁴⁶, S. Kuehn³⁶,
 A. Kugel^{61a}, T. Kuhl⁴⁶, V. Kukhtin⁷⁹, R. Kukla¹⁰¹, Y. Kulchitsky^{107,al}, S. Kuleshov^{147c}, Y.P. Kulinich¹⁷³,
 M. Kuna⁵⁸, T. Kunigo⁸⁵, A. Kupco¹⁴¹, T. Kupfer⁴⁷, O. Kuprash⁵², H. Kurashige⁸², L.L. Kurchaninov^{168a},
 Y.A. Kurochkin¹⁰⁷, A. Kurova¹¹¹, M.G. Kurth^{15a,15d}, E.S. Kuwertz³⁶, M. Kuze¹⁶⁵, A.K. Kvam¹⁴⁸,
 J. Kvita¹³⁰, T. Kwan¹⁰³, A. La Rosa¹¹⁴, L. La Rotonda^{41b,41a}, F. La Ruffa^{41b,41a}, C. Lacasta¹⁷⁴,
 F. Lacava^{72a,72b}, D.P.J. Lack¹⁰⁰, H. Lacker¹⁹, D. Lacour¹³⁶, E. Ladygin⁷⁹, R. Lafaye⁵, B. Laforge¹³⁶,
 T. Lagouri^{33c}, S. Lai⁵³, S. Lammers⁶⁵, W. Lampi⁷, C. Lampoudis¹⁶², E. Lançon²⁹, U. Landgraf⁵²,
 M.P.J. Landon⁹², M.C. Lanfermann⁵⁴, V.S. Lang⁴⁶, J.C. Lange⁵³, R.J. Langenberg³⁶, A.J. Lankford¹⁷¹,
 F. Lanni²⁹, K. Lantzsch²⁴, A. Lanza^{70a}, A. Lapertosa^{55b,55a}, S. Laplace¹³⁶, J.F. Laporte¹⁴⁵, T. Lari^{68a},
 F. Lasagni Manghi^{23b,23a}, M. Lassnig³⁶, T.S. Lau^{63a}, A. Laudrain¹³², A. Laurier³⁴, M. Lavorgna^{69a,69b},

M. Lazzaroni^{68a,68b}, B. Le¹⁰⁴, E. Le Guirriec¹⁰¹, M. LeBlanc⁷, T. LeCompte⁶, F. Ledroit-Guillon⁵⁸,
 C.A. Lee²⁹, G.R. Lee¹⁷, L. Lee⁵⁹, S.C. Lee¹⁵⁸, S.J. Lee³⁴, B. Lefebvre^{168a}, M. Lefebvre¹⁷⁶, F. Legger¹¹³,
 C. Leggett¹⁸, K. Lehmann¹⁵², N. Lehmann¹⁸², G. Lehmann Miotto³⁶, W.A. Leight⁴⁶, A. Leisos^{162,y},
 M.A.L. Leite^{80d}, C.E. Leitgeb¹¹³, R. Leitner¹⁴³, D. Lellouch^{180,*}, K.J.C. Leney⁴², T. Lenz²⁴, B. Lenzi³⁶,
 R. Leone⁷, S. Leone^{71a}, C. Leonidopoulos⁵⁰, A. Leopold¹³⁶, G. Lerner¹⁵⁶, C. Leroy¹⁰⁹, R. Les¹⁶⁷,
 C.G. Lester³², M. Levchenko¹³⁸, J. Levêque⁵, D. Levin¹⁰⁵, L.J. Levinson¹⁸⁰, D.J. Lewis²¹, B. Li^{15b},
 B. Li¹⁰⁵, C.-Q. Li^{60a}, F. Li^{60c}, H. Li^{60a}, H. Li^{60b}, J. Li^{60c}, K. Li¹⁵³, L. Li^{60c}, M. Li^{15a}, Q. Li^{15a,15d},
 Q.Y. Li^{60a}, S. Li^{60d,60c}, X. Li⁴⁶, Y. Li⁴⁶, Z. Li^{60b}, Z. Liang^{15a}, B. Liberti^{73a}, A. Liblong¹⁶⁷, K. Lie^{63c},
 S. Liem¹¹⁹, C.Y. Lin³², K. Lin¹⁰⁶, T.H. Lin⁹⁹, R.A. Linck⁶⁵, J.H. Lindon²¹, A.L. Lionti⁵⁴, E. Lipeles¹³⁷,
 A. Lipniacka¹⁷, M. Lisovyi^{61b}, T.M. Liss^{173,aw}, A. Lister¹⁷⁵, A.M. Litke¹⁴⁶, J.D. Little⁸, B. Liu^{78,ae},
 B.L. Liu⁶, H.B. Liu²⁹, H. Liu¹⁰⁵, J.B. Liu^{60a}, J.K.K. Liu¹³⁵, K. Liu¹³⁶, M. Liu^{60a}, P. Liu¹⁸, Y. Liu^{15a,15d},
 Y.L. Liu¹⁰⁵, Y.W. Liu^{60a}, M. Livan^{70a,70b}, A. Lleres⁵⁸, J. Llorente Merino^{15a}, S.L. Lloyd⁹², C.Y. Lo^{63b},
 F. Lo Sterzo⁴², E.M. Lobodzinska⁴⁶, P. Loch⁷, S. Loffredo^{73a,73b}, T. Lohse¹⁹, K. Lohwasser¹⁴⁹,
 M. Lokajicek¹⁴¹, J.D. Long¹⁷³, R.E. Long⁸⁹, L. Longo³⁶, K.A.Looper¹²⁶, J.A. Lopez^{147c}, I. Lopez Paz¹⁰⁰,
 A. Lopez Solis¹⁴⁹, J. Lorenz¹¹³, N. Lorenzo Martinez⁵, M. Losada²², P.J. Lösel¹¹³, A. Lösle⁵², X. Lou⁴⁶,
 X. Lou^{15a}, A. Lounis¹³², J. Love⁶, P.A. Love⁸⁹, J.J. Lozano Bahilo¹⁷⁴, M. Lu^{60a}, Y.J. Lu⁶⁴, H.J. Lubatti¹⁴⁸,
 C. Luci^{72a,72b}, A. Lucotte⁵⁸, C. Luedtke⁵², F. Luehring⁶⁵, I. Luise¹³⁶, L. Luminari^{72a}, B. Lund-Jensen¹⁵⁴,
 M.S. Lutz¹⁰², D. Lynn²⁹, R. Lysak¹⁴¹, E. Lytken⁹⁶, F. Lyu^{15a}, V. Lyubushkin⁷⁹, T. Lyubushkina⁷⁹,
 H. Ma²⁹, L.L. Ma^{60b}, Y. Ma^{60b}, G. Maccarrone⁵¹, A. Macchiolo¹¹⁴, C.M. Macdonald¹⁴⁹,
 J. Machado Miguens¹³⁷, D. Madaffari¹⁷⁴, R. Madar³⁸, W.F. Mader⁴⁸, N. Madysa⁴⁸, J. Maeda⁸²,
 K. Maekawa¹⁶³, S. Maeland¹⁷, T. Maeno²⁹, M. Maerker⁴⁸, A.S. Maevskiy¹¹², V. Magerl⁵², N. Magini⁷⁸,
 D.J. Mahon³⁹, C. Maidantchik^{80b}, T. Maier¹¹³, A. Maio^{140a,140b,140d}, K. Maj⁸⁴, O. Majersky^{28a},
 S. Majewski¹³¹, Y. Makida⁸¹, N. Makovec¹³², B. Malaescu¹³⁶, Pa. Malecki⁸⁴, V.P. Maleev¹³⁸, F. Malek⁵⁸,
 U. Mallik⁷⁷, D. Malon⁶, C. Malone³², S. Maltezos¹⁰, S. Malyukov⁷⁹, J. Mamuzic¹⁷⁴, G. Mancini⁵¹,
 I. Mandić⁹¹, L. Manhaes de Andrade Filho^{80a}, I.M. Maniatis¹⁶², J. Manjarres Ramos⁴⁸, K.H. Mankinen⁹⁶,
 A. Mann¹¹³, A. Manousos⁷⁶, B. Mansoulie¹⁴⁵, I. Manthos¹⁶², S. Manzoni¹¹⁹, A. Marantis¹⁶²,
 G. Marceca³⁰, L. Marchese¹³⁵, G. Marchiori¹³⁶, M. Marcisovsky¹⁴¹, C. Marcon⁹⁶, C.A. Marin Tobon³⁶,
 M. Marjanovic³⁸, Z. Marshall¹⁸, M.U.F Martensson¹⁷², S. Marti-Garcia¹⁷⁴, C.B. Martin¹²⁶,
 T.A. Martin¹⁷⁸, V.J. Martin⁵⁰, B. Martin dit Latour¹⁷, L. Martinelli^{74a,74b}, M. Martinez^{14,z},
 V.I. Martinez Outschoorn¹⁰², S. Martin-Haugh¹⁴⁴, V.S. Martoiu^{27b}, A.C. Martyniuk⁹⁴, A. Marzin³⁶,
 S.R. Maschek¹¹⁴, L. Masetti⁹⁹, T. Mashimo¹⁶³, R. Mashinistov¹¹⁰, J. Masik¹⁰⁰, A.L. Maslennikov^{121b,121a},
 L.H. Mason¹⁰⁴, L. Massa^{73a,73b}, P. Massarotti^{69a,69b}, P. Mastrandrea^{71a,71b}, A. Mastroberardino^{41b,41a},
 T. Masubuchi¹⁶³, A. Matic¹¹³, P. Mättig²⁴, J. Maurer^{27b}, B. Maček⁹¹, D.A. Maximov^{121b,121a},
 R. Mazini¹⁵⁸, I. Maznas¹⁶², S.M. Mazza¹⁴⁶, S.P. Mc Kee¹⁰⁵, T.G. McCarthy¹¹⁴, L.I. McClymont⁹⁴,
 W.P. McCormack¹⁸, E.F. McDonald¹⁰⁴, J.A. McFayden³⁶, M.A. McKay⁴², K.D. McLean¹⁷⁶,
 S.J. McMahon¹⁴⁴, P.C. McNamara¹⁰⁴, C.J. McNicol¹⁷⁸, R.A. McPherson^{176,af}, J.E. Mdhluli^{33c},
 Z.A. Meadows¹⁰², S. Meehan¹⁴⁸, T. Megy⁵², S. Mehlhase¹¹³, A. Mehta⁹⁰, T. Meideck⁵⁸, B. Meirose⁴³,
 D. Melini¹⁷⁴, B.R. Mellado Garcia^{33c}, J.D. Mellenthin⁵³, M. Melo^{28a}, F. Meloni⁴⁶, A. Melzer²⁴,
 S.B. Menary¹⁰⁰, E.D. Mendes Gouveia^{140a,140e}, L. Meng³⁶, X.T. Meng¹⁰⁵, S. Menke¹¹⁴, E. Meoni^{41b,41a},
 S. Mergelmeyer¹⁹, S.A.M. Merkt¹³⁹, C. Merlassino²⁰, P. Mermod⁵⁴, L. Merola^{69a,69b}, C. Meroni^{68a},
 O. Meshkov^{112,110}, J.K.R. Meshreki¹⁵¹, A. Messina^{72a,72b}, J. Metcalfe⁶, A.S. Mete¹⁷¹, C. Meyer⁶⁵,
 J. Meyer¹⁶⁰, J.-P. Meyer¹⁴⁵, H. Meyer Zu Theenhausen^{61a}, F. Miano¹⁵⁶, R.P. Middleton¹⁴⁴, L. Mijović⁵⁰,
 G. Mikenberg¹⁸⁰, M. Mikestikova¹⁴¹, M. Mikuž⁹¹, H. Mildner¹⁴⁹, M. Milesi¹⁰⁴, A. Milic¹⁶⁷,
 D.A. Millar⁹², D.W. Miller³⁷, A. Milov¹⁸⁰, D.A. Milstead^{45a,45b}, R.A. Mina^{153,r}, A.A. Minaenko¹²²,
 M. Miñano Moya¹⁷⁴, I.A. Minashvili^{159b}, A.I. Mincer¹²⁴, B. Mindur^{83a}, M. Mineev⁷⁹, Y. Minegishi¹⁶³,
 Y. Ming¹⁸¹, L.M. Mir¹⁴, A. Mirto^{67a,67b}, K.P. Mistry¹³⁷, T. Mitani¹⁷⁹, J. Mitrevski¹¹³, V.A. Mitsou¹⁷⁴,
 M. Mittal^{60c}, A. Miucci²⁰, P.S. Miyagawa¹⁴⁹, A. Mizukami⁸¹, J.U. Mjörnmark⁹⁶, T. Mkrtchyan¹⁸⁴,

M. Mlynarikova¹⁴³, T. Moa^{45a,45b}, K. Mochizuki¹⁰⁹, P. Mogg⁵², S. Mohapatra³⁹, R. Moles-Valls²⁴,
 M.C. Mondragon¹⁰⁶, K. Mönig⁴⁶, J. Monk⁴⁰, E. Monnier¹⁰¹, A. Montalbano¹⁵², J. Montejo Berlingen³⁶,
 M. Montella⁹⁴, F. Monticelli⁸⁸, S. Monzani^{68a}, N. Morange¹³², D. Moreno²², M. Moreno Llácer³⁶,
 C. Moreno Martinez¹⁴, P. Morettini^{55b}, M. Morgenstern¹¹⁹, S. Morgenstern⁴⁸, D. Mori¹⁵², M. Morii⁵⁹,
 M. Morinaga¹⁷⁹, V. Morisbak¹³⁴, A.K. Morley³⁶, G. Mornacchi³⁶, A.P. Morris⁹⁴, L. Morvaj¹⁵⁵,
 P. Moschovakos³⁶, B. Moser¹¹⁹, M. Mosidze^{159b}, T. Moskalets¹⁴⁵, H.J. Moss¹⁴⁹, J. Moss^{31,0},
 K. Motohashi¹⁶⁵, E. Mountricha³⁶, E.J.W. Moyse¹⁰², S. Muanza¹⁰¹, J. Mueller¹³⁹, R.S.P. Mueller¹¹³,
 D. Muenstermann⁸⁹, G.A. Mullier⁹⁶, J.L. Munoz Martinez¹⁴, F.J. Munoz Sanchez¹⁰⁰, P. Murin^{28b},
 W.J. Murray^{178,144}, A. Murrone^{68a,68b}, M. Muškinja¹⁸, C. Mwewa^{33a}, A.G. Myagkov^{122,aq}, J. Myers¹³¹,
 M. Myska¹⁴², B.P. Nachman¹⁸, O. Nackenhorst⁴⁷, A.Nag Nag⁴⁸, K. Nagai¹³⁵, K. Nagano⁸¹, Y. Nagasaka⁶²,
 M. Nagel⁵², E. Nagy¹⁰¹, A.M. Nairz³⁶, Y. Nakahama¹¹⁶, K. Nakamura⁸¹, T. Nakamura¹⁶³, I. Nakano¹²⁷,
 H. Nanjo¹³³, F. Napolitano^{61a}, R.F. Naranjo Garcia⁴⁶, R. Narayan⁴², D.I. Narrias Villar^{61a}, I. Naryshkin¹³⁸,
 T. Naumann⁴⁶, G. Navarro²², H.A. Neal^{105,*}, P.Y. Nechaeva¹¹⁰, F. Nechansky⁴⁶, T.J. Neep²¹,
 A. Negri^{70a,70b}, M. Negrini^{23b}, C. Nellist⁵³, M.E. Nelson¹³⁵, S. Nemecek¹⁴¹, P. Nemethy¹²⁴, M. Nessi^{36,e},
 M.S. Neubauer¹⁷³, M. Neumann¹⁸², P.R. Newman²¹, T.Y. Ng^{63c}, Y.S. Ng¹⁹, Y.W.Y. Ng¹⁷¹,
 H.D.N. Nguyen¹⁰¹, T. Nguyen Manh¹⁰⁹, E. Nibigira³⁸, R.B. Nickerson¹³⁵, R. Nicolaïdou¹⁴⁵,
 D.S. Nielsen⁴⁰, J. Nielsen¹⁴⁶, N. Nikiforou¹¹, V. Nikolaenko^{122,aq}, I. Nikolic-Audit¹³⁶, K. Nikolopoulos²¹,
 P. Nilsson²⁹, H.R. Nindhito⁵⁴, Y. Ninomiya⁸¹, A. Nisati^{72a}, N. Nishu^{60c}, R. Nisius¹¹⁴, I. Nitsche⁴⁷,
 T. Nitta¹⁷⁹, T. Nobe¹⁶³, Y. Noguchi⁸⁵, I. Nomidis¹³⁶, M.A. Nomura²⁹, M. Nordberg³⁶,
 N. Norjoharuddeen¹³⁵, T. Novak⁹¹, O. Novgorodova⁴⁸, R. Novotny¹⁴², L. Nozka¹³⁰, K. Ntekas¹⁷¹,
 E. Nurse⁹⁴, F.G. Oakham^{34,az}, H. Oberlack¹¹⁴, J. Ocariz¹³⁶, A. Ochi⁸², I. Ochoa³⁹, J.P. Ochoa-Ricoux^{147a},
 K. O'Connor²⁶, S. Oda⁸⁷, S. Odaka⁸¹, S. Oerdekk⁵³, A. Ogródniak^{83a}, A. Oh¹⁰⁰, S.H. Oh⁴⁹, C.C. Ohm¹⁵⁴,
 H. Oide^{55b,55a}, M.L. Ojeda¹⁶⁷, H. Okawa¹⁶⁹, Y. Okazaki⁸⁵, Y. Okumura¹⁶³, T. Okuyama⁸¹, A. Olariu^{27b},
 L.F. Oleiro Seabra^{140a}, S.A. Olivares Pino^{147a}, D. Oliveira Damazio²⁹, J.L. Oliver¹, M.J.R. Olsson¹⁷¹,
 A. Olszewski⁸⁴, J. Olszowska⁸⁴, D.C. O'Neil¹⁵², A. Onofre^{140a,140e}, K. Onogi¹¹⁶, P.U.E. Onyisi¹¹,
 H. Oppen¹³⁴, M.J. Oreglia³⁷, G.E. Orellana⁸⁸, D. Orestano^{74a,74b}, N. Orlando¹⁴, R.S. Orr¹⁶⁷, V. O'Shea⁵⁷,
 R. Ospanov^{60a}, G. Otero y Garzon³⁰, H. Otono⁸⁷, M. Ouchrif^{35d}, J. Ouellette²⁹, F. Ould-Saada¹³⁴,
 A. Ouraou¹⁴⁵, Q. Ouyang^{15a}, M. Owen⁵⁷, R.E. Owen²¹, V.E. Ozcan^{12c}, N. Ozturk⁸, J. Pacalt¹³⁰,
 H.A. Pacey³², K. Pachal⁴⁹, A. Pacheco Pages¹⁴, C. Padilla Aranda¹⁴, S. Pagan Griso¹⁸, M. Paganini¹⁸³,
 G. Palacino⁶⁵, S. Palazzo⁵⁰, S. Palestini³⁶, M. Palka^{83b}, D. Pallin³⁸, I. Panagoulias¹⁰, C.E. Pandini³⁶,
 J.G. Panduro Vazquez⁹³, P. Pani⁴⁶, G. Panizzo^{66a,66c}, L. Paolozzi⁵⁴, C. Papadatos¹⁰⁹, K. Papageorgiou^{9,i},
 A. Paramonov⁶, D. Paredes Hernandez^{63b}, S.R. Paredes Saenz¹³⁵, B. Parida¹⁶⁶, T.H. Park¹⁶⁷, A.J. Parker⁸⁹,
 M.A. Parker³², F. Parodi^{55b,55a}, E.W. Parrish¹²⁰, J.A. Parsons³⁹, U. Parzefall⁵², L. Pascual Dominguez¹³⁶,
 V.R. Pascuzzi¹⁶⁷, J.M.P. Pasner¹⁴⁶, E. Pasqualucci^{72a}, S. Passaggio^{55b}, F. Pastore⁹³, P. Pasuwant^{43a,45b},
 S. Pataria⁹⁹, J.R. Pater¹⁰⁰, A. Pathak¹⁸¹, T. Pauly³⁶, B. Pearson¹¹⁴, M. Pedersen¹³⁴, L. Pedraza Diaz¹¹⁸,
 R. Pedro^{140a}, T. Peiffer⁵³, S.V. Peleganchuk^{121b,121a}, O. Penc¹⁴¹, H. Peng^{60a}, B.S. Peralva^{80a},
 M.M. Perego¹³², A.P. Pereira Peixoto^{140a}, D.V. Perepelitsa²⁹, F. Peri¹⁹, L. Perini^{68a,68b}, H. Pernegger³⁶,
 S. Perrella^{69a,69b}, K. Peters⁴⁶, R.F.Y. Peters¹⁰⁰, B.A. Petersen³⁶, T.C. Petersen⁴⁰, E. Petit¹⁰¹, A. Petridis¹,
 C. Petridou¹⁶², P. Petroff¹³², M. Petrov¹³⁵, F. Petrucci^{74a,74b}, M. Pettee¹⁸³, N.E. Pettersson¹⁰²,
 K. Petukhova¹⁴³, A. Peyaud¹⁴⁵, R. Pezoa^{147c}, L. Pezzotti^{70a,70b}, T. Pham¹⁰⁴, F.H. Phillips¹⁰⁶,
 P.W. Phillips¹⁴⁴, M.W. Phipps¹⁷³, G. Piacquadio¹⁵⁵, E. Pianori¹⁸, A. Picazio¹⁰², R.H. Pickles¹⁰⁰,
 R. Piegaia³⁰, D. Pietreanu^{27b}, J.E. Pilcher³⁷, A.D. Pilkington¹⁰⁰, M. Pinamonti^{73a,73b}, J.L. Pinfold³,
 M. Pitt¹⁸⁰, L. Pizzimenti^{73a,73b}, M.-A. Pleier²⁹, V. Pleskot¹⁴³, E. Plotnikova⁷⁹, D. Pluth⁷⁸,
 P. Podberezko^{121b,121a}, R. Poettgen⁹⁶, R. Poggi⁵⁴, L. Poggioli¹³², I. Pogrebnyak¹⁰⁶, D. Pohl²⁴,
 I. Pokharel⁵³, G. Polesello^{70a}, A. Poley¹⁸, A. Policicchio^{72a,72b}, R. Polifka¹⁴³, A. Polini^{23b}, C.S. Pollard⁴⁶,
 V. Polychronakos²⁹, D. Ponomarenko¹¹¹, L. Pontecorvo³⁶, S. Popa^{27a}, G.A. Popeneciu^{27d},
 D.M. Portillo Quintero⁵⁸, S. Pospisil¹⁴², K. Potamianos⁴⁶, I.N. Potrap⁷⁹, C.J. Potter³², H. Potti¹¹,

T. Poulsen⁹⁶, J. Poveda³⁶, T.D. Powell¹⁴⁹, G. Pownall⁴⁶, M.E. Pozo Astigarraga³⁶, P. Pralavorio¹⁰¹, S. Prell⁷⁸, D. Price¹⁰⁰, M. Primavera^{67a}, S. Prince¹⁰³, M.L. Proffitt¹⁴⁸, N. Proklova¹¹¹, K. Prokofiev^{63c}, F. Prokoshin⁷⁹, S. Protopopescu²⁹, J. Proudfoot⁶, M. Przybycien^{83a}, D. Pudzha¹³⁸, A. Puri¹⁷³, P. Puzo¹³², J. Qian¹⁰⁵, Y. Qin¹⁰⁰, A. Quadt⁵³, M. Queitsch-Maitland⁴⁶, A. Qureshi¹, P. Rados¹⁰⁴, F. Ragusa^{68a,68b}, G. Rahal⁹⁷, J.A. Raine⁵⁴, S. Rajagopalan²⁹, A. Ramirez Morales⁹², K. Ran^{15a,15d}, T. Rashid¹³², S. Raspopov⁵, M.G. Ratti^{68a,68b}, D.M. Rauch⁴⁶, F. Rauscher¹¹³, S. Rave⁹⁹, B. Ravina¹⁴⁹, I. Ravinovich¹⁸⁰, J.H. Rawling¹⁰⁰, M. Raymond³⁶, A.L. Read¹³⁴, N.P. Readioff⁵⁸, M. Reale^{67a,67b}, D.M. Rebuzzi^{70a,70b}, A. Redelbach¹⁷⁷, G. Redlinger²⁹, K. Reeves⁴³, L. Rehnisch¹⁹, J. Reichert¹³⁷, D. Reikher¹⁶¹, A. Reiss⁹⁹, A. Rej¹⁵¹, C. Rembser³⁶, M. Renda^{27b}, M. Rescigno^{72a}, S. Resconi^{68a}, E.D. Resseguie¹³⁷, S. Rettie¹⁷⁵, E. Reynolds²¹, O.L. Rezanova^{121b,121a}, P. Reznicek¹⁴³, E. Ricci^{75a,75b}, R. Richter¹¹⁴, S. Richter⁴⁶, E. Richter-Was^{83b}, O. Ricken²⁴, M. Ridel¹³⁶, P. Rieck¹¹⁴, C.J. Riegel¹⁸², O. Rifki⁴⁶, M. Rijssenbeek¹⁵⁵, A. Rimoldi^{70a,70b}, M. Rimoldi⁴⁶, L. Rinaldi^{23b}, G. Ripellino¹⁵⁴, B. Ristic⁸⁹, E. Ritsch³⁶, I. Riu¹⁴, J.C. Rivera Vergara¹⁷⁶, F. Rizatdinova¹²⁹, E. Rizvi⁹², C. Rizzi³⁶, R.T. Roberts¹⁰⁰, S.H. Robertson^{103,af}, M. Robin⁴⁶, D. Robinson³², J.E.M. Robinson⁴⁶, C.M. Robles Gajardo^{147c}, A. Robson⁵⁷, E. Rocco⁹⁹, C. Roda^{71a,71b}, S. Rodriguez Bosca¹⁷⁴, A. Rodriguez Perez¹⁴, D. Rodriguez Rodriguez¹⁷⁴, A.M. Rodríguez Vera^{168b}, S. Roe³⁶, O. Røhne¹³⁴, R. Röhrlig¹¹⁴, C.P.A. Roland⁶⁵, J. Roloff⁵⁹, A. Romaniouk¹¹¹, M. Romano^{23b,23a}, N. Rompotis⁹⁰, M. Ronzani¹²⁴, L. Roos¹³⁶, S. Rosati^{72a}, K. Rosbach⁵², G. Rosin¹⁰², B.J. Rosser¹³⁷, E. Rossi⁴⁶, E. Rossi^{74a,74b}, E. Rossi^{69a,69b}, L.P. Rossi^{55b}, L. Rossini^{68a,68b}, R. Rosten¹⁴, M. Rotaru^{27b}, J. Rothberg¹⁴⁸, D. Rousseau¹³², G. Rovelli^{70a,70b}, D. Roy^{33c}, A. Rozanov¹⁰¹, Y. Rozen¹⁶⁰, X. Ruan^{33c}, F. Rubbo¹⁵³, F. Rühr⁵², A. Ruiz-Martinez¹⁷⁴, A. Rummler³⁶, Z. Rurikova⁵², N.A. Rusakovich⁷⁹, H.L. Russell¹⁰³, L. Rustige^{38,47}, J.P. Rutherford⁷, E.M. Rüttinger^{46,k}, M. Rybar³⁹, G. Rybkin¹³², A. Ryzhov¹²², G.F. Rzehorz⁵³, P. Sabatini⁵³, G. Sabato¹¹⁹, S. Sacerdoti¹³², H.F-W. Sadrozinski¹⁴⁶, R. Sadykov⁷⁹, F. Safai Tehrani^{72a}, B. Safarzadeh Samani¹⁵⁶, P. Saha¹²⁰, S. Saha¹⁰³, M. Sahinsoy^{61a}, A. Sahu¹⁸², M. Saimpert⁴⁶, M. Saito¹⁶³, T. Saito¹⁶³, H. Sakamoto¹⁶³, A. Sakharov^{124,ap}, D. Salamani⁵⁴, G. Salamanna^{74a,74b}, J.E. Salazar Loyola^{147c}, P.H. Sales De Bruin¹⁷², D. Salihagic^{114,*}, A. Salnikov¹⁵³, J. Salt¹⁷⁴, D. Salvatore^{41b,41a}, F. Salvatore¹⁵⁶, A. Salvucci^{63a,63b,63c}, A. Salzburger³⁶, J. Samarati³⁶, D. Sammel⁵², D. Sampsonidis¹⁶², D. Sampsonidou¹⁶², J. Sánchez¹⁷⁴, A. Sanchez Pineda^{66a,66c}, H. Sandaker¹³⁴, C.O. Sander⁴⁶, I.G. Sanderswood⁸⁹, M. Sandhoff¹⁸², C. Sandoval²², D.P.C. Sankey¹⁴⁴, M. Sannino^{55b,55a}, Y. Sano¹¹⁶, A. Sansoni⁵¹, C. Santoni³⁸, H. Santos^{140a,140b}, S.N. Santpur¹⁸, A. Santra¹⁷⁴, A. Sapronov⁷⁹, J.G. Saraiva^{140a,140d}, O. Sasaki⁸¹, K. Sato¹⁶⁹, E. Sauvan⁵, P. Savard^{167,az}, N. Savic¹¹⁴, R. Sawada¹⁶³, C. Sawyer¹⁴⁴, L. Sawyer^{95,an}, C. Sbarra^{23b}, A. Sbrizzi^{23a}, T. Scanlon⁹⁴, J. Schaarschmidt¹⁴⁸, P. Schacht¹¹⁴, B.M. Schachtner¹¹³, D. Schaefer³⁷, L. Schaefer¹³⁷, J. Schaeffer⁹⁹, S. Schaepe³⁶, U. Schäfer⁹⁹, A.C. Schaffer¹³², D. Schaile¹¹³, R.D. Schamberger¹⁵⁵, N. Scharmberg¹⁰⁰, V.A. Schegelsky¹³⁸, D. Scheirich¹⁴³, F. Schenck¹⁹, M. Schernau¹⁷¹, C. Schiavi^{55b,55a}, S. Schier¹⁴⁶, L.K. Schildgen²⁴, Z.M. Schillaci²⁶, E.J. Schioppa³⁶, M. Schioppa^{41b,41a}, K.E. Schleicher⁵², S. Schlenker³⁶, K.R. Schmidt-Sommerfeld¹¹⁴, K. Schmieden³⁶, C. Schmitt⁹⁹, S. Schmitt⁴⁶, S. Schmitz⁹⁹, J.C. Schmoekel⁴⁶, U. Schnoor⁵², L. Schoeffel¹⁴⁵, A. Schoening^{61b}, P.G. Scholer⁵², E. Schopf¹³⁵, M. Schott⁹⁹, J.F.P. Schouwenberg¹¹⁸, J. Schovancova³⁶, S. Schramm⁵⁴, F. Schroeder¹⁸², A. Schulte⁹⁹, H-C. Schultz-Coulon^{61a}, M. Schumacher⁵², B.A. Schumm¹⁴⁶, Ph. Schune¹⁴⁵, A. Schwartzman¹⁵³, T.A. Schwarz¹⁰⁵, Ph. Schwemling¹⁴⁵, R. Schwienhorst¹⁰⁶, A. Sciandra¹⁴⁶, G. Sciolla²⁶, M. Scodeggio⁴⁶, M. Scornajenghi^{41b,41a}, F. Scuri^{71a}, F. Scutti¹⁰⁴, L.M. Scyboz¹¹⁴, C.D. Sebastiani^{72a,72b}, P. Seema¹⁹, S.C. Seidel¹¹⁷, A. Seiden¹⁴⁶, T. Seiss³⁷, J.M. Seixas^{80b}, G. Sekhniaidze^{69a}, K. Sekhon¹⁰⁵, S.J. Sekula⁴², N. Semprini-Cesari^{23b,23a}, S. Sen⁴⁹, S. Senkin³⁸, C. Serfon⁷⁶, L. Serin¹³², L. Serkin^{66a,66b}, M. Sessa^{60a}, H. Severini¹²⁸, T. Šfiligoj⁹¹, F. Sforza¹⁷⁰, A. Sfyrla⁵⁴, E. Shabalina⁵³, J.D. Shahinian¹⁴⁶, N.W. Shaikh^{45a,45b}, D. Shaked Renous¹⁸⁰, L.Y. Shan^{15a}, R. Shang¹⁷³, J.T. Shank²⁵, M. Shapiro¹⁸, A. Sharma¹³⁵, A.S. Sharma¹, P.B. Shatalov¹²³, K. Shaw¹⁵⁶, S.M. Shaw¹⁰⁰, A. Shcherbakova¹³⁸, Y. Shen¹²⁸, N. Sherafati³⁴, A.D. Sherman²⁵,

P. Sherwood⁹⁴, L. Shi^{158,av}, S. Shimizu⁸¹, C.O. Shimmin¹⁸³, Y. Shimogama¹⁷⁹, M. Shimojima¹¹⁵, I.P.J. Shipsey¹³⁵, S. Shirabe⁸⁷, M. Shiyakova^{79,ac}, J. Shlomi¹⁸⁰, A. Shmeleva¹¹⁰, M.J. Shochet³⁷, J. Shojaii¹⁰⁴, D.R. Shope¹²⁸, S. Shrestha¹²⁶, E. Shulga¹⁸⁰, P. Sicho¹⁴¹, A.M. Sickles¹⁷³, P.E. Sidebo¹⁵⁴, E. Sideras Haddad^{33c}, O. Sidiropoulou³⁶, A. Sidoti^{23b,23a}, F. Siegert⁴⁸, Dj. Sijacki¹⁶, M.Jr. Silva¹⁸¹, M.V. Silva Oliveira^{80a}, S.B. Silverstein^{45a}, S. Simion¹³², E. Simioni⁹⁹, R. Simoniello⁹⁹, S. Simsek^{12b}, P. Sinervo¹⁶⁷, N.B. Sinev¹³¹, M. Sioli^{23b,23a}, I. Siral¹⁰⁵, S.Yu. Sivoklokov¹¹², J. Sjölin^{45a,45b}, E. Skorda⁹⁶, P. Skubic¹²⁸, M. Slawinska⁸⁴, K. Sliwa¹⁷⁰, R. Slovak¹⁴³, V. Smakhtin¹⁸⁰, B.H. Smart¹⁴⁴, J. Smiesko^{28a}, N. Smirnov¹¹¹, S.Yu. Smirnov¹¹¹, Y. Smirnov¹¹¹, L.N. Smirnova^{112,v}, O. Smirnova⁹⁶, J.W. Smith⁵³, M. Smizanska⁸⁹, K. Smolek¹⁴², A. Smykiewicz⁸⁴, A.A. Snesarev¹¹⁰, H.L. Snoek¹¹⁹, I.M. Snyder¹³¹, S. Snyder²⁹, R. Sobie^{176,af}, A.M. Soffa¹⁷¹, A. Soffer¹⁶¹, A. Søgaard⁵⁰, F. Sohns⁵³, C.A. Solans Sanchez³⁶, E.Yu. Soldatov¹¹¹, U. Soldevila¹⁷⁴, A.A. Solodkov¹²², A. Soloshenko⁷⁹, O.V. Solovyanov¹²², V. Solovyev¹³⁸, P. Sommer¹⁴⁹, H. Son¹⁷⁰, W. Song¹⁴⁴, W.Y. Song^{168b}, A. Sopczak¹⁴², F. Sopkova^{28b}, C.L. Sotiropoulou^{71a,71b}, S. Sottocornola^{70a,70b}, R. Soualah^{66a,66c,h}, A.M. Soukharev^{121b,121a}, D. South⁴⁶, S. Spagnolo^{67a,67b}, M. Spalla¹¹⁴, M. Spangenberg¹⁷⁸, F. Spanò⁹³, D. Sperlich⁵², T.M. Speker^{61a}, R. Spighi^{23b}, G. Spigo³⁶, M. Spina¹⁵⁶, D.P. Spiteri⁵⁷, M. Spousta¹⁴³, A. Stabile^{68a,68b}, B.L. Stamas¹²⁰, R. Stamen^{61a}, M. Stamenkovic¹¹⁹, E. Stanecka⁸⁴, R.W. Stanek⁶, B. Stanislaus¹³⁵, M.M. Stanitzki⁴⁶, M. Stankaityte¹³⁵, B. Stapf¹¹⁹, E.A. Starchenko¹²², G.H. Stark¹⁴⁶, J. Stark⁵⁸, S.H. Stark⁴⁰, P. Staroba¹⁴¹, P. Starovoitov^{61a}, S. Stärz¹⁰³, R. Staszewski⁸⁴, G. Stavropoulos⁴⁴, M. Stegler⁴⁶, P. Steinberg²⁹, A.L. Steinhebel¹³¹, B. Stelzer¹⁵², H.J. Stelzer¹³⁹, O. Stelzer-Chilton^{168a}, H. Stenzel⁵⁶, T.J. Stevenson¹⁵⁶, G.A. Stewart³⁶, M.C. Stockton³⁶, G. Stoicea^{27b}, M. Stolarski^{140a}, P. Stolte⁵³, S. Stonjek¹¹⁴, A. Straessner⁴⁸, J. Strandberg¹⁵⁴, S. Strandberg^{45a,45b}, M. Strauss¹²⁸, P. Strizenec^{28b}, R. Ströhmer¹⁷⁷, D.M. Strom¹³¹, R. Stroynowski⁴², A. Strubig⁵⁰, S.A. Stucci²⁹, B. Stugu¹⁷, J. Stupak¹²⁸, N.A. Styles⁴⁶, D. Su¹⁵³, S. Suchek^{61a}, V.V. Sulin¹¹⁰, M.J. Sullivan⁹⁰, D.M.S. Sultan⁵⁴, S. Sultansoy^{4c}, T. Sumida⁸⁵, S. Sun¹⁰⁵, X. Sun³, K. Suruliz¹⁵⁶, C.J.E. Suster¹⁵⁷, M.R. Sutton¹⁵⁶, S. Suzuki⁸¹, M. Svatos¹⁴¹, M. Swiatlowski³⁷, S.P. Swift², T. Swirski¹⁷⁷, A. Sydorenko⁹⁹, I. Sykora^{28a}, M. Sykora¹⁴³, T. Sykora¹⁴³, D. Ta⁹⁹, K. Tackmann^{46,aa}, J. Taenzer¹⁶¹, A. Taffard¹⁷¹, R. Tafirout^{168a}, H. Takai²⁹, R. Takashima⁸⁶, K. Takeda⁸², T. Takeshita¹⁵⁰, E.P. Takeva⁵⁰, Y. Takubo⁸¹, M. Talby¹⁰¹, A.A. Talyshev^{121b,121a}, N.M. Tamir¹⁶¹, J. Tanaka¹⁶³, M. Tanaka¹⁶⁵, R. Tanaka¹³², S. Tapia Araya¹⁷³, S. Tapprogge⁹⁹, A. Tarek Abouelfadl Mohamed¹³⁶, S. Tarem¹⁶⁰, G. Tarna^{27b,d}, G.F. Tartarelli^{68a}, P. Tas¹⁴³, M. Tasevsky¹⁴¹, T. Tashiro⁸⁵, E. Tassi^{41b,41a}, A. Tavares Delgado^{140a,140b}, Y. Tayalati^{35e}, A.J. Taylor⁵⁰, G.N. Taylor¹⁰⁴, W. Taylor^{168b}, A.S. Tee⁸⁹, R. Teixeira De Lima¹⁵³, P. Teixeira-Dias⁹³, H. Ten Kate³⁶, J.J. Teoh¹¹⁹, S. Terada⁸¹, K. Terashi¹⁶³, J. Terron⁹⁸, S. Terzo¹⁴, M. Testa⁵¹, R.J. Teuscher^{167,af}, S.J. Thais¹⁸³, T. Theveneaux-Pelzer⁴⁶, F. Thiele⁴⁰, D.W. Thomas⁹³, J.O. Thomas⁴², J.P. Thomas²¹, A.S. Thompson⁵⁷, P.D. Thompson²¹, L.A. Thomsen¹⁸³, E. Thomson¹³⁷, Y. Tian³⁹, R.E. Ticse Torres⁵³, V.O. Tikhomirov^{110,ar}, Yu.A. Tikhonov^{121b,121a}, S. Timoshenko¹¹¹, P. Tipton¹⁸³, S. Tisserant¹⁰¹, K. Todome^{23b,23a}, S. Todorova-Nova⁵, S. Todt⁴⁸, J. Tojo⁸⁷, S. Tokár^{28a}, K. Tokushuku⁸¹, E. Tolley¹²⁶, K.G. Tomiwa^{33c}, M. Tomoto¹¹⁶, L. Tompkins^{153,r}, B. Tong⁵⁹, P. Tornambe¹⁰², E. Torrence¹³¹, H. Torres⁴⁸, E. Torró Pastor¹⁴⁸, C. Toscirci¹³⁵, J. Toth^{101,ad}, D.R. Tovey¹⁴⁹, A. Traeet¹⁷, C.J. Treado¹²⁴, T. Trefzger¹⁷⁷, F. Tresoldi¹⁵⁶, A. Tricoli²⁹, I.M. Trigger^{168a}, S. Trincatz-Duvoid¹³⁶, W. Trischuk¹⁶⁷, B. Trocmé⁵⁸, A. Trofymov¹⁴⁵, C. Troncon^{68a}, M. Trovatelli¹⁷⁶, F. Trovatq¹⁵⁶, L. Truong^{33b}, M. Trzebinski⁸⁴, A. Trzupek⁸⁴, F. Tsai⁴⁶, J.C.-L. Tseng¹³⁵, P.V. Tsiareshka^{107,al}, A. Tsirigotis¹⁶², N. Tsirintanis⁹, V. Tsiskaridze¹⁵⁵, E.G. Tskhadadze^{159a}, M. Tsopoulou¹⁶², I.I. Tsukerman¹²³, V. Tsulaia¹⁸, S. Tsuno⁸¹, D. Tsybychev¹⁵⁵, Y. Tu^{63b}, A. Tudorache^{27b}, V. Tudorache^{27b}, T.T. Tulbure^{27a}, A.N. Tuna⁵⁹, S. Turchikhin⁷⁹, D. Turgeman¹⁸⁰, I. Turk Cakir^{4b,w}, R.J. Turner²¹, R.T. Turra^{68a}, P.M. Tuts³⁹, S. Tzamarias¹⁶², E. Tzovara⁹⁹, G. Ucchielli⁴⁷, K. Uchida¹⁶³, I. Ueda⁸¹, M. Ughetto^{45a,45b}, F. Ukegawa¹⁶⁹, G. Unal³⁶, A. Undrus²⁹, G. Unel¹⁷¹, F.C. Ungaro¹⁰⁴, Y. Unno⁸¹, K. Uno¹⁶³, J. Urban^{28b}, P. Urquijo¹⁰⁴, G. Usai⁸, J. Usui⁸¹, Z. Uysal^{12d}, L. Vacavant¹⁰¹, V. Vacek¹⁴², B. Vachon¹⁰³, K.O.H. Vadla¹³⁴, A. Vaidya⁹⁴,

C. Valderanis¹¹³, E. Valdes Santurio^{45a,45b}, M. Valente⁵⁴, S. Valentinetto^{23b,23a}, A. Valero¹⁷⁴, L. Valéry⁴⁶, R.A. Vallance²¹, A. Vallier³⁶, J.A. Valls Ferrer¹⁷⁴, T.R. Van Daalen¹⁴, P. Van Gemmeren⁶, I. Van Vulpen¹¹⁹, M. Vanadia^{73a,73b}, W. Vandelli³⁶, A. Vaniachine¹⁶⁶, D. Vannicola^{72a,72b}, R. Vari^{72a}, E.W. Varnes⁷, C. Varni^{55b,55a}, T. Varol⁴², D. Varouchas¹³², K.E. Varvell¹⁵⁷, M.E. Vasile^{27b}, G.A. Vasquez¹⁷⁶, J.G. Vasquez¹⁸³, F. Vazeille³⁸, D. Vazquez Furelos¹⁴, T. Vazquez Schroeder³⁶, J. Veatch⁵³, V. Vecchio^{74a,74b}, M.J. Veen¹¹⁹, L.M. Veloce¹⁶⁷, F. Veloso^{140a,140c}, S. Veneziano^{72a}, A. Ventura^{67a,67b}, N. Venturi³⁶, A. Verbytskyi¹¹⁴, V. Vercesi^{70a}, M. Verducci^{74a,74b}, C.M. Vergel Infante⁷⁸, C. Vergis²⁴, W. Verkerke¹¹⁹, A.T. Vermeulen¹¹⁹, J.C. Vermeulen¹¹⁹, M.C. Vetterli^{152,az}, N. Viaux Maira^{147c}, M. Vicente Barreto Pinto⁵⁴, T. Vickey¹⁴⁹, O.E. Vickey Boeriu¹⁴⁹, G.H.A. Viehhauser¹³⁵, L. Vigani¹³⁵, M. Villa^{23b,23a}, M. Villaplana Perez^{68a,68b}, E. Vilucchi⁵¹, M.G. Vincter³⁴, V.B. Vinogradov⁷⁹, A. Vishwakarma⁴⁶, C. Vittori^{23b,23a}, I. Vivarelli¹⁵⁶, M. Vogel¹⁸², P. Vokac¹⁴², S.E. von Buddenbrock^{33c}, E. Von Toerne²⁴, V. Vorobel¹⁴³, K. Vorobej¹¹¹, M. Vos¹⁷⁴, J.H. Vossebeld⁹⁰, M. Vozak¹⁰⁰, N. Vranjes¹⁶, M. Vranjes Milosavljevic¹⁶, V. Vrba¹⁴², M. Vreeswijk¹¹⁹, R. Vuillermet³⁶, I. Vukotic³⁷, P. Wagner²⁴, W. Wagner¹⁸², J. Wagner-Kuhr¹¹³, H. Wahlberg⁸⁸, K. Wakamiya⁸², V.M. Walbrecht¹¹⁴, J. Walder⁸⁹, R. Walker¹¹³, S.D. Walker⁹³, W. Walkowiak¹⁵¹, V. Wallangen^{45a,45b}, A.M. Wang⁵⁹, C. Wang^{60b}, F. Wang¹⁸¹, H. Wang¹⁸, H. Wang³, J. Wang¹⁵⁷, J. Wang^{61b}, P. Wang⁴², Q. Wang¹²⁸, R.-J. Wang⁹⁹, R. Wang^{60a}, R. Wang⁶, S.M. Wang¹⁵⁸, W.T. Wang^{60a}, W. Wang^{15c,ag}, W.X. Wang^{60a,ag}, Y. Wang^{60a,ao}, Z. Wang^{60c}, C. Wanotayaroj⁴⁶, A. Warburton¹⁰³, C.P. Ward³², D.R. Wardrope⁹⁴, N. Warrack⁵⁷, A. Washbrook⁵⁰, A.T. Watson²¹, M.F. Watson²¹, G. Watts¹⁴⁸, B.M. Waugh⁹⁴, A.F. Webb¹¹, S. Webb⁹⁹, C. Weber¹⁸³, M.S. Weber²⁰, S.A. Weber³⁴, S.M. Weber^{61a}, A.R. Weidberg¹³⁵, J. Weingarten⁴⁷, M. Weirich⁹⁹, C. Weiser⁵², P.S. Wells³⁶, T. Wenaus²⁹, T. Wengler³⁶, S. Wenig³⁶, N. Wermes²⁴, M.D. Werner⁷⁸, P. Werner³⁶, M. Wessels^{61a}, T.D. Weston²⁰, K. Whalen¹³¹, N.L. Whallon¹⁴⁸, A.M. Wharton⁸⁹, A.S. White¹⁰⁵, A. White⁸, M.J. White¹, D. Whiteson¹⁷¹, B.W. Whitmore⁸⁹, F.J. Wickens¹⁴⁴, W. Wiedenmann¹⁸¹, M. Wielers¹⁴⁴, N. Wieseotte⁹⁹, C. Wiglesworth⁴⁰, L.A.M. Wiik-Fuchs⁵², F. Wilk¹⁰⁰, H.G. Wilkens³⁶, L.J. Wilkins⁹³, H.H. Williams¹³⁷, S. Williams³², C. Willis¹⁰⁶, S. Willocq¹⁰², J.A. Wilson²¹, I. Wingerter-Seez⁵, E. Winkels¹⁵⁶, F. Winklmeier¹³¹, O.J. Winston¹⁵⁶, B.T. Winter⁵², M. Wittgen¹⁵³, M. Wobisch⁹⁵, A. Wolf⁹⁹, T.M.H. Wolf¹¹⁹, R. Wolff¹⁰¹, R.W. Wölker¹³⁵, J. Wollrath⁵², M.W. Wolter⁸⁴, H. Wolters^{140a,140c}, V.W.S. Wong¹⁷⁵, N.L. Woods¹⁴⁶, S.D. Worm²¹, B.K. Wosiek⁸⁴, K.W. Woźniak⁸⁴, K. Wraight⁵⁷, S.L. Wu¹⁸¹, X. Wu⁵⁴, Y. Wu^{60a}, T.R. Wyatt¹⁰⁰, B.M. Wynne⁵⁰, S. Xella⁴⁰, Z. Xi¹⁰⁵, L. Xia¹⁷⁸, D. Xu^{15a}, H. Xu^{60a,d}, L. Xu²⁹, T. Xu¹⁴⁵, W. Xu¹⁰⁵, Z. Xu^{60b}, Z. Xu¹⁵³, B. Yabsley¹⁵⁷, S. Yacoob^{33a}, K. Yajima¹³³, D.P. Yallup⁹⁴, D. Yamaguchi¹⁶⁵, Y. Yamaguchi¹⁶⁵, A. Yamamoto⁸¹, T. Yamanaka¹⁶³, F. Yamane⁸², M. Yamatani¹⁶³, T. Yamazaki¹⁶³, Y. Yamazaki⁸², Z. Yan²⁵, H.J. Yang^{60c,60d}, H.T. Yang¹⁸, S. Yang⁷⁷, X. Yang^{60b,58}, Y. Yang¹⁶³, W.-M. Yao¹⁸, Y.C. Yap⁴⁶, Y. Yasu⁸¹, E. Yatsenko^{60c,60d}, J. Ye⁴², S. Ye²⁹, I. Yeletskikh⁷⁹, M.R. Yexley⁸⁹, E. Yigitbasi²⁵, E. Yildirim⁹⁹, K. Yorita¹⁷⁹, K. Yoshihara¹³⁷, C.J.S. Young³⁶, C. Young¹⁵³, J. Yu⁷⁸, R. Yuan^{60b}, X. Yue^{61a}, S.P.Y. Yuen²⁴, B. Zabinski⁸⁴, G. Zacharis¹⁰, E. Zaffaroni⁵⁴, J. Zahreddine¹³⁶, A.M. Zaitsev^{122,az}, T. Zakareishvili^{159b}, N. Zakharchuk³⁴, S. Zambito⁵⁹, D. Zanzi³⁶, D.R. Zaripovas⁵⁷, S.V. Zeißner⁴⁷, C. Zeitnitz¹⁸², G. Zemaityte¹³⁵, J.C. Zeng¹⁷³, O. Zenin¹²², T. Ženiš^{28a}, D. Zerwas¹³², M. Zgubič¹³⁵, D.F. Zhang^{15b}, F. Zhang¹⁸¹, G. Zhang^{60a}, G. Zhang^{15b}, H. Zhang^{15c}, J. Zhang⁶, L. Zhang^{15c}, L. Zhang^{60a}, M. Zhang¹⁷³, R. Zhang^{60a}, R. Zhang²⁴, X. Zhang^{60b}, Y. Zhang^{15a,15d}, Z. Zhang^{63a}, Z. Zhang¹³², P. Zhao⁴⁹, Y. Zhao^{60b}, Z. Zhao^{60a}, A. Zhemchugov⁷⁹, Z. Zheng¹⁰⁵, D. Zhong¹⁷³, B. Zhou¹⁰⁵, C. Zhou¹⁸¹, M.S. Zhou^{15a,15d}, M. Zhou¹⁵⁵, N. Zhou^{60c}, Y. Zhou⁷, C.G. Zhu^{60b}, H.L. Zhu^{60a}, H. Zhu^{15a}, J. Zhu¹⁰⁵, Y. Zhu^{60a}, X. Zhuang^{15a}, K. Zhukov¹¹⁰, V. Zhulanov^{121b,121a}, D. Zieminska⁶⁵, N.I. Zimine⁷⁹, S. Zimmermann⁵², Z. Zinonos¹¹⁴, M. Ziolkowski¹⁵¹, L. Živković¹⁶, G. Zobernig¹⁸¹, A. Zoccoli^{23b,23a}, K. Zoch⁵³, T.G. Zorbas¹⁴⁹, R. Zou³⁷, L. Zwalinski³⁶.

¹Department of Physics, University of Adelaide, Adelaide; Australia.

- ²Physics Department, SUNY Albany, Albany NY; United States of America.
- ³Department of Physics, University of Alberta, Edmonton AB; Canada.
- ^{4(a)}Department of Physics, Ankara University, Ankara; ^(b)Istanbul Aydin University, Istanbul; ^(c)Division of Physics, TOBB University of Economics and Technology, Ankara; Turkey.
- ⁵LAPP, Université Grenoble Alpes, Université Savoie Mont Blanc, CNRS/IN2P3, Annecy; France.
- ⁶High Energy Physics Division, Argonne National Laboratory, Argonne IL; United States of America.
- ⁷Department of Physics, University of Arizona, Tucson AZ; United States of America.
- ⁸Department of Physics, University of Texas at Arlington, Arlington TX; United States of America.
- ⁹Physics Department, National and Kapodistrian University of Athens, Athens; Greece.
- ¹⁰Physics Department, National Technical University of Athens, Zografou; Greece.
- ¹¹Department of Physics, University of Texas at Austin, Austin TX; United States of America.
- ^{12(a)}Bahcesehir University, Faculty of Engineering and Natural Sciences, Istanbul; ^(b)Istanbul Bilgi University, Faculty of Engineering and Natural Sciences, Istanbul; ^(c)Department of Physics, Bogazici University, Istanbul; ^(d)Department of Physics Engineering, Gaziantep University, Gaziantep; Turkey.
- ¹³Institute of Physics, Azerbaijan Academy of Sciences, Baku; Azerbaijan.
- ¹⁴Institut de Física d'Altes Energies (IFAE), Barcelona Institute of Science and Technology, Barcelona; Spain.
- ^{15(a)}Institute of High Energy Physics, Chinese Academy of Sciences, Beijing; ^(b)Physics Department, Tsinghua University, Beijing; ^(c)Department of Physics, Nanjing University, Nanjing; ^(d)University of Chinese Academy of Science (UCAS), Beijing; China.
- ¹⁶Institute of Physics, University of Belgrade, Belgrade; Serbia.
- ¹⁷Department for Physics and Technology, University of Bergen, Bergen; Norway.
- ¹⁸Physics Division, Lawrence Berkeley National Laboratory and University of California, Berkeley CA; United States of America.
- ¹⁹Institut für Physik, Humboldt Universität zu Berlin, Berlin; Germany.
- ²⁰Albert Einstein Center for Fundamental Physics and Laboratory for High Energy Physics, University of Bern, Bern; Switzerland.
- ²¹School of Physics and Astronomy, University of Birmingham, Birmingham; United Kingdom.
- ²²Facultad de Ciencias y Centro de Investigaciones, Universidad Antonio Nariño, Bogota; Colombia.
- ^{23(a)}INFN Bologna and Universita' di Bologna, Dipartimento di Fisica; ^(b)INFN Sezione di Bologna; Italy.
- ²⁴Physikalisch Institut, Universität Bonn, Bonn; Germany.
- ²⁵Department of Physics, Boston University, Boston MA; United States of America.
- ²⁶Department of Physics, Brandeis University, Waltham MA; United States of America.
- ^{27(a)}Transilvania University of Brasov, Brasov; ^(b)Horia Hulubei National Institute of Physics and Nuclear Engineering, Bucharest; ^(c)Department of Physics, Alexandru Ioan Cuza University of Iasi, Iasi; ^(d)National Institute for Research and Development of Isotopic and Molecular Technologies, Physics Department, Cluj-Napoca; ^(e)University Politehnica Bucharest, Bucharest; ^(f)West University in Timisoara, Timisoara; Romania.
- ^{28(a)}Faculty of Mathematics, Physics and Informatics, Comenius University, Bratislava; ^(b)Department of Subnuclear Physics, Institute of Experimental Physics of the Slovak Academy of Sciences, Kosice; Slovak Republic.
- ²⁹Physics Department, Brookhaven National Laboratory, Upton NY; United States of America.
- ³⁰Departamento de Física, Universidad de Buenos Aires, Buenos Aires; Argentina.
- ³¹California State University, CA; United States of America.
- ³²Cavendish Laboratory, University of Cambridge, Cambridge; United Kingdom.
- ^{33(a)}Department of Physics, University of Cape Town, Cape Town; ^(b)Department of Mechanical Engineering Science, University of Johannesburg, Johannesburg; ^(c)School of Physics, University of the

Witwatersrand, Johannesburg; South Africa.

³⁴Department of Physics, Carleton University, Ottawa ON; Canada.

^{35(a)}Faculté des Sciences Ain Chock, Réseau Universitaire de Physique des Hautes Energies - Université Hassan II, Casablanca;^(b)Faculté des Sciences, Université Ibn-Tofail, Kénitra;^(c)Faculté des Sciences Semlalia, Université Cadi Ayyad, LPHEA-Marrakech;^(d)Faculté des Sciences, Université Mohamed Premier and LPTPM, Oujda;^(e)Faculté des sciences, Université Mohammed V, Rabat; Morocco.

³⁶CERN, Geneva; Switzerland.

³⁷Enrico Fermi Institute, University of Chicago, Chicago IL; United States of America.

³⁸LPC, Université Clermont Auvergne, CNRS/IN2P3, Clermont-Ferrand; France.

³⁹Nevis Laboratory, Columbia University, Irvington NY; United States of America.

⁴⁰Niels Bohr Institute, University of Copenhagen, Copenhagen; Denmark.

^{41(a)}Dipartimento di Fisica, Università della Calabria, Rende;^(b)INFN Gruppo Collegato di Cosenza, Laboratori Nazionali di Frascati; Italy.

⁴²Physics Department, Southern Methodist University, Dallas TX; United States of America.

⁴³Physics Department, University of Texas at Dallas, Richardson TX; United States of America.

⁴⁴National Centre for Scientific Research "Demokritos", Agia Paraskevi; Greece.

^{45(a)}Department of Physics, Stockholm University;^(b)Oskar Klein Centre, Stockholm; Sweden.

⁴⁶Deutsches Elektronen-Synchrotron DESY, Hamburg and Zeuthen; Germany.

⁴⁷Lehrstuhl für Experimentelle Physik IV, Technische Universität Dortmund, Dortmund; Germany.

⁴⁸Institut für Kern- und Teilchenphysik, Technische Universität Dresden, Dresden; Germany.

⁴⁹Department of Physics, Duke University, Durham NC; United States of America.

⁵⁰SUPA - School of Physics and Astronomy, University of Edinburgh, Edinburgh; United Kingdom.

⁵¹INFN e Laboratori Nazionali di Frascati, Frascati; Italy.

⁵²Physikalischs Institut, Albert-Ludwigs-Universität Freiburg, Freiburg; Germany.

⁵³II. Physikalischs Institut, Georg-August-Universität Göttingen, Göttingen; Germany.

⁵⁴Département de Physique Nucléaire et Corpusculaire, Université de Genève, Genève; Switzerland.

^{55(a)}Dipartimento di Fisica, Università di Genova, Genova;^(b)INFN Sezione di Genova; Italy.

⁵⁶II. Physikalischs Institut, Justus-Liebig-Universität Giessen, Giessen; Germany.

⁵⁷SUPA - School of Physics and Astronomy, University of Glasgow, Glasgow; United Kingdom.

⁵⁸LPSC, Université Grenoble Alpes, CNRS/IN2P3, Grenoble INP, Grenoble; France.

⁵⁹Laboratory for Particle Physics and Cosmology, Harvard University, Cambridge MA; United States of America.

^{60(a)}Department of Modern Physics and State Key Laboratory of Particle Detection and Electronics, University of Science and Technology of China, Hefei;^(b)Institute of Frontier and Interdisciplinary Science and Key Laboratory of Particle Physics and Particle Irradiation (MOE), Shandong University, Qingdao;^(c)School of Physics and Astronomy, Shanghai Jiao Tong University, KLPPAC-MoE, SKLPPC, Shanghai;^(d)Tsung-Dao Lee Institute, Shanghai; China.

^{61(a)}Kirchhoff-Institut für Physik, Ruprecht-Karls-Universität Heidelberg, Heidelberg;^(b)Physikalischs Institut, Ruprecht-Karls-Universität Heidelberg, Heidelberg; Germany.

⁶²Faculty of Applied Information Science, Hiroshima Institute of Technology, Hiroshima; Japan.

^{63(a)}Department of Physics, Chinese University of Hong Kong, Shatin, N.T., Hong Kong;^(b)Department of Physics, University of Hong Kong, Hong Kong;^(c)Department of Physics and Institute for Advanced Study, Hong Kong University of Science and Technology, Clear Water Bay, Kowloon, Hong Kong; China.

⁶⁴Department of Physics, National Tsing Hua University, Hsinchu; Taiwan.

⁶⁵Department of Physics, Indiana University, Bloomington IN; United States of America.

^{66(a)}INFN Gruppo Collegato di Udine, Sezione di Trieste, Udine;^(b)ICTP, Trieste;^(c)Dipartimento Politecnico di Ingegneria e Architettura, Università di Udine, Udine; Italy.

- ^{67(a)}INFN Sezione di Lecce; ^(b)Dipartimento di Matematica e Fisica, Università del Salento, Lecce; Italy.
^{68(a)}INFN Sezione di Milano; ^(b)Dipartimento di Fisica, Università di Milano, Milano; Italy.
^{69(a)}INFN Sezione di Napoli; ^(b)Dipartimento di Fisica, Università di Napoli, Napoli; Italy.
^{70(a)}INFN Sezione di Pavia; ^(b)Dipartimento di Fisica, Università di Pavia, Pavia; Italy.
^{71(a)}INFN Sezione di Pisa; ^(b)Dipartimento di Fisica E. Fermi, Università di Pisa, Pisa; Italy.
^{72(a)}INFN Sezione di Roma; ^(b)Dipartimento di Fisica, Sapienza Università di Roma, Roma; Italy.
^{73(a)}INFN Sezione di Roma Tor Vergata; ^(b)Dipartimento di Fisica, Università di Roma Tor Vergata, Roma; Italy.
^{74(a)}INFN Sezione di Roma Tre; ^(b)Dipartimento di Matematica e Fisica, Università Roma Tre, Roma; Italy.
^{75(a)}INFN-TIFPA; ^(b)Università degli Studi di Trento, Trento; Italy.
⁷⁶Institut für Astro- und Teilchenphysik, Leopold-Franzens-Universität, Innsbruck; Austria.
⁷⁷University of Iowa, Iowa City IA; United States of America.
⁷⁸Department of Physics and Astronomy, Iowa State University, Ames IA; United States of America.
⁷⁹Joint Institute for Nuclear Research, Dubna; Russia.
^{80(a)}Departamento de Engenharia Elétrica, Universidade Federal de Juiz de Fora (UFJF), Juiz de Fora; ^(b)Universidade Federal do Rio De Janeiro COPPE/EE/IF, Rio de Janeiro; ^(c)Universidade Federal de São João del Rei (UFSJ), São João del Rei; ^(d)Instituto de Física, Universidade de São Paulo, São Paulo; Brazil.
⁸¹KEK, High Energy Accelerator Research Organization, Tsukuba; Japan.
⁸²Graduate School of Science, Kobe University, Kobe; Japan.
^{83(a)}AGH University of Science and Technology, Faculty of Physics and Applied Computer Science, Krakow; ^(b)Marian Smoluchowski Institute of Physics, Jagiellonian University, Krakow; Poland.
⁸⁴Institute of Nuclear Physics Polish Academy of Sciences, Krakow; Poland.
⁸⁵Faculty of Science, Kyoto University, Kyoto; Japan.
⁸⁶Kyoto University of Education, Kyoto; Japan.
⁸⁷Research Center for Advanced Particle Physics and Department of Physics, Kyushu University, Fukuoka ; Japan.
⁸⁸Instituto de Física La Plata, Universidad Nacional de La Plata and CONICET, La Plata; Argentina.
⁸⁹Physics Department, Lancaster University, Lancaster; United Kingdom.
⁹⁰Oliver Lodge Laboratory, University of Liverpool, Liverpool; United Kingdom.
⁹¹Department of Experimental Particle Physics, Jožef Stefan Institute and Department of Physics, University of Ljubljana, Ljubljana; Slovenia.
⁹²School of Physics and Astronomy, Queen Mary University of London, London; United Kingdom.
⁹³Department of Physics, Royal Holloway University of London, Egham; United Kingdom.
⁹⁴Department of Physics and Astronomy, University College London, London; United Kingdom.
⁹⁵Louisiana Tech University, Ruston LA; United States of America.
⁹⁶Fysiska institutionen, Lunds universitet, Lund; Sweden.
⁹⁷Centre de Calcul de l’Institut National de Physique Nucléaire et de Physique des Particules (IN2P3), Villeurbanne; France.
⁹⁸Departamento de Física Teorica C-15 and CIAFF, Universidad Autónoma de Madrid, Madrid; Spain.
⁹⁹Institut für Physik, Universität Mainz, Mainz; Germany.
¹⁰⁰School of Physics and Astronomy, University of Manchester, Manchester; United Kingdom.
¹⁰¹CPPM, Aix-Marseille Université, CNRS/IN2P3, Marseille; France.
¹⁰²Department of Physics, University of Massachusetts, Amherst MA; United States of America.
¹⁰³Department of Physics, McGill University, Montreal QC; Canada.
¹⁰⁴School of Physics, University of Melbourne, Victoria; Australia.
¹⁰⁵Department of Physics, University of Michigan, Ann Arbor MI; United States of America.

- ¹⁰⁶Department of Physics and Astronomy, Michigan State University, East Lansing MI; United States of America.
- ¹⁰⁷B.I. Stepanov Institute of Physics, National Academy of Sciences of Belarus, Minsk; Belarus.
- ¹⁰⁸Research Institute for Nuclear Problems of Byelorussian State University, Minsk; Belarus.
- ¹⁰⁹Group of Particle Physics, University of Montreal, Montreal QC; Canada.
- ¹¹⁰P.N. Lebedev Physical Institute of the Russian Academy of Sciences, Moscow; Russia.
- ¹¹¹National Research Nuclear University MEPhI, Moscow; Russia.
- ¹¹²D.V. Skobeltsyn Institute of Nuclear Physics, M.V. Lomonosov Moscow State University, Moscow; Russia.
- ¹¹³Fakultät für Physik, Ludwig-Maximilians-Universität München, München; Germany.
- ¹¹⁴Max-Planck-Institut für Physik (Werner-Heisenberg-Institut), München; Germany.
- ¹¹⁵Nagasaki Institute of Applied Science, Nagasaki; Japan.
- ¹¹⁶Graduate School of Science and Kobayashi-Maskawa Institute, Nagoya University, Nagoya; Japan.
- ¹¹⁷Department of Physics and Astronomy, University of New Mexico, Albuquerque NM; United States of America.
- ¹¹⁸Institute for Mathematics, Astrophysics and Particle Physics, Radboud University Nijmegen/Nikhef, Nijmegen; Netherlands.
- ¹¹⁹Nikhef National Institute for Subatomic Physics and University of Amsterdam, Amsterdam; Netherlands.
- ¹²⁰Department of Physics, Northern Illinois University, DeKalb IL; United States of America.
- ^{121(a)}Budker Institute of Nuclear Physics and NSU, SB RAS, Novosibirsk;^(b)Novosibirsk State University Novosibirsk; Russia.
- ¹²²Institute for High Energy Physics of the National Research Centre Kurchatov Institute, Protvino; Russia.
- ¹²³Institute for Theoretical and Experimental Physics named by A.I. Alikhanov of National Research Centre "Kurchatov Institute", Moscow; Russia.
- ¹²⁴Department of Physics, New York University, New York NY; United States of America.
- ¹²⁵Ochanomizu University, Otsuka, Bunkyo-ku, Tokyo; Japan.
- ¹²⁶Ohio State University, Columbus OH; United States of America.
- ¹²⁷Faculty of Science, Okayama University, Okayama; Japan.
- ¹²⁸Homer L. Dodge Department of Physics and Astronomy, University of Oklahoma, Norman OK; United States of America.
- ¹²⁹Department of Physics, Oklahoma State University, Stillwater OK; United States of America.
- ¹³⁰Palacký University, RCPTM, Joint Laboratory of Optics, Olomouc; Czech Republic.
- ¹³¹Center for High Energy Physics, University of Oregon, Eugene OR; United States of America.
- ¹³²LAL, Université Paris-Sud, CNRS/IN2P3, Université Paris-Saclay, Orsay; France.
- ¹³³Graduate School of Science, Osaka University, Osaka; Japan.
- ¹³⁴Department of Physics, University of Oslo, Oslo; Norway.
- ¹³⁵Department of Physics, Oxford University, Oxford; United Kingdom.
- ¹³⁶LPNHE, Sorbonne Université, Université de Paris, CNRS/IN2P3, Paris; France.
- ¹³⁷Department of Physics, University of Pennsylvania, Philadelphia PA; United States of America.
- ¹³⁸Konstantinov Nuclear Physics Institute of National Research Centre "Kurchatov Institute", PNPI, St. Petersburg; Russia.
- ¹³⁹Department of Physics and Astronomy, University of Pittsburgh, Pittsburgh PA; United States of America.
- ^{140(a)}Laboratório de Instrumentação e Física Experimental de Partículas - LIP, Lisboa;^(b)Departamento de Física, Faculdade de Ciências, Universidade de Lisboa, Lisboa;^(c)Departamento de Física, Universidade de Coimbra, Coimbra;^(d)Centro de Física Nuclear da Universidade de Lisboa, Lisboa;^(e)Departamento de

Física, Universidade do Minho, Braga;^(f)Departamento de Física Teórica y del Cosmos, Universidad de Granada, Granada (Spain);^(g)Dep Física and CEFITEC of Faculdade de Ciências e Tecnologia, Universidade Nova de Lisboa, Caparica;^(h)Instituto Superior Técnico, Universidade de Lisboa, Lisboa; Portugal.

¹⁴¹Institute of Physics of the Czech Academy of Sciences, Prague; Czech Republic.

¹⁴²Czech Technical University in Prague, Prague; Czech Republic.

¹⁴³Charles University, Faculty of Mathematics and Physics, Prague; Czech Republic.

¹⁴⁴Particle Physics Department, Rutherford Appleton Laboratory, Didcot; United Kingdom.

¹⁴⁵IRFU, CEA, Université Paris-Saclay, Gif-sur-Yvette; France.

¹⁴⁶Santa Cruz Institute for Particle Physics, University of California Santa Cruz, Santa Cruz CA; United States of America.

^{147(a)}Departamento de Física, Pontificia Universidad Católica de Chile, Santiago;^(b)Universidad Andres Bello, Department of Physics, Santiago;^(c)Departamento de Física, Universidad Técnica Federico Santa María, Valparaíso; Chile.

¹⁴⁸Department of Physics, University of Washington, Seattle WA; United States of America.

¹⁴⁹Department of Physics and Astronomy, University of Sheffield, Sheffield; United Kingdom.

¹⁵⁰Department of Physics, Shinshu University, Nagano; Japan.

¹⁵¹Department Physik, Universität Siegen, Siegen; Germany.

¹⁵²Department of Physics, Simon Fraser University, Burnaby BC; Canada.

¹⁵³SLAC National Accelerator Laboratory, Stanford CA; United States of America.

¹⁵⁴Physics Department, Royal Institute of Technology, Stockholm; Sweden.

¹⁵⁵Departments of Physics and Astronomy, Stony Brook University, Stony Brook NY; United States of America.

¹⁵⁶Department of Physics and Astronomy, University of Sussex, Brighton; United Kingdom.

¹⁵⁷School of Physics, University of Sydney, Sydney; Australia.

¹⁵⁸Institute of Physics, Academia Sinica, Taipei; Taiwan.

^{159(a)}E. Andronikashvili Institute of Physics, Iv. Javakhishvili Tbilisi State University, Tbilisi;^(b)High Energy Physics Institute, Tbilisi State University, Tbilisi; Georgia.

¹⁶⁰Department of Physics, Technion, Israel Institute of Technology, Haifa; Israel.

¹⁶¹Raymond and Beverly Sackler School of Physics and Astronomy, Tel Aviv University, Tel Aviv; Israel.

¹⁶²Department of Physics, Aristotle University of Thessaloniki, Thessaloniki; Greece.

¹⁶³International Center for Elementary Particle Physics and Department of Physics, University of Tokyo, Tokyo; Japan.

¹⁶⁴Graduate School of Science and Technology, Tokyo Metropolitan University, Tokyo; Japan.

¹⁶⁵Department of Physics, Tokyo Institute of Technology, Tokyo; Japan.

¹⁶⁶Tomsk State University, Tomsk; Russia.

¹⁶⁷Department of Physics, University of Toronto, Toronto ON; Canada.

^{168(a)}TRIUMF, Vancouver BC;^(b)Department of Physics and Astronomy, York University, Toronto ON; Canada.

¹⁶⁹Division of Physics and Tomonaga Center for the History of the Universe, Faculty of Pure and Applied Sciences, University of Tsukuba, Tsukuba; Japan.

¹⁷⁰Department of Physics and Astronomy, Tufts University, Medford MA; United States of America.

¹⁷¹Department of Physics and Astronomy, University of California Irvine, Irvine CA; United States of America.

¹⁷²Department of Physics and Astronomy, University of Uppsala, Uppsala; Sweden.

¹⁷³Department of Physics, University of Illinois, Urbana IL; United States of America.

¹⁷⁴Instituto de Física Corpuscular (IFIC), Centro Mixto Universidad de Valencia - CSIC, Valencia; Spain.

- ¹⁷⁵Department of Physics, University of British Columbia, Vancouver BC; Canada.
- ¹⁷⁶Department of Physics and Astronomy, University of Victoria, Victoria BC; Canada.
- ¹⁷⁷Fakultät für Physik und Astronomie, Julius-Maximilians-Universität Würzburg, Würzburg; Germany.
- ¹⁷⁸Department of Physics, University of Warwick, Coventry; United Kingdom.
- ¹⁷⁹Waseda University, Tokyo; Japan.
- ¹⁸⁰Department of Particle Physics, Weizmann Institute of Science, Rehovot; Israel.
- ¹⁸¹Department of Physics, University of Wisconsin, Madison WI; United States of America.
- ¹⁸²Fakultät für Mathematik und Naturwissenschaften, Fachgruppe Physik, Bergische Universität Wuppertal, Wuppertal; Germany.
- ¹⁸³Department of Physics, Yale University, New Haven CT; United States of America.
- ¹⁸⁴Yerevan Physics Institute, Yerevan; Armenia.
- ^a Also at Borough of Manhattan Community College, City University of New York, New York NY; United States of America.
- ^b Also at Centre for High Performance Computing, CSIR Campus, Rosebank, Cape Town; South Africa.
- ^c Also at CERN, Geneva; Switzerland.
- ^d Also at CPPM, Aix-Marseille Université, CNRS/IN2P3, Marseille; France.
- ^e Also at Département de Physique Nucléaire et Corpusculaire, Université de Genève, Genève; Switzerland.
- ^f Also at Departament de Fisica de la Universitat Autonoma de Barcelona, Barcelona; Spain.
- ^g Also at Departamento de Física, Instituto Superior Técnico, Universidade de Lisboa, Lisboa; Portugal.
- ^h Also at Department of Applied Physics and Astronomy, University of Sharjah, Sharjah; United Arab Emirates.
- ⁱ Also at Department of Financial and Management Engineering, University of the Aegean, Chios; Greece.
- ^j Also at Department of Physics and Astronomy, University of Louisville, Louisville, KY; United States of America.
- ^k Also at Department of Physics and Astronomy, University of Sheffield, Sheffield; United Kingdom.
- ^l Also at Department of Physics, Ben Gurion University of the Negev, Beer Sheva; Israel.
- ^m Also at Department of Physics, California State University, East Bay; United States of America.
- ⁿ Also at Department of Physics, California State University, Fresno; United States of America.
- ^o Also at Department of Physics, California State University, Sacramento; United States of America.
- ^p Also at Department of Physics, King's College London, London; United Kingdom.
- ^q Also at Department of Physics, St. Petersburg State Polytechnical University, St. Petersburg; Russia.
- ^r Also at Department of Physics, Stanford University, Stanford CA; United States of America.
- ^s Also at Department of Physics, University of Adelaide, Adelaide; Australia.
- ^t Also at Department of Physics, University of Fribourg, Fribourg; Switzerland.
- ^u Also at Department of Physics, University of Michigan, Ann Arbor MI; United States of America.
- ^v Also at Faculty of Physics, M.V. Lomonosov Moscow State University, Moscow; Russia.
- ^w Also at Giresun University, Faculty of Engineering, Giresun; Turkey.
- ^x Also at Graduate School of Science, Osaka University, Osaka; Japan.
- ^y Also at Hellenic Open University, Patras; Greece.
- ^z Also at Institutio Catalana de Recerca i Estudis Avancats, ICREA, Barcelona; Spain.
- ^{aa} Also at Institut für Experimentalphysik, Universität Hamburg, Hamburg; Germany.
- ^{ab} Also at Institute for Mathematics, Astrophysics and Particle Physics, Radboud University Nijmegen/Nikhef, Nijmegen; Netherlands.
- ^{ac} Also at Institute for Nuclear Research and Nuclear Energy (INRNE) of the Bulgarian Academy of Sciences, Sofia; Bulgaria.
- ^{ad} Also at Institute for Particle and Nuclear Physics, Wigner Research Centre for Physics, Budapest;

Hungary.

- ae* Also at Institute of High Energy Physics, Chinese Academy of Sciences, Beijing; China.
af Also at Institute of Particle Physics (IPP), Vancouver; Canada.
ag Also at Institute of Physics, Academia Sinica, Taipei; Taiwan.
ah Also at Institute of Physics, Azerbaijan Academy of Sciences, Baku; Azerbaijan.
ai Also at Institute of Theoretical Physics, Ilia State University, Tbilisi; Georgia.
aj Also at Instituto de Fisica Teorica, IFT-UAM/CSIC, Madrid; Spain.
ak Also at Istanbul University, Dept. of Physics, Istanbul; Turkey.
al Also at Joint Institute for Nuclear Research, Dubna; Russia.
am Also at LAL, Université Paris-Sud, CNRS/IN2P3, Université Paris-Saclay, Orsay; France.
an Also at Louisiana Tech University, Ruston LA; United States of America.
ao Also at LPNHE, Sorbonne Université, Université de Paris, CNRS/IN2P3, Paris; France.
ap Also at Manhattan College, New York NY; United States of America.
aq Also at Moscow Institute of Physics and Technology State University, Dolgoprudny; Russia.
ar Also at National Research Nuclear University MEPhI, Moscow; Russia.
as Also at Physics Department, An-Najah National University, Nablus; Palestine.
at Also at Physics Dept, University of South Africa, Pretoria; South Africa.
au Also at Physikalisch-es Institut, Albert-Ludwigs-Universität Freiburg, Freiburg; Germany.
av Also at School of Physics, Sun Yat-sen University, Guangzhou; China.
aw Also at The City College of New York, New York NY; United States of America.
ax Also at The Collaborative Innovation Center of Quantum Matter (CICQM), Beijing; China.
ay Also at Tomsk State University, Tomsk, and Moscow Institute of Physics and Technology State University, Dolgoprudny; Russia.
az Also at TRIUMF, Vancouver BC; Canada.
ba Also at Universita di Napoli Parthenope, Napoli; Italy.

* Deceased